POLITECHNIKA GDAŃSKA

Faculty of Applied Physics and Mathematics

The author of the PhD dissertation: Jan Tuziemski
Scientific discipline: Physics

DOCTORAL DISSERTATION

Title of PhD dissertation: Quantum decoherence and correlation structures

Title of PhD dissertation (in Polish): Kwantowa dekoherencja i struktury korelacyjne

Supervisor *signature*	Second supervisor *signature*
prof. dr hab. Paweł Horodecki	dr Jarosław Korbicz

Gdańsk, 2016

POLITECHNIKA GDAŃSKA

FTiMS PG

Faculty of Applied Physics and Mathematics

STATEMENT

The author of the PhD dissertation: Jan Tuziemski

I, the undersigned, agree/~~do not agree~~* that my PhD dissertation entitled:
Quantum decoherence and correlation structures
may be used for scientific or didactic purposes.[1]

Gdańsk, 9.09.2016 .....

signature of the PhD student

Aware of criminal liability for violations of the Act of 4th February 1994 on Copyright and Related Rights (Journal of Laws 2006, No. 90, item 631) and disciplinary actions set out in the Law on Higher Education (Journal of Laws 2012, item 572 with later amendments),[2] as well as civil liability, I declare, that the submitted PhD dissertation is my own work.

I declare, that the submitted PhD dissertation is my own work performed under and in cooperation with the supervision of prof. dr hab. Paweł Horodecki and the cosupervision of dr Jarosław Korbicz.

This submitted PhD dissertation has never before been the basis of an official procedure associated with the awarding of a PhD degree.

All the information contained in the above thesis which is derived from written and electronic sources is documented in a list of relevant literature in accordance with art. 34 of the Copyright and Related Rights Act.

I confirm that this PhD dissertation is identical to the attached electronic version.

Gdańsk, 9.09.2016 .....

signature of the PhD student

I, the undersigned, agree/do not agree* to include an electronic version of the above PhD dissertation in the open, institutional, digital repository of Gdańsk University of Technology, Pomeranian Digital Library, and for it to be submitted to the processes of verification and protection against misappropriation of authorship.

Gdańsk, 9.09.2016 .....

signature of the PhD student

[1] Decree of Rector of Gdansk University of Technology No. 34/2009 of 9th November 2009, TUG archive instruction addendum No. 8.

[2] Act of 27th July 2005, Law on Higher Education: Chapter 7, Criminal responsibility of PhD students, Article 226.

POLITECHNIKA GDAŃSKA

FTiMS PG

Faculty of Applied Physics and Mathematics

DESCRIPTION OF DOCTORAL DISSERTATION

The Author of the PhD dissertation: Jan Tuziemski

Title of PhD dissertation: Quantum decoherence and correlation structures

Title of PhD dissertation in Polish: Kwantowa dekoherencja I struktury korelacyjne

Language of PhD dissertation: English

Supervision: prof. dr hab. Paweł Horodecki

Second supervisor: dr Jarosław Korbicz

Date of doctoral defense:

Keywords of PhD dissertation in Polish: informacja kwantowa, kwantowe korelacja, dekoherencja, przejście kwantowo-klasyczne

Keywords of PhD dissertation in English: quantum information, quantum correlations, decoherence, quantum to classical transition

Summary of PhD dissertation in Polish:

W rozprawie przedstawiono teoretyczne rozważania dotyczące roli struktur korelacyjnych w wybranych problemach kwantowej teorii informacji oraz zagadnienia wyłaniania się klasycznej rzeczywistości ze świata rządzonego prawami mechaniki kwantowej. W szczególności, odnośnie tematyki związanej z kwantowym przetwarzaniem informacji, badano protokół zdalnego przygotowania stanu (ang. Remote State Preparation), w celu ustalenia, który rodzaj korelacji kwantowych ma kluczowy wpływ na wydajność protokołu. Udowodniono, że w najogólniejszym przepadku kwantowe korelacje reprezentowane zawarte w stanach splątanych nie mogą prowadzić do niższej wydajności protokołu niż korelacje zawarte w stanach separowalnych. Tym samym rozwiązano problem wzbudzający duże zainteresowanie wśród naukowców zajmujących się kwantową teorią informacji. Odnośnie zagadnienia przejścia kwantowo-klasycznego zbadano nową teorię struktur rozgłaszających (ang. Spectrum Broadcast Structures) w modelach układów fizycznych, w których rozprawy przewidywania teorii nie zostały dotychczas sprawdzone. W szczególności badano modele, w których wyróżniony układ oddziałuje ze środowiskiem złożonym z oscylatorów harmonicznych, a zwłaszcza model kwantowego ruchu Browna. Przy pomocy opracowanych w rozprawie narzędzi wykazano, że w modelu kwantowego ruchu Browna, w pewnym reżimie parametrów, dynamika prowadzi do powstania struktur rozgłaszających oraz zwrócono uwagę na ich dynamiczne cechu.

Summary of PhD dissertation in English:

In this thesis we theoretically investigate selected problems concerning correlation structures in Quantum Information Theory and Quantum to Classical transition. In particular, regarding the former we would like to answer the question: what kind of quantum correlations is responsible for quantum advantage in Remote State Preparation protocol? This is an important question that has recently received a considerable amount of attention. Here we prove that, in the most general setting, separable states cannot exceed the efficiency of entangled states in the protocol. The second aim concerns the investigation of recently developed theory of Spectrum Broadcast

Structures in physical models, where it has not been studied so far. More precisely, we focus on the case, in which the environment is composed of harmonic oscillators, especially on Quantum Brownian Motion model. We study the model and show that there is a regime of parameters, in which Spectrum Broadcast Structures are formed. We comment on novel dynamical features of the Spectrum Broadcast Structures formed in the model.

Abstract

In this thesis we theoretically investigate selected problems concerning correlation structures in Quantum Information Theory and Quantum to Classical transition. In particular, regarding the former we would like to answer the question: what kind of quantum correlations is responsible for quantum advantage in Remote State Preparation protocol? This is an important question that has recently received a considerable amount of attention. Here we prove that, in the most general setting, separable states cannot exceed the efficiency of entangled states in the protocol. We show also that the previous statement is not true in cases, in which there are some additional restrictions imposed on the protocol.

The second aim concerns verification of the hypothesis that Spectrum Broadcast Structures are formed in previously unstudied physical models and, in case of it's confirmation, characterization of this process. More precisely we focus on cases, in which the environment is composed of harmonic oscillators, especially on Quantum Brownian Motion model. We study the model in the recoilless limit and show that there is a regime of parameters, in which Spectrum Broadcast Structures are formed. We analyze the process by providing it's timescales and comment on novel dynamical features of the Spectrum Broadcast Structures formed in the model.

List of publications

This work is based on results from the following publications:

- Paweł Horodecki, Jan Tuziemski Paweł Mazurek, Ryszard Horodecki
  Can Communication Power of Separable Correlations Exceed That of Entanglement Resource?
  Physical Review Letters 112, 140507 (2014)

- Jan Tuziemski, Jarosław K. Korbicz
  Objectivisation In Simplified Quantum Brownian Motion Models
  Photonics 2, 228 (2015)

- Jan Tuziemski, Jarosław K. Korbicz
  Dynamical objectivity in quantum Brownian motion
  EPL (Europhysics Letters) 112, 40008 (2015)

- Jan Tuziemski, Jarosław K. Korbicz
  Analytical studies of Spectrum Broadcast Structures in Quantum Brownian Motion
  To appear in Journal of Physics A

Not related to the content of the thesis

- Adam Miranowicz, Paweł Horodecki, Ravindra W. Chhajlany, Jan Tuziemski, and Jan Sperling
  Analytical progress on symmetric geometric discord: Measurement-based upper bounds
  Physical Review A 86, 042123 (2012)

- Jan Tuziemski, Karol Horodecki
  On the non-locality of tripartite non-signaling boxes emerging from wirings
  Quantum Information and Computation 15, 13&14 (2015)

- Ravishankar Ramanathan, Jan Tuziemski, Michał Horodecki, and Paweł Horodecki
  No quantum realization of extremal no-signaling boxes
  Physical Review Letters 117, 050401 (2016)

Acknowledgements

I would like to express my gratitude to my supervisor prof. dr hab. Paweł Horodecki for accepting me as his student, his support, encouragement and advice.

I am grateful to my co-supervisor dr Jarosław Korbicz for many interesting discussions as well as helpful remarks concerning research and scientific life.

I would like to thank prof. dr hab. Ryszard Horodecki, Jadwiga Horodecka, prof dr hab. Józef Sienkiewicz, prof dr hab. Michał Horodecki, dr Karol Horodecki and dr Ravishankar Ramanathan for their help and support at various stages of my studies.

I am deeply indebted to my family. My Grandmother was always eager to sher her invaluable wisdom and tirelessly participated in preparations of my presentations. My Parents always encouraged me in my choice of career. I would like to give special thanks to my Brother for motivating me to take various physical and intellectual activities.

I would like to thank my wife Marta for her love and trust in me.

I acknowledge the financial support by means of project no. 2015/16/T/ST2/00354 of the Polish National Science Center for the preparation of PhD thesis.

Contents

To my Grandmother.

Chapter 1

Introduction

1.1 Introduction and Motivations

Investigation of a composite system gives a variety of opportunities, for example one can study the mutual relations between its parts. The possible number of such relations – correlations – increases with number of subsystems constituting a system. Taking into account the size of the universe it is reasonable to expect that correlations are ubiquitous in nature and indeed this is the case. However, as with other phenomena, the fact of being widespread does not automatically imply that correlations are relevant from physical point of view. Therefore, to fully understand their importance in physics, it is necessary to study situations, in which they may play a role. As a matter of fact, many investigations along this lines have been preformed proving that the presence of correlations in the surrounding us world is not a mere coincidence. This realization is reflected already at the level of names of subfields such as "strongly correlated systems" or tools such as "correlation function" but it has also much deeper consequences. However, as the universe is such a complex system, it is no surprise that our comprehension of the role of correlations is far from being complete.

The ongoing studies of correlations in physics are important not only form conceptual but also from practical point of view. One of the best examples of the latter statement is Quantum Information Theory, in which one investigates how the non-classical correlations predicted by Quantum Theory influence the way in which information can be processed. It turned out that many tasks impossible to achieve using classical systems can be preformed with the help of quantum correlations and simultaneously that in the quantum setting there are fundamental restrictions, which do not affect directly the classical domain. Although much research has been carried out in this field, there are still interesting open problems to work on. Besides, one should also appreciate that some techniques developed in the context of information processing with quantum systems start to enter other fields like Condensed Matter Theory.

The findings of Quantum Information Theory show also that there is no clear distinction between practical and conceptual importance: although developed for practical purposes they

stress yet from another perspective the fundamental difference between the classical and quantum domain. This discrepancy has been realized since early days of Quantum Theory, was (and still is) a source of prejudice against it and lead to famous quotes, debates [1] and research works [2, 3, 4]. Although some time has passed since then, the relation between Quantum and Classical physics is still not fully understood. On the one hand, to the best of our knowledge, the quantum physics provides the most accurate description of nature that has been verified in series of experiments, with no contradiction found. On the other, the reason why this theory challenges our understanding of physics in such a significant way is quite apparent: the phenomena predicted by Quantum Theory cannot be directly seen outside the quantum domain, especially we do not encounter them in our everyday experience. As the experiments testing validity of the theory slowly enter the regimes of everyday (macroscopic) scales, there are no obvious reasons to exclude the possibility that Quantum Theory is the universal theory that can be applied to the whole universe. However, in such a case one needs to clarify the mechanism (or mechanisms) standing behind emergence of the familiar classical behavior out of the quantum universe. This problem, known also as Quantum to Classical transition has been studied for decades [5, 6, 7, 8, 9, 10, 11, 12, 13] and continues to be the subject of discussions not only among physicists but also philosophers of science [14]. It is commonly agreed that a full description of the problem should explain at least three main issues: 1) the lack of non-classical states of single and many body macroscopic systems – the features such as quantum coherences or quantum correlations are absent at the macroscopic level; 2) the redundancy of information about the states of classical systems – in most cases it can be found in many places whereas from "no-cloning" theorem we know that the quantum information cannot be copied [15]; 3) the measurement problem [16] – disappearance of randomness and disturbance associated with quantum measurements in the classical setting. None of the existing approaches aiming at explaining the Quantum to Classical transition has been able to satisfactory address all the points mentioned above. However, most of them underline the role of correlations in this process. It is apparent especially in theories of Quantum Darwinism [11] and Spectrum Broadcast Structures [13], which originate from information-theoretic considerations in the spirit of Quantum Information Theory.

In this thesis we theoretically investigate selected problems concerning correlation structures in Quantum Information Theory and Quantum to Classical transition. In particular, regarding the former we would like to answer the question: what kind of quantum correlations is responsible for quantum advantage in Remote State Preparation protocol? This is an important question that has recently received a considerable amount of attention [17]. The second aim concerns verification of the hypothesis that recently found Spectrum Broadcast Structures [13] are formed in previously unstudied physical models and, in case of it's confirmation, characterization of this process. More precisely we focus on cases, in which the environment is

composed of harmonic oscillators, especially on Quantum Brownian Motion model.

1.2 Structure of the thesis and summary of the results

In Chapter 2 we recall the basin notions from Quantum Theory and Quantum Information Theory that are relevant from our perspective. In this Chapter we discuss the correlation structures in Quantum Theory and provide a short introduction to the role of correlations in quantum information protocols focusing on Remote State Preparation protocol and the problem of Quantum to Classical transition by summarizing Decoherence theory, Quantum Darwinism and approach based on Spectrum Broadcast Structures.

In Chapter 3 we investigate in detail the relation between different kinds of quantum correlations and the efficiency of Remote State Preparation protocol. This issue has been considered recently in a work [17] and received a lot of attention since it has been argued there that it is not the strongest form of quantum correlations - quantum entanglement but a weaker form of separable quantum correlations that is responsible for enabling this task. We start by introducing the most general settings for the considered protocol and compare them to those used in the mentioned work. Subsequently, we stress the importance of choosing the proper way of measuring an accuracy of the protocol by showing that the wrong choice made in [17] leads to inconsistent results. Adopting the right tool we revisit the problem and prove that, contrary to claims made in [17], in the most general setting the weaker form of quantum correlations cannot provide better efficiency in the protocol than the stronger one. Furthermore, we discuss two variants of the protocol, in which the allowed operations in the protocol are restricted in a natural way, and show that in these cases the general conclusion from the previous sentence does not hold.

In Chapter 4 we turn our attention to some aspects of the Quantum to Classical transition problem. We investigate a case in which a distinguished system interacts with an environment consisting of quantum harmonic oscillators. In this Chapter we do not specify the central system, we just assume that it is a sources of time dependent external force acting on the environment. In this setting we derive expressions for two functions indicating Spectrum Broadcast Structure formation - the decoherence factor governing the suppressions of possible coherences and generalized overlap that provides information about the information content of the environment. The obtained expressions are valid in the case when the environment is in a thermal state but subsequently we generalize them for arbitrary single-mode Gaussian states of the environment. We discuss also the dependence of indicator functions on temperature of environment showing that the information content of the environment decreases with temperature, whereas, apart from such behavior, the modulus of decoherence factor can be constant with temperature.

In Chapter 5 we investigate the formation of Spectrum Broadcast Structures in Quantum Brownian Motion model, consisting of a central harmonic oscillator interacting with harmonic oscillators forming an environment. We discuss two different approaches of modeling the environment: the most common one, in which the properties of the environment are encapsulated in a continuous spectral-density function and the one, in which one does not use this function and keeps the description in terms of individual parameters characterizing environmental subsystems. To gain some intuition about the model we begin our considerations with the simplified cases, when firstly the self-Hamiltonians of the system and the environment are omitted (this case in known in the decoherence literature as the measurement-limit) and secondly the Hamiltonian of the environment is restored (we call this partial measurement limit). In both cases we derive expressions for functions indicating Spectrum Broadcast Structure formation and timescales of these process, assuming that the environment is composed of finite number of subsystems with frequencies chosen at random. Subsequently we include into considerations the self-Hamiltonian of the central system and in the recoilless limit we derive an approximate solution of the dynamics suitable for the purposes of our study. This allows us to use the results of Chapter 4 and obtain the expressions for indicator functions - the decoherence factor and generalized overlap. Then we begin their analysis, firstly with the help of a continuous spectral-density function, afterwards investigating the description in terms of discrete environmental spectra. As in the latter setting the analytical expressions for indicator functions lead to almost periodic functions of time, we initially perform analysis by plotting them. We study how possible choices of the frequencies of environment with respect to the central system frequency influence the formation of Spectrum Broadcast Structure in the considered model. Subsequently, we develop a fully analytical method, based on the Law of Large Numbers, that allows us to analyze the functions. In particular, we determine the timescales of the process and provide an answer to an important question: how many environmental subsystems are needed for the decoherence factor and the generalized overlap to be below a given threshold.

In Chapter 6 we summarize our results and list some open problems.

Chapter 2

Preliminaries

2.1 Brief introduction to the formalism of Quantum Theory

The framework of each physical theory consists of mathematical structures and relations between them and physical world they aim to describe. The presentation of the detailed mathematical formulation of Quantum Theory can be found in textbooks (see e.g. [18, 19]). Here we present the main notions and tools that are used in the thesis. Additionally we discuss some, relevant for our purpose, concepts of Quantum Information Theory. The detailed presentation of the latter can be found for example in [20, 21].

2.1.1 States

The description of a quantum state depends on the amount of knowledge that one posses about it. If a state of a given system is known exactly then it is described by a vector $|\Psi\rangle$ belonging to a Hilbert space H and the state is said to be pure. The dimension of the Hilbert space H depends on the considered problem. In Quantum Information Theory one usually is able to restrict considerations to finite-dimensional spaces. However, in problems regarding physical systems such as quantum harmonic oscillators infinite dimensional Hilbert spaces are unavoidable. In this case the Hilbert space must be separable, this means that it must admit a countable orthonormal basis. If for some reasons the knowledge of the system is not perfect, then the state is said to be mixed. In such a case one can write a density operator (matrix)

$$\rho = \sum_i p_i |\Psi_i\rangle\langle\Psi_i|, \tag{2.1}$$

where p_i are probabilities of finding the system in one of pure state $|\Psi_i\rangle$. In order to describe a proper physical system, the density operator cannot be just an arbitrary matrix. It must be: i) Hermitian $\rho = \rho^\dagger$ ii) non-negative $\forall_{|\phi\rangle\in H}\langle\phi|\rho|\phi\rangle > 0$, iii) of unit trace $Tr(\rho) = 1$.

2.1.2 Composite Quantum Systems

In the case when a given physical system consists of many subsystems we say that it is composite. Let us consider a situation in which there are two isolated (uncorrelated) subsystems A and B that are described by density matrices ρ_A, ρ_B. Then the joint state of subsystems is given by a density matrix ρ_{AB} that is constructed via the tensor (Kronecker) product

$$\rho_{AB} = \rho_A \otimes \rho_B. \tag{2.2}$$

One may be interested in the reverse problem. Suppose that a joint systems is described by ρ_{AB} and one has access only to the subsystem A. Then the state corresponding to subsystem A is obtained by taking the partial trace with respect to the subsystem B $\rho_A = Tr_B \rho_{AB}$. The above discussion can be easily generalized to situations involving any (finite) number of subsystems.

So far we excluded from our considerations the notion of correlations. Due to the fact that quantum systems may be correlated in many different ways we postpone the discussion of correlations till Subsection 2.2.

2.1.3 Measurements

The physical quantities such as energy, momentum or position, correspond to operators acting on a Hilbert space of considered physical systems. These operators are self-adjoint. Apart from being Hermitian it means also that operator $\hat{O}$ and its adjoint $\hat{O}^\dagger$ must have domains that coincide. For details see [22].

In finite dimensional systems Hermicity implies self-adjointness. The self-adjoint operators can be always decomposed as $\hat{O} = \sum_i o_i \Pi_i$, where o_i are real eigenvalues and Π_i are orthogonal projectors $\Pi_i \Pi_j = \delta_{ij} \Pi_j$. Projectors Π_i form the complete set $\sum_i \Pi_i = I$, where I is the identity operator. This decomposition is noteworthy since the eigenvalues o_i are the possible outcomes in an experiment measuring observable $\hat{O}$. Let us suppose that an observable $\hat{O}$ is measured on a state ρ. Then the probability of obtaining outcome o_i equals $p_i = Tr\left(\rho \Pi_i\right)$ and the theory predicts that the state after the measurement is $\rho_i = \frac{\Pi_i \rho \Pi_i}{Tr(\rho \Pi_i)}$.

In general it is possible to perform measurements in which the projectors Π_i are replaced by non-orthogonal operators V_i such that $\sum_i V_i^\dagger V_i = I$. Such measurements are referred to as POVMs [20].

2.1.4 General operations on quantum states

Although the measurements described in the previous Subsection are very natural from the physical point of view, they are not the most general operation that can be performed on quantum states. One may ask, in abstract terms, what is the structure of operations, which transform

quantum states into other quantum states. The obvious requirement for such an operation is to preserve the positivity of quantum states, this is $\Lambda(\rho) \geq 0$. However, one should also take into account that a given state ρ_A can be a subsystem of a larger state ρ_{AB} so a general operation applied to ρ_A should also transform the whole state ρ_{AB} to a valid quantum state. Therefore one requires that a map Λ is a completely positive one. Restricting the discussion to finite dimensional case, a complete positivity means that when we extend action of Λ to a higher dimensional system by mens of an identity map I_d, the resulting state must be positive regardless of the dimension d:

$$\forall_d \;\; I_d \otimes \Lambda\rho_{AB} \geq 0. \tag{2.3}$$

The state $\tilde{\rho}$ being a result of action of an operation Λ on a state ρ is

$$\tilde{\rho} = \frac{\Lambda(\rho)}{Tr[\Lambda(\rho)]}. \tag{2.4}$$

The completely positive operations can be represented in the so-called operator-sum or Kraus-Choi representation. Let us denote the set of linear bounded operators from space H into H $B(H)$. Then we have the following theorem [23, 24].

Theorem 1. *A map $\Lambda : B(H_A^d) \to B(H_A^{d'})$ is completely positive if and only if it admits a representation*

$$\Lambda(\rho) = \sum_{i=0}^{M} V_i \rho V_i^{\dagger}, \tag{2.5}$$

where d, d' are dimensions of Hilbert spaces H_A, H_B respectively, $\{V_i\}_{i=0}^{M}$ is set of $d' \times d$ matrices, and $M \leq dd'$.

One can further classify completely positive maps according to the value of $Tr[\Lambda(\rho)]$.
If $Tr[\Lambda(\rho)] = 1$ the operation is called a deterministic quantum operation or quantum channel. Moreover in this case $\sum_{i=0}^{M} V_i^{\dagger} V_i = I$. To this subclass belong POVM and projective measurements described in previous Subsection.
On the other hand, if $Tr[\Lambda(\rho)] < 1$ the operation Λ is called stochastic. Then $\sum_{i=0}^{M} V_i^{\dagger} V_i \leq I$. Such operations are sometimes encountered in some quantum information protocols.

2.1.5 Dynamics of quantum systems

The evolution of an isolated physical system is governed by the Schrödinger equation

$$i\hbar \frac{d}{dt} |\Psi(t)\rangle = \hat{H} |\Psi(t)\rangle, \tag{2.6}$$

where $\hat{H}$ is Hamiltonian operator of a given physical system. Formally, the evolution of the system from initial time $t_i = 0$ till $t_f = t$ is thus given by an unitary operator

$$\hat{U}(t) = \exp\left(-\frac{i}{\hbar}\hat{H}t\right). \tag{2.7}$$

The case, in which the Hamiltonian is time dependent $\hat{H}(t)$ is more involved. Symbolically one can write that the evolution operator as

$$\hat{U}(t) = \mathcal{T}\exp\left(-\frac{i}{\hbar}\int_0^t dt'\hat{H}(t')\right), \tag{2.8}$$

where $\mathcal{T}$ is time ordering operator. The above expression should be understood in terms of a series

$$\hat{U}(t) = \sum_{n=0}^{\infty}\frac{-i^n}{\hbar^n n!}\int_0^t dt_1 \ldots \int_0^t dt_n \mathcal{T}[\hat{H}(t_1)\ldots\hat{H}(t_n)]. \tag{2.9}$$

The global unitary evolution of a composite quantum system does not imply the unitary evolution of its subsystems. In general, let us assume that the composite quantum state $\rho_{S:E}$ describes a system of interest and its environment and that they undergo an unitary evolution $\hat{U}_{S:E}(t)$

$$\rho_{S:E}(t) = \hat{U}_{S:E}(t)\rho_{S:E}\hat{U}^{\dagger}_{S:E}(t). \tag{2.10}$$

If we are interested in the description of the state alone, we need to trace out the environment

$$\rho_S(t) = Tr_E\left(\hat{U}_{S:E}(t)\rho_{S:E}\hat{U}^{\dagger}_{S:E}(t)\right). \tag{2.11}$$

Since any reduced dynamics of the system must change its state into another valid state of a physical system and the dynamics preserve trace $Tr(\rho_S(t)) = Tr(\rho_S)$, we can treat the reduced evolution as an example of a quantum channel introduced in previous Subsection. Then it follows that the reduced evolution admits decomposition into Choi-Kraus operators V_i

$$\rho_S(t) = Tr_E\left(\hat{U}_{S:E}(t)\rho_{S:E}\hat{U}^{\dagger}_{S:E}(t)\right) = \Lambda_t(\rho_S) = \sum_i V_i\rho_S V_i^{\dagger}. \tag{2.12}$$

In fact one can not only interpret the reduced evolution of the system as a quantum channel but the reverse interpretation is also true. This is the statement of the Stinespring dilation theorem [25].

Theorem 2. *Any completely positive trace preserving map may always be written as a unitary evolution on an enlarged space with the environmental subsystems eventually traced out.*

The study of reduced dynamics can be also performed form another perspective. One can take time derivative of (2.12) and try to solve the resulting differential equation, which is of a form

$$\frac{d}{dt}\rho_S(t) = \hat{\mathcal{L}}_t\rho_S. \tag{2.13}$$

It turns out that after certain approximations on the state of the environment and the character of system-environment interaction are imposed, the master equation can be solved. Thus one gains insights into the evolution of the system even though the analytical description of a total evolution operator can be too complex to use or even impossible to obtain. An important class of master equations consists of first order differential equations local in time. Their general form is

$$\frac{d}{dt}\rho_S(t) = \hat{\mathcal{L}}_t\rho_S = -\frac{i}{\hbar}\left[\hat{H}'_S, \rho_S(t)\right] + \hat{L}(\rho_S(t)). \tag{2.14}$$

The first part of the right hand side of the above equation, given by the commutator $-\frac{i}{\hbar}\left[\hat{H}'_S, \rho_S(t)\right]$, describes the unitary evolution of the system under the Hamiltonian $\hat{H}'_S$. Note that this Hamiltonian in general is not identical to the unperturbed Hamiltonian of the system $\hat{H}_S$. The interaction with the environment may lead to effects such as a renormalization of the energy levels of the system. Thus the environment may affect the unitary evolution of the system. Moreover, the second term $\hat{L}(\rho_S(t))$ describes possible non-unitary effects induced by the environment. The non-unitary character of the reduced evolution is of great importance to the problem of Quantum to Classical transition and will be discussed in Section 2.4.

2.2 Correlation Structures in Quantum Theory

The detailed structure of correlations in Quantum Theory is rather complex. Despite this fact, correlations encountered in quantum theory can be divided into two groups: to the first one belong correlations that are common to quantum and classical theory, whereas to the second all non-classical correlations. Entanglement is the most prominent example from the second group [26], however it is not the only non-classical type of correlations. In recent years a considerable effort was put into investigation of so called correlations beyond entanglement [27]. Since there is no general agreement on which correlations are essentially classical we adopt here approach form [28].

As different types of correlations are at heart of problems tackled in this thesis, we introduce basic concepts regarding them. The presentation is restricted to bipartite case. We start with entanglement.

2.2.1 Quantum Entanglement

One of the most striking features exhibited by composed quantum systems is entanglement, which initially was a subject of research concerning foundational issues of Quantum Theory. However, with the development of Quantum Information Theory it has been realized that entanglement can be viewed as a resource for quantum-information protocols. Moreover, phenomenon of entanglement is also important in addressing the problem of Quantum to Classical transition. Therefore it is necessary to introduce this concept in the thesis.

The definition of quantum entanglement is not straightforward. One firstly define set of separable states [26].

Definition 2.1. *A pure state of composite system, consisting of subsystems A and B, is called to be separable if and only if it can be written as*

$$|\Psi\rangle_{AB} = |\phi\rangle_A \otimes |\psi\rangle_B. \tag{2.15}$$

In the case of mixed states one needs to consider the convex hull of pure product states [26].

Definition 2.2. *A mixed state of composite system, consisting of subsystems A and B, is called to be separable if and only if it can be written as*

$$\rho_{AB} = \sum_i p_i \rho_A^i \otimes \rho_B^i. \tag{2.16}$$

A state is entangled, if it is not separable. We conclude this subsection with stressing the fact that there is no universal feasible method of detection, if a given state is entangled or not [26].

2.2.2 Quantum Correlations beyond entanglement

One may ask if entangled states are the only non-classical correlated states predicted by the Quantum Theory? The negative answer to this question is closely related to the fact that in Quantum Theory measurement, in general, disturbs a state of a system. Due to this feature, even some separable states cannot be regarded as classical. By imposing additional requirement, namely invariance of a state with respect to a complete local measurement, defined by a complete set of projectors $\{\Pi_i^A\}$, performed on one subsystem (say A)

$$\rho_{AB} = \sum_i \Pi_i^A \otimes I_B \rho_{AB} \Pi_i^A \otimes I_B, \tag{2.17}$$

we arrive at the definition of so called classical-quantum states [28].

Definition 2.3. *A bipartite state is classical-quantum (CQ) if it can be written as*

$$\rho_{AB} = \sum_i p_i |i\rangle\langle i|_A \otimes \sigma_i^B, \tag{2.18}$$

where $\{|i\rangle\}$ is an orthonormal set, p_i a probability distribution and σ_i^B are quantum states.

Note that one can also define this set with respect to the subsystem B, which in our notation leads to QC states.

For some authors [27] the classical-quantum states are essentially classical, due to the fact that one can gain maximal accessible information about one subsystem without perturbing the whole state. However, in general, such a statement may not be true for the second subsystem. As a result some CQ states do not have their classical analogues. Therefore, it is necessary to define the set of classical-classical states, which are embedding of a classical joint probability distributions into the quantum formalism [28].

Definition 2.4. *A bipartite state is classical-classical if it can be written as*

$$\rho_{AB} = \sum_i p_{ij} |i\rangle\langle i|_A \otimes |j\rangle\langle j|_B, \tag{2.19}$$

where $\{|i\rangle_A\}$, $\{|j\rangle_B\}$ are orthonormal sets and p_{ij} is a joint probability distribution.

There are many interesting problems connected to the introduced classes od states. For example, one may be interested in quantifying how much non-classical correlations a given state contains. The topic is very broad for all type of quantum correlations [26, 27]. One possible way of defining a measure is based on a notion of a distance between an investigated state and a class of states that does not contain correlations interesting from the point of view of the problem. As a distance function one can choose for example the relative entropy, which for density matrices ρ, σ is defined as

$$S(\rho||\sigma) = Tr\left[\rho(\log\rho - \log\sigma)\right]. \tag{2.20}$$

The resulting measures are of general structure

$$E_{Class} = \inf_{\sigma \in Class} S(\rho||\sigma), \tag{2.21}$$

where the infimum is taken with respect to some class of states $Class = \{CC, CQ, QC, SEP\}$. This measure has been investigated in entanglement theory (where it is usually referred to as Relative Entropy of Entanglement [26]) and for other types of correlations [29, 30]. In a strict sense, the relative entropy cannot be treated as a proper distance measure since it is not symmetric. This motivated some authors to choose Hilbert-Schmidt metric for constructing

correlations measures. As an example let us consider the geometric measure of discord that will be important in further parts of the thesis.

Definition 2.5. *The geometric discord is defined as*

$$D(\rho) \equiv \min_{\chi \in CQ} \|\rho - \chi\|^2 = \min_{\chi \in C} Tr\left[(\rho - \chi)^2\right], \tag{2.22}$$

where CQ stands for classical-quantum states.

Performing minimum with respect to separable states results in Hilbert-Schmidt measure of entanglement [1].

2.3 Role of correlations in quantum information protocols

As has been mentioned in the introduction, the development of Quantum Information Theory has changed the view on entanglement. It has been realized that entanglement is the resource that enables to perform some tasks, which are impossible form classical point of view. To make this statement more precise we briefly introduce the general structure of quantum resource theories [32]. They consists of three ingredients:

1. the resource states,
2. the free states or non-resource states,
3. the restricted set of allowed or free operations.

In the resource theories it is assumed that, if one does not have access to some resource state, then one can use only free operations and free states. From the this point of view, the resource state allows to overcome the limitations imposed by the structure of free states and operations. In the entanglement theory entangled states serve as a resource, separable states are assumed to be free and the allowed set of operations consists of the so called Local Operations and Classical Communication (LOCC). To give an intuitive explanation of LOCC operations let us introduce the so called distant lab paradigm. Here one assumes that a composite quantum system is distributed among various parties. The parties are spatially separated, what leads to a natural restriction: they are only able to perform local operations (LO) on the subsystems of the composite state being in their possession, such as measurements or more general quantum operations. However, to enable collaboration between parties it is also assumed that they can communicate any classical data, such as measurements' results or can share randomness, by means of classical communication channel (CC). Apart from the structure of the entanglement theory, the assumption of classical communication is motivated also from a technological point

[1] Note that this measure does not fulfill all usually required properties [31].

of view: currently communicating quantum systems is much more difficult than the classical data. From now we restrict our discussion to the case of bipartite LOCC operations. The two separated parties are usually denoted as Alice and Bob. Then we can introduce the following subclasses of LOCC operations:

1. Zero-way LOCC operations. Here one assumes that parties do not communicate with each other, what leads to the following structure of operations

$$\Lambda^0(\rho_{AB}) = \Lambda_A \otimes \Lambda_B(\rho_{AB}), \tag{2.23}$$

where Λ_A, Λ_B are deterministic quantum operations.

2. One-way LOCC operations. Here we assume that one party can send classical message to the other. If we fix the direction of communication (say from A to B) the structure of operations is

$$\Lambda^{\rightarrow}(\rho_{AB}) = \sum_i (V_i^A \otimes I)[I \otimes \Lambda_i^B](\rho_{AB})(V_i^A \otimes I)^\dagger, \tag{2.24}$$

where Bob is assumed to perform deterministic quantum operations Λ_i^B due to the fact that he is not able to communicate to Alice. On the other hand, Alice can perform some stochastic quantum operation that satisfy $\sum_i (V_i^A)^\dagger V_i^A \leq I$. After obtaining the result she send it to Bob who performs a quantum channel Λ_i^B. In fact, one can impose an additional constraint on the $\Lambda^{\rightarrow}$ operations, namely on the amount of classical communication that parties are allowed to send. For example, one can require that Alice can send 2 classical bits to Bob. We denote the resulting class as $LOCC^{\rightarrow,2}$. Using this operations and entanglement as a resource it is possible to perform the famous teleportation protocol [33]. Remote State Preparation is an example of a LOCC protocol with restriction of one bit of classical communication ($LOCC^{\rightarrow,1}$ in our notation). We provide its description as it is the main topic of interest in Chapter 3. In the original version of the protocol [34] the task is to prepare a quantum state, which is known to Alice, at Bob's site. One assumes that initially they share a maximally entangled state as a resource. Under such assumptions, the task can be performed in a single run of experiment with just one bit of classical communication, provided that the state to be prepared is drawn from a special ensemble. In an asymptotic setting such a rate – one classical communication bit per one quantum two-dimensional system (qubit) – is achieved for arbitrary states to be sent [35]. Let us now sketch the main steps of the non-asymptotic protocol.

In general, one use can any maximally entangled state of two qubits

$$|\Psi_{\pm}\rangle_{AB} = \frac{1}{\sqrt{2}}\left(|00\rangle_{AB} \pm |11\rangle_{AB}\right) \quad |\Phi_{\pm}\rangle = \frac{1}{\sqrt{2}}\left(|01\rangle_{AB} \pm |10\rangle_{AB}\right) \tag{2.25}$$

as the shared state. However, the choice $|\Phi_{-}\rangle = \frac{1}{\sqrt{2}}\left(|01\rangle - |10\rangle\right)$ results in the simplest version of the protocol. Alice aims at preparing state $|\varphi\rangle$. She performs a measurement $\hat{M}_A = |\varphi_{\perp}\rangle\langle\varphi_{\perp}|_A - |\varphi\rangle\langle\varphi|_A$ on her part of the shared state, where $|\varphi_{\perp}\rangle_A$ is a state orthogonal to $|\varphi\rangle_A$. There are two possible measurement outcomes. If she obtains 1 the post-measurement state is $|\varphi_{\perp}\varphi\rangle_{AB}$, to -1 corresponds the state $|\varphi\varphi_{\perp}\rangle_{AB}$. She then sends her measurement outcome to Bob, who learns that either he is in the possession of the desired state $|\varphi\rangle$ (if in the message he obtains 1) or that he needs to perform some transformation since his state is $|\varphi_{\perp}\rangle$. In general, the required transformation $|\varphi\rangle \to |\varphi_{\perp}\rangle$ may be non-unitary and thus impossible to perform, however it is not the case for special classes of states such as $|\varphi\rangle = \frac{1}{\sqrt{2}}\left(|0\rangle + e^{i\theta}|1\rangle\right)$, with arbitrary phase θ. Then Bob needs to apply to his part of state one of the Pauli matrices

$$\sigma_1 = \begin{pmatrix} 0 & 1 \\ 1 & 0 \end{pmatrix} \quad \sigma_2 = \begin{pmatrix} 0 & i \\ -i & 0 \end{pmatrix} \quad \sigma_3 = \begin{pmatrix} 1 & 0 \\ 0 & -1 \end{pmatrix}, \tag{2.26}$$

namely σ_3.

One may interpret Remote State Preparation protocol as a task, in which a single real number θ is sent from Alice to Bob. Classical procedure would require sending infinite number of classical bits that specify θ. The Remote State Preparation protocol shows that it is possible to achieve the same task using only one bit of communication with the help of quantum entanglement.

3. Two-way LOCC. Here the both parties can communicate. The mathematical structure of allowed operations is more involved

$$\begin{aligned} \Lambda^{\leftrightarrow}(\rho_{AB}) = \sum_{i,j,k,\ldots} \ldots (I \otimes V^B_{i,j,k})(I \otimes V^A_{i,j})(I \otimes V^B_i)(\rho_{AB}) \times \\ (I \otimes V^B_i)^{\dagger}(I \otimes V^A_{i,j})^{\dagger}(I \otimes V^B_{i,j,k})^{\dagger} \ldots, \end{aligned} \tag{2.27}$$

where Bob starts by performing an operation described by operators V^B_i sends his result to Alice, who performs an operation described by operators $V^A_{i,j}$ and the process repeats. In this case all set of operators $\left\{V^B_i\right\}$, $\left\{V^A_{i,j}\right\}\ldots$ must obey $\sum_i (V^B_i)^{\dagger}(V^B_i) \leq I$, $\sum_j (V^A_{i,j})^{\dagger}(V^A_{i,j}) \leq I, \ldots$ to be a valid stochastic quantum operations. As in the case of one-way LOCC, here one can also introduce subclasses, in which the amount of classical communication is restricted. In general the protocols can be asymmetric, this is one can allow parties to send different number of bits.

If such a convention is adopted then natural inclusion relations hold. For example, one-way LOCC is a subclass of two-way LOCC, in which one party is allowed to communicate 0 bits.

The entanglement theory studies which restrictions imposed by LOCC paradigm can be overcome, if one has access to entangled states. It turned out that entanglement is a powerful resource enabling many, impossible from classical point of view, tasks such as already mentioned Remote State Preparation protocol, Teleportation [33], Dense Coding [36] or computing [37]. Initially, the advantage of these quantum protocols over their classical counterparts was linked to the quantum entanglement. However, the notion of quantum correlations is broader than entanglement since there are separable states that still are correlated in a non-classically way. Therefore, two interesting problems may be posed here. The first one concerns the question, if the separable states can be also useful for such tasks. In fact, it was shown that efficiency of the protocols involving separable non-classical states may also exceed the efficiency of any classical solution of Deutsch-Jozsa problem [38, 39] or Knill-Laflamme scheme [40]. These results provided further insights into the relations between quantum and classical correlations as they show that notion of entanglement does not suffice to understand quantumness. They are also important from operational point of view, as entanglement sates are usually very fragile to noise. As a result, in experiments entangled states are usually degraded and one achieves worse performance than that derived in theoretical schemes. From such a perspective, one can automatically assume that, even though separable quantum correlations still provide an advantage, they can never be regarded as a better resource than the entanglement states. Therefore the result of recent work [17], in which it is claimed that indeed the converse statement is true – some separable states can lead to better performance in Remote State Preparation protocol, is so surprising. As Remote State Preparation is an important building block of quantum communication protocols the problem is of grate importance and will be readdressed in Chapter 3.

We end this subsection with a remark that also other, interesting from physical point of view, problems can be recast in form of resources theories. As an example one can consider resource theories of: coherence [41, 42, 43], thermodynamics [44, 45, 46] and asymmetry [47].

2.4 Role of correlations in Quantum to Classical transition

One can argue that Quantum Theory is one of the most successful scientific descriptions of nature. Its predictions have been verified experimentally to an unprecedented accuracy, however some problems still remain open. One of them concerns the relation of Quantum Theory to the familiar laws of Classical Physics. As an example, let us consider the superposition principle. In the classical domain its validity is restricted to wave phenomena. Contrary to this fact, in

Quantum Theory superposition principle is a universal rule, which applies to all physical systems. As a result, there are quantum states being superpositions of two (or more) classically distinct properties. The most well example of such a state is found in the famous Schrödinger's gedenken-experiment, in which a cat is in a superposition of being alive or dead. Absence of such states on the macroscopic scales indicates that there should be a way in which classical world of everyday experience emerge naturally from the quantum formalism.

However, the fully satisfactory explanation of Quantum to Classical transition has not been formulated yet. One of the most promising approaches to address this problem is based on the realization that, in this case, the notion of idealized isolated system may be an obstacle in understanding how quantum systems become essentially classical [6, 7, 8, 12]. A considerable progress has been made when it was recognized that the interaction of system with environment may correlate the system to the environment in a non-classical way. Then, at the level of the reduced state of system, possible quantum features may disappear. Responsible for this effect are quantum correlations that cause delocalization of an initial state of the system. This is the essence of Decoherence theory that is discussed in more detail in the next Subsection.

Nevertheless, the Decoherence theory alone does not suffice to explain another important aspect of our everyday experience. Not only we do not encounter superpositions of states, but also the information about physical systems is robust and can be found independently by many observers, who learn about systems indirectly using some fragments of the environment. This observation lead to research program known as Quantum Darwinism [10, 11, 48]. Its details are discussed in Subsection 2.4.2.

Development of Quantum Darwinism was a major breakthrough in studies on Quantum to Classical transition. However, this approach was not formulated in terms of the most fundamental description provided by Quantum Theory, namely in terms of quantum states. The further step in understanding of the emergence of classical reality was achieved in [13], where a universal structure of quantum states providing clasicallity, which precise meaning will be clarified later, was derived. This structure is known as Spectrum Broadcast Structure and is described in Subsection 2.4.3.

2.4.1 Decoherence

As has been mentioned in Subsection 2.1.5 the global unitary evolution of the whole state does not imply that the reduced evolution of subsystems is also some unitary transformation. This statement is of a great importance in situations that one usually encounters while dealing with physical systems. Namely, in most cases a system of interest interacts with its environment. However, from various reasons, the state of the environment is not taken into account in the considerations and one focuses on the state of the system alone. The Decoherence theory stresses that this fact leads to a disappearance of coherences in the system's state. To illustrate

this statement, let us consider a situation, in which a system S interacts with the environment E that consists of N subsystems. The general form of the Hamiltonian is

$$\hat{H}_{S:E} = \hat{H}_S + \hat{H}_E + \hat{H}_{INT}. \tag{2.28}$$

For the purpose of this Subsection in what follows we are going to neglect the self Hamiltonians of system $\hat{H}_S$ and environment $\hat{H}_E$. This simplification is known as a quantum measurement limit and allows to gain better understanding in the processes underlying decoherence. We specify the interaction Hamiltonian to be

$$\hat{H}_{INT} = \hat{X} \otimes \sum_{k=1}^{N} \hat{Y}_k, \tag{2.29}$$

where $\hat{X}$, $\hat{Y}_k$ are some observables of the system and the k-th environment respectively, assumed for simplicity to have discrete spectra. The dynamics of the system and environment is thus governed by the unitary operator

$$\hat{U}(t) = \sum_j |x_j\rangle\langle x_j| \otimes \hat{U}_1(x_j,t) \otimes \cdots \otimes \hat{U}_N(x_j,t), \quad \hat{U}_k(x_j,t) \equiv e^{-ix_j t\hat{Y}_k/\hbar}, \tag{2.30}$$

where we spectrally decomposed observable $\hat{X}$ in terms of its eigenvalues x_j and eigenvectors $|x_j\rangle$. Operator $\hat{U}(t)$ is of a controlled unitary type, where the system controls the environments through eigenvalues x_j of $\hat{X}$. We are mainly interested in the correlations between the system and environment that are created in the course of evolution. Therefore, we assume that initial system-environment state factorizes

$$\rho(0)_{S:E} = \rho_{0S} \otimes \bigotimes_{k=1}^{N} \rho_{0k}. \tag{2.31}$$

The joint state of the system and the environment at time t is thus given by

$$\begin{aligned} \rho(t)_{S:E} = \quad & \sum_j \langle x_j|\rho_{0S}\,|x_j\rangle |x_j\rangle\langle x_j| \otimes \bigotimes_{k=1}^{N} \hat{U}_k(x_j,t)\rho_{0k}\hat{U}_k^\dagger(x_j,t) + \\ & \sum_{j,j',j\neq j'} \langle x_j|\rho_{0S}\,|x_{j'}\rangle |x_j\rangle\langle x_{j'}| \otimes \bigotimes_{k=1}^{N} \hat{U}_k(x_j,t)\rho_{0k}\hat{U}_k^\dagger(x_{j'},t). \end{aligned} \tag{2.32}$$

In decoherence theory the main object of study is the reduced state of the system. It is obtained by taking the partial trace with respect to the environment

$$\rho_S(t) = Tr_E(\rho_{S:E}(t)) = \sum_j \langle x_j|\rho_{0S}\,|x_j\rangle|x_j\rangle\langle x_j| + \sum_{j,j',j\neq j'} \Gamma_{j,j'}(t)\langle x_j|\rho_{0S}\,|x_{j'}\rangle|x_j\rangle\langle x_{j'}|, \tag{2.33}$$

where $\Gamma_{j,j'}$ is the so-called decoherence factor

$$\Gamma_{j,j'}(t) = \prod_{k=1}^{N} Tr\left(\hat{U}_k(x_j,t)\rho_{0k}\hat{U}_k^\dagger(x_{j'},t)\right). \tag{2.34}$$

If for given all different pairs j, j' one has that $|\Gamma_{j,j'}(t)| = 0$ for some time t, the off-diagonal part of the reduced density matrix vanish

$$\rho_S(t) = \sum_j \langle x_j|\rho_{0S}\,|x_j\rangle|x_j\rangle\langle x_j|. \tag{2.35}$$

As a result, in the description of the state of the system the coherences between eigenstates of observable $\hat{X}$ are suppressed - the decoherence process occurred. The superposition terms are still present at the global level of joint system-environment state (2.32), however at the local level of the system's state (2.35) they become unobservable. The classical mixture of $\hat{X}$ eigenstates (2.35) is not affected by the system-environment interaction. In a sense, such mixtures are selected by the interaction. This concept, known also as environment-induced superselection or einselection, was developed in [6, 7], where the eigenstates of $\hat{X}$ were called pointer states. Decoherence theory has attracted considerable amount of attention both from theoretical and experimental perspective and has been successfully investigated in many physical models [12]. The decoherence process is not the only non-unitary effect that can be induced by the environment on the system. In general the interaction may lead to effects such as dissipation [49, 50, 51].

Let us mention that in the literature one also considers other mechanisms leading to the lost of coherence in the reduced state of the system [8].

The false decoherence [8] happens when states forming coherent superposition disappear. For example the interaction with the environment may lead to a relaxation process, in which some states of the system decay into others. As an example let us consider a situation in which

$$\begin{aligned} |0\rangle|\phi\rangle_E &\to |0\rangle|\phi'\rangle_E \\ |1\rangle|\phi\rangle_E &\to |0\rangle|\phi''\rangle_E. \end{aligned} \tag{2.36}$$

Then, clearly, the coherence between states $|0\rangle, |1\rangle$ is lost.

The fake decoherence [8] is a process, in which the system's density matrix becomes diagonal due to the fact that it is averaged over some ensemble of states. Then the lost of coherence is connected to lack of knowledge about the state rather than a physical process. If the experiment revealing coherence is performed on the members of the ensemble separately, the interference effects can still be observed.

The coherence between $|0\rangle$ and $|1\rangle$ can also be transformed to some other states $|i\rangle$ of the system, effectively causing disappearance of coherence from the relevant subspace. Then simply the role of the environment is played by some states of the system.

2.4.2 Quantum Darwinism

Decoherence theory only stress the fact that the initial coherent state of the system becomes delocalized on many degrees of freedom due to the interaction with the environment. It assumes that the environment, even some fragments of it, is not observed. However, due to the interaction, the some information about the system is constantly imprinted on the environment. Therefore, it is plausible to expect that some pieces of information can be recovered from it. Moreover, it is important to realize that this is indeed the case in most physical situations. The best example here is eyesight that enables to acquire information about objects by registration of scattered photons rather than by direct interaction with the objects in question. An additional remark should be made here, namely in classical physics many observers can independently gain information about a state of a system, without disturbing it and they agree on what they learned. In a sense, the state of a system preexists objectively. This is the intuition behind the Quantum Darwinism program, which is a major breakthrough in explanation of Quantum to Classical transition. Quantum Darwinism was developed in series of papers [10, 48, 52, 53, 54] and studied in many models known from decoherence theory [55, 56, 57, 58, 59, 60, 61, 62, 62]. We begin presentation of the program by introducing the definition of objectivity [11].

Definition 2.6. *A state of the system S exists objectively if many observers can find out the state of S independently, and without perturbing it.*

Quantum Darwinism assumes that the process of finding out a state of a system is achieved using fragments of an environment, which are available to observers. Therefore, in contrary to Decoherence theory, here the emphasis is put on properties of a partially reduced state, describing the system and fragments of the environment accessible to observers. In particular, of interest are correlations between the system and the fragments.

In the classical setting if a system is perfectly correlated with one fragment of an environment, then the fragment can be used to recover properties of the system. Moreover, access to additional perfectly correlated fragments of the environment does not result in information

gain since all is already known from the single fragment. This statement can be formulated in a quantitative way, using classical information theory. The system and fragment of its environment are modeled as (for simplicity discrete) joint random variable S, E^k. The correlations between them are measured by mutual information

$$I(S : E^k) = H(S) + H(E^k) - H(S, E^k), \tag{2.37}$$

where $H(S)$ and $H(E^k)$ are marginal Shanon entropies and $H(S, E^k)$ is the joint Shannon entropy. For a random variable X Shanon entropy is defined as

$$H(X) = -\sum_i p(x_i) \log p(x_i). \tag{2.38}$$

If the random variable S is perfectly correlated with E^k then $H(S) = H(E^k) = H(S, E^k)$ and as a result

$$I(S : E^k) = H(S). \tag{2.39}$$

Inclusion of another perfectly correlated system $E^{k'}$ in the description does not change the mutual information. We have $H(S) = H(E^k E^{k'}) = H(S, E^k E^{k'})$ and $I(S : E^k E^{k'}) = H(S)$.

Quantum Darwinism adopts this approach to the quantum setting. The joint and marginal random variables are replaced by density matrices. The joint state of the system and environment is described by a partially reduced state

$$\rho_{S:fE} = Tr_{(1-f)E}(\rho_{S:E}), \tag{2.40}$$

where f denotes the observed fraction of the environment ($f \in [0, 1]$). The correlations are measured by quantum mutual information

$$I(\rho_{S:fE}) = H(\rho_S) + H(\rho_{fE}) - H(\rho_{S:fE}), \tag{2.41}$$

$H(\rho_S)$, $H(\rho_{fE})$, are von Neumann entropies of reduced states and $H(\rho_{S:fE})$ is join von Neumann entropy. For a density matrix ρ von Neumann entropy is defined as

$$H(\rho) = -Tr(\rho \log \rho) = -\sum_i \lambda_i \log \lambda_i, \tag{2.42}$$

where $\{\lambda_i\}$ are eigenvalues of ρ.

Quantum Darwinism studies behavior of quantum mutual information as a function of the environment fraction f. Since in many cases it may be unclear, which environmental subsystems should form fraction f it is assumed that one performs analysis for a given partition into

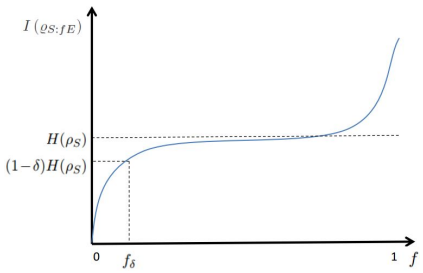

FIGURE 2.1: The partial information plot: quantum mutual information $I(\rho_{S:fE})$ as a function of fragment f. The region in which $I(\rho_{S:fE}) \approx H(\rho_S)$ is called the classical plateau. In the also the fraction f_δ providing $I(\rho_{S:fE}) = (1-\delta)H(\rho_S)$ information of the system was depicted. For more details see for example [63].

observed and unobserved environment and the results are then averaged over many partitions. The main claim of Quantum Darwinism is that if a state is objective in the sense of Definition 2.6, then for broad range of f

$$I(\rho_{S:fE}) \approx H(\rho_S). \tag{2.43}$$

More precisely, the expected behavior of $I(\rho_{S:fE})$ as a function of f for an objective state $\rho_{S:fE}$ is as follows. Initially $I(\rho_{S:fE})$ quickly rises, this indicates that acquisition of parts of the environment leads to gain of information about the system. When $I(\rho_{S:fE})$ approaches $H(\rho_S)$, the information provided by subsequent fragments of environment becomes redundant and therefore $I(\rho_{S:fE})$ remains constant. Finally $I(\rho_{S:fE})$ rises to value of $2H(\rho_S)$ for f close to 1, which is a purely quantum phenomena caused by the property of pure entanglement states, for which $H(\rho_{S:fE}) = 0$ but $H(\rho_S) = H(\rho_{fE}) > 0$.

In the Quantum Darwinism literature usually the analysis of $I(\rho_{S:fE})$ is performed on a plot - the so-called partial information plot, thus the range, in which $I(\rho_{S:fE})$ remains constant, is called classical plateau. As an example let us consider Figure 2.1. The appearance of the plateau is the crucial feature pointing towards objectification of a system's state. One can also estimate the number of independent fragments of the environment that supply classical information about system. In order to do so, an information deficit δ is specified and it is checked for which value of f_δ $I(\rho_{S:f_\delta E}) = (1-\delta)H(\rho_S)$. The number of records providing almost all (up to δ) classical information about the state is then $R_\delta = f_\delta^{-1}$.

Let us again stress that Quantum Darwinism represents an important breakthrough in investigations of Quantum to Classical transition. The shift of paradigm from environment as a sink of information to environment as information carrier postulated by the authors of Quantum Darwinism allowed to gain new and significant insights into the relation between Quantum and Classical theory. However, the question if the scalar condition based on $I(\rho_{S:fE})$ is sufficient to decide, if a state of a system becomes objective remains open. Sufficiency of the

condition was proved in [13]. However also there circumstantial evidence was given that there may exist a state $\rho_{S:E}$, whose partial reduction $\rho_{S:fE}$ is entangled (hence non-classical and non-objective) still fulfilling the scalar condition of Quantum Darwinism.

2.4.3 Spectrum Broadcast Structures

The inconclusiveness of Quantum Darwinism's arguments denotes that emergence of the objective world from Quantum Theory deserves a more rigorous treatment. Indeed, in [13] the problem of Quantum to Classical transition was addressed at the most fundamental level of quantum states and canonical structure of an objective quantum system-environment state was derived. Before presenting it one needs to formalize Definition 2.6 according to [13]. The setting is the same as in Quantum Darwinism. Namely, the quantum system S interacts with many environments $E_1, \ldots, E_N$. Some fragments of environment must pass unobserved to account for information loss causing decoherence. The remaining system-environment state is $\rho_{S:fE}$. The process of "finding out the state of the system" by an observer is understood in terms of von Neumann measurement performed by the observer on an accessible to him fragment of the environment. The independence condition is guaranteed by requiring that there are no correlations between observers (their measurements). As a result, their von Neumann measurements are given by tensor product of local measurements

$$\Pi_j^{M_S} \otimes \Pi_{j_1}^{M_1} \otimes \ldots \Pi_{j_{fn}}^{M_{fN}}. \tag{2.44}$$

Moreover, Definition 2.6 is made more precise by adding an agreement condition, which states that many observers find independently *the same* state of S.

The notion of non-disturbance is adopted from Bohr's works [3, 1], in which he argued that local measurements on the subsystems are non-disturbing if they leave the whole joint state invariant (after forgetting the results of particular measurements). As a result, the state should have the following property

$$\sum_{j,j_1,\ldots j_{fN}} \Pi_j^{M_S} \otimes \Pi_{j_1}^{M_1} \otimes \ldots \Pi_{j_{fn}}^{M_{fN}} \rho_{S:fE} \Pi_j^{M_S} \otimes \Pi_{j_1}^{M_1} \otimes \ldots \Pi_{j_{fn}}^{M_{fN}} = \rho_{S:fE}. \tag{2.45}$$

This is the key step, the only states fulfilling the above requirement are classical-quantum states [64] of the form

$$\rho_{S:fE} = \sum_i p_i |i\rangle\langle i| \otimes \mathbf{R}_i^{fE}, \tag{2.46}$$

where $\mathbf{R}_i^{fE}$ are environmental states with mutually orthogonal supports $\mathbf{R}_i^{fE}\mathbf{R}_{i'\neq i}^{fE} = 0$. Working under these assumptions and using the so-called strong independence condition (firstly

formulated in [64]), which states that the only correlation between the environments should be the common information about the system (in a state conditioned by the information about the system there should be no correlations between the environments), the authors of [13] prove that objective system-environment states admit a canonical form

$$\rho_{S:fE} = \sum_i p_i |i\rangle\langle i| \otimes \rho_i^{E_1} \otimes \ldots \rho_i^{E_{fN}}, \tag{2.47}$$

where $\{|i\rangle\}$ is orthonormal pointer basis and $\rho_i^{E_k}$ are states of individual environmental degrees of freedom with mutually orthogonal supports $\rho_i^{E_k}\rho_{i'}^{E_k} = 0 \ \forall_{i\neq i'}, \ k = 1, \ldots, fN$. The latter property enables observers to distinguish between states of central system using their fragments of the environment: they just need to perform a projective measurement on subspaces of supported by spectra of $\rho_i^{E_k}$ (for all i). As these spectra are disjoint (due to the the condition $\rho_i^{E_k}\rho_{i'}^{E_k} = 0 \ \forall_{i\neq i'}$), the measurement's result i will reveal the state of the system. The structure of the state (2.47) is called spectrum broadcast form. It is a special form of so-called classical-classical state, which was defined in [28].

Due to its structure (equation (2.47)) and the disjoint supports of environmental states $\rho_i^{E_k}$ it formally follows that if the Spectrum Broadcast Structure was formed, then for every non-zero fraction f' of environment forming the structure the condition proposed by Quantum Darwinism is fulfilled

$$I\left(\rho_{S:f'E}\right) = H\left(\rho_S\right). \tag{2.48}$$

It remains unclear if there are are states, which do not admit Spectrum Broadcast Structure but fulfill the scalar condition of Quantum Darwinism. If this was the case, it would mean that the condition is insufficient to show objectivity in the sense of Definition 2.6.

For some readers the form (2.47) may seem to be too restrictive as a candidate for a structure providing the observers with objective information about the system. For example, one may wonder why such a structure could not encompass some kind of separable quantum correlations? In Chapter 3 we show that in some variants of Remote State Preparation protocol some separable quantum correlations lead to better efficiency of the protocol than that obtain with entangled states and hence should not be regarded as classical.

Any theory aiming at describing Quantum to Classical transition remains just a concept unless one is able to show that its predictions are realized in some physical scenario. This is also the case for the Spectrum Broadcast Structures, which would be just a theoretical idea if they were not formed over the course of an evolution in some models relevant from the physical point of view. In fact, their formation has been shown in one of the well know and appealing models of decoherence [5] – an illuminated sphere model, in which the decoherence is caused by photons that scatter at a delocalized sphere [65] . However, this result does not

suffice to conclude that the formation of Spectrum Broadcast Structures is the key mechanism responsible for an appearance of objective classical reality form Quantum Theory.

In general it is unknown if Spectrum Broadcast Structures are formed typically during evolution. The only known exception is the case, in which one assumes the specific form of the problem Hamiltonian [66]. Note however, that it is also possible to consider another approach to Quantum to Classical transition, in which one treats the dynamics as a quantum channel. In such a setting it has been shown that, under some conditions, then the effective dynamics from the system to some fragment of the environment is of a "prepare and measure" form, which in simple terms can be understood as follows: firstly some specific observable of the system is measured and subsequently the corresponding state of the environment is prepared [67]. Although very general, this approach does not allow to study continuous systems, as the results were proven only in the finite-dimensional setting. Moreover, one does not gain insight into timescales of the process and the information content of the environment remains unclear. This discussion shows that the investigation of particular physical models is still needed.

There are many situations in which some physical system interacts with some of environment. However, some of them are more interesting and important than the others. To the former group belong the so-called canonical models of decoherence [12]. In order to determine the set of canonical models one has to specify the central system and the environment. The common choice is between the continuous variables and discrete systems. Usually the latter are restricted to the two-dimensional systems (referred to also as spin $\frac{1}{2}$ particles). As a result one arrives at the conclusion that there are four canonical models, since there are two possible choices for the central system as well as the environment. This fact, taking also into account that there are approximations allowing to map some systems onto canonical models, is of a great importance. Although the canonical models cannot encompass all the richness of the physical world, they should be considered as ideal candidates to test a theory. If the results are negative, one should not expect them to hold in more complex settings.

The above discussion shows that a method to check, if in a given model a Spectrum Broadcast Structure was formed, is needed. Let us now present the direct procedure of verifying Spectrum Broadcast Structure formation. We introduce two indicator functions, whose analysis allow us to conclude if a given model leads to the Spectrum Broadcast Structure or not.

As in the case of decoherence theory, we illustrate the procedure in a case when only the interaction Hamiltonian of the form $\hat{H}_{INT} = \hat{X} \otimes \sum_{k=1}^{N} \hat{Y}_k$ is relevant for the problem (in case when both $[\hat{H}_S, \hat{H}_{INT}] \neq 0$ and $[\hat{H}_E, \hat{H}_{INT}] \neq 0$ there is no general procedure of checking if the Spectrum Broadcast Structure is formed). Thus, our starting point is equation (2.32), describing time evolution of joint system-environment state. Subsequently, an unobserved fragment of

environment is traced out, leading to the partially reduced system-environmental state

$$\rho_{S:fE}(t) = \quad Tr_{(1-f)E}(\rho_{S:E}(t)) = \sum_j \langle x_j|\rho_{0S}\,|x_j\rangle|x_j\rangle\langle x_j| \otimes \bigotimes_{k=1}^{fN} \rho_j^{E_k} + \tag{2.49}$$

$$\sum_{j,j',j\neq j'} \Gamma_{j,j'}(t)\langle x_j|\rho_{0S}\,|x_{j'}\rangle|x_j\rangle\langle x_{j'}| \otimes \bigotimes_{k=1}^{fN} \hat{U}_k(x_j,t)\rho_{0k}\hat{U}_k^\dagger(x_{j'},t), \tag{2.50}$$

where $\Gamma_{j,j'}(t)$ the decoherence factor

$$\Gamma_{j,j'}(t) = \prod_{(1-f)E} Tr\left(\hat{U}_k(x_j,t)\rho_{0k}\hat{U}_k^\dagger(x_{j'},t)\right), \tag{2.51}$$

and $\rho_j^{E_k}$ are

$$\rho_j^{E_k} = \hat{U}_k(x_j,t)\rho_{0k}\hat{U}_k^\dagger(x_j,t). \tag{2.52}$$

In order to verify formation of Spectrum Broadcast Structure one proceeds in two steps. First of all, the coherent part (2.50) of the partially reduced system-environment state should vanish. This will imply that there is no entanglement between the system and the environment and that the coherence (with respect to the eigenbasis of system's observable $\hat{X}$) is suppressed (at the level of partially reduced state). In a nontrivial case, the only possibility for off-diagonal part (2.50) to vanish is when with time the modulus of decoherence factor $\left|\Gamma_{j,j'}(t)\right| = 0$ for all pairs $j \neq j'$. The decoherence process is necessary condition for Spectrum Broadcast Structure formation. However, it is not a sufficient one so the second step in analysis is needed.

To conclude that the Spectrum Broadcast Structure was formed, one checks the information content of remaining environmental states $\rho_j^{E_k}$. In accordance with the paradigm introduced by the Quantum Darwinism, presented earlier in this Subsection, observers find out the state of the system indirectly by measuring accessible to them environmental subsystems. They can only do so if the information about the central system has been imprinted on these subsystems and moreover can be extracted from them. As a result, states of subsystems evolving accordingly to different eigenstates of observable $\hat{X}$ of the system should also be distinguishable. One can put this requirement in mathematical terms: density operators corresponding to different eigenstates of $\hat{X}$ must have non-overlapping supports $\rho_i^{E_k}\rho_{i'}^{E_k} = 0$. In such a case an observer can perform projective measurement on different supports of the spectra and by learning the result he in principle learns also the state of the central system.

Among many different ways of measuring the distinguishability of quantum states, the most convenient one for our purposes is the generalized overlap. For two density matrices ρ, σ

it is defined as

$$B(\rho,\sigma) = Tr\sqrt{\sqrt{\rho}\sigma\sqrt{\rho}}. \tag{2.53}$$

This quantity is known also as fidelity of quantum states and in this case is denoted by $F(\rho,\sigma)$. If the states ρ,σ are indistinguishable $B(\rho,\sigma) = 1$, on the other hand, if they can be distinguished without an error $B(\rho,\sigma) = 0$. In general, if $B(\rho,\sigma) = \epsilon$ then there exits an operator $\hat{M}$ defined as

$$\hat{M} \equiv \sigma^{-1/2}\sqrt{\sqrt{\sigma}\rho\sqrt{\sigma}}\sigma^{-1/2}, \tag{2.54}$$

whose spectral decomposition $\hat{M} = \sum_i m_i\hat{M}_i$, more precisely the projectors $\hat{M}_i$ provide set of operators distinguishing ρ,σ up to an error ϵ [68].

It can be seen from the definition that the generalized overlap is invariant under unitary operators $B(\hat{U}\rho\hat{U}^\dagger,\hat{U}\sigma\hat{U}^\dagger) = B(\rho,\sigma)$. Generalized overlap is also symmetric in its arguments, which is not so obvious and requires a bit of effort to show [68]. The property making generalized overlap the most suitable tool, among many different possible measures, for studying information deposited in environment is its scaling with tensor product. Namely $B(\rho_A\otimes\rho_B,\sigma_A\otimes\sigma_B) = B(\rho_A,\sigma_A)B(\rho_B,\sigma_B)$. This is a very important property, as usually the interaction between system and an individual of the environment is weak in the sense that the individual environmental subsystem is not affected by the interaction in a significant way and the states $\rho_j^{E_k},\ \rho_{j'}^{E_k}$ remain almost indistinguishable. In such a case, the only possibility to construct the state with perfect correlations between the central system and the environment, leading to the formation of Spectrum Broadcast Structure, is to coarse-grain the environmental degrees of freedom. In other words, one can form groups consisting of environmental subsystems, which are called macrofractions $\rho_j^{mac} = \bigotimes_{k\in mac}\rho_j^{E_k}$. Such an approach was firstly applied in [65]. When the initial state of the environment is uncorrelated (2.31) and the evolution operator consists of tensor product of individual unitary operators with respect to subsystems (2.30), then the generalized overlap of a macrofraction amounts to taking product over individual subsystems constituting it

$$B^{mac}_{j,j'}(t) = B\Big(\rho_j^{mac}(t),\rho_{j'}^{mac}(t)\Big) = \prod_{k\in mac} B\Big(\rho_j^{E_k}(t),\rho_{j'}^{E_k}(t)\Big). \tag{2.55}$$

A few additional remarks are in order. Firstly, there is a connection between the generalized overlap and the scalar product. For pure states $B(|\psi\rangle\langle\psi|,|\varphi\rangle\langle\varphi|) = |\langle\psi|\varphi\rangle|$. As a result if one considers a scenario in which the environment is in a pure state then there is no distinction between the modulus of decoherence factor and generalized overlap as for a single subsystem

system k since from (2.51) follows

$$\left|\Gamma^k_{j,j'}(t)\right| = \left|Tr\left(\hat{U}_k(x_j,t)\rho_{0k}\hat{U}^\dagger_k(x_{j'},t)\right)\right| = \left|Tr\left(\hat{U}_k(x_j,t)|\phi_0\rangle\langle\phi_0|_k\hat{U}^\dagger_k(x_{j'},t)\right)\right| = \tag{2.56}$$
$$\left|\langle\phi_0|\hat{U}^\dagger_k(x_{j'},t)(\hat{U}_k(x_j,t)|\phi_0\rangle\right| = \left|\langle\phi_{j'}|\phi_j\rangle\right| = B^k(|\phi_j\rangle\langle\phi_j|,|\phi_{j'}\rangle\langle\phi_{j'}|).$$

Therefore in the considered scenario there is a single quantity governing the process of Spectrum Broadcast Structure formation: the modulus of overlap of post-interaction environmental states. The decoherence factor and the generalized overlap have the same origin, the only difference between them is based on the splitting of the environment into observed and non-observed part. To calculate decoherence factor one simply performs product over individual overlaps for non-observed parts of the environment, to check the distiguishability the product is taken over subsystems forming macrofraction.

If the environment is initially in a mixed state one can in principle purify state of each subsystem ρ_{0k} by introducing artificial subsystem k' and state $|\phi_0\rangle_{kk'}$ such that $\rho_{0k} = Tr_{k'}\left(|\phi_0\rangle\langle\phi_0|_{kk'}\right)$. In such the case the dynamics is trivially extended to take into account additional subsystems $\hat{U}_{S:EE'}(t) = \hat{U}_{S:E}(t)\otimes\bigotimes_{k'}^N I_k$. This procedure is perfectly valid to calculate the decoherence factor as (assuming that the evolution $\hat{U}_{S:E}(t)$ is of the controlled type)

$$\left|\Gamma^k_{j,j'}(t)\right| = \left|Tr\left(\hat{U}_k(x_j,t)\rho_{0k}\hat{U}^\dagger_k(x_{j'},t)\right)\right| = \tag{2.57}$$
$$\left|Tr_{kk'}\left(\hat{U}_k(x_j,t)\otimes I_{k'}|\phi_0\rangle\langle\phi_0|_{kk'}\hat{U}^\dagger_k(x_{j'},t)\otimes I_{k'}\right)\right| = \left|\langle\phi_0|\hat{U}^\dagger_k(x_{j'},t)\hat{U}_k(x_j,t)\otimes I_{k'}|\phi_0\rangle_{kk'}\right|.$$

As a result, whenever in a mixed state case we find that the decoherence factor equals zero, it is possible to introduce a larger Hilbert in which the initial state evolves into two orthogonal ones. Putting aside the problem of interpretation (should one consider the introduced system as a real one?), the purification procedure does not allow to put decoherence factor and generalized overlap on the equal footing - even then they are two separated quantities having different origin. The distinguishability of the environment depends only on the information content of the evolving observed environmental subsystems. Even if they are subsystems of global pure states, which are physically meaningful, the observers do not have access to these global states so they can not use them to extract information. To illustrate this point let us consider a simple example, in which a central 2 dimensional system interacts with the 2 dimensional environment via controlled unitary

$$\hat{U}_{S:E}(t) = |0\rangle\langle 0|\otimes\bigotimes_k^N I_k + |1\rangle\langle 1|\otimes\bigotimes_k^N \sigma_1^k. \tag{2.58}$$

The environment is initially in a maximally mixed state $\rho_{0k} = \frac{1}{2}I_k$ and the system in an arbitrary state $\rho_{0S} = |\Psi\rangle\langle\Psi|,\ |\Psi\rangle = \sqrt{p}|0\rangle + \sqrt{1-p}|1\rangle$. Its straightforward to verify that the

decoherence factor $\left|\Gamma_{01}^k\right| = \left|Tr(\sigma_1^k)\right| = 0$ and that both post-interaction states are equal ρ_{0k} so $B(\rho_{0k}, \sigma_1^k \rho_{0k} \sigma_1^k) = 1$. We can also investigate this example by firstly purifying the state of the environment $|\phi_0\rangle_{kk'} = \frac{1}{\sqrt{2}}\left(|00\rangle_{kk'} + |11\rangle_{kk'}\right)$. Now the post interaction states are

$$\begin{aligned} |\phi\rangle_{kk'} &= |\phi_0\rangle_{kk'} = \frac{1}{\sqrt{2}}\left(|00\rangle_{kk'} + |11\rangle_{kk'}\right), \\ |\phi'\rangle_{kk'} &= \sigma_1^k \otimes I_{k'} |\phi_0\rangle_{kk'} = \frac{1}{\sqrt{2}}\left(|10\rangle_{kk'} + |01\rangle_{kk'}\right). \end{aligned} \tag{2.59}$$

Obviously they are orthogonal, what is reflected in the fact that the decoherence factor is $\left|\Gamma_{01}^k\right| = 0$. However, at the local level of subsystems the reduced states are still maximally mixed so they are indistinguishable as we found previously.

It is possible to express the generalized overlap for mixed states as an overlap of purifications. However, the above discussed problems needs to be taken into account so not all purifications will give rise to the correct definition. It can be shown that expression for generalized overlap can be written as $B(\rho_A, \sigma_A) = \max_{|\psi\rangle_{AB}} |\langle\psi|\varphi\rangle_{AB}|$, where states $|\psi\rangle_{AB}, |\varphi\rangle_{AB}$ are purifications of ρ_A, σ_A. The additional step in calculating generalized overlap via purifications is the maximization over all possible purification of state $|\psi\rangle_{AB}$. In the example that we considered the maximization procedure would result in two identical indistinguishable post-interaction states $|\phi\rangle_{kk'}$.

Summing up the discussion: the decoherence factor and generalized overlap are in general different quantities having different origin. The only case, in which they can be put on the equal footing happens when the environment is initially in some pure state. Otherwise, even after purification procedure is performed, both quantities must be calculated in two different ways.

Moreover, the generalized overlap is related to another important measure of distinguishability, this is the trace norm

$$T(\rho, \sigma) = \frac{1}{2}\left\|\rho - \sigma\right\|_1 = \frac{1}{2} Tr\left[\sqrt{(\rho - \sigma)(\rho - \sigma)^\dagger}\right], \tag{2.60}$$

via inequalities that were proven in [69]

$$1 - B(\rho, \sigma) \leq T(\rho, \sigma) \leq \sqrt{1 - B^2(\rho, \sigma)}. \tag{2.61}$$

The method of verifying the formation of spectrum broadcast structures can be summarized in the following points

1. Find the evolution of a particular model describing system and environment.

2. Trace out the unobserved fragment of the environment.

3. Determine if the coherences in the partially reduced state vanish by calculating decoherence factor $\Gamma_{j,j'}(t)$ and checking if with time $\left|\Gamma_{j,j'}(t)\right| = 0$.

4. Investigate the information content of remaining fragments of environment by calculating $B^{mac}_{j,j'}(t)$ and checking if with time for some grouping of environmental subsystems $B^{mac}_{j,j'}(t) = 0$.

It is in an interesting open problem if the formation of spectrum broadcast structure can be verified in an alternative feasible way. In Chapter 4 we will begin to apply the direct procedure in order to investigate the formation of Spectrum Broadcast Structures in Quantum Brownian Motion model.

Chapter 3

Quantum Correlations beyond entanglement and Remote State Preparation protocol

3.1 Introduction

In this chapter we study in detail the role of quantum correlations in Remote State Preparation protocol. As has been mentioned in the previous Chapter, it has usually been assumed that the most powerful quantum resource is entanglement. From this point of view other types of quantum correlations can also be useful for various communicational and computational tasks. However, a strict hierarchy should hold: separable states should not outperform entangled ones.

Therefor, the claims of the recent paper [17], in which the surprising possibility of the fact that in some cases the communication power of quantum correlations beyond entanglement represented by separable states may exceed that of some entangled ones in Remote State Preparation protocol was announced, attracted a grate interest. The authors of the paper have also provided the direct connection of the transfer fidelity of the protocol they have chosen to measure of quantum correlations of the resource state – geometrical discord, which was introduced in Definition 2.5. Details of the protocol presented in [17] are discussed in Subsection 3.2.1. The result seems to be a breakthrough not only from fundamental but also from practical perspective as Remote State Preparation protocol is one of the significant building blocks in quantum communication. Due to the fact that a potential impact of the results on our understanding of the power and usefulness of different non-classical resources is so significant, the paper is worth analyzing. However, after the analysis is made it turns out the results are disputable. One can rise several doubts about the author's approach.

First of all, a non-standard quadratic fidelity is chosen as a figure of merit for the protocol. An introduction of a new tool cannot be regarded as an objection, however the careful analysis

presented in Section 3.3 shows clearly that the quadratic fidelity is not a correct tool and leads to wrong statements.

Moreover, whenever one intends to make a statement about some protocol, considered settings should correspond to the generality of the statement. From the results of [17] it can be concluded that the result of the paper is generic for Remote State Preparation protocol. Putting the objection made in the previous paragraph aside, the version of the protocol considered by the authors of [17] is restricted in the sense that only projective measurements on Alice's side – instead of the most general POVM measurements allowed by quantum formalism and only unitary operations on Bob's side – instead of general quantum channels are considered. In fact, the latter issue has been noticed already in [70], where it has been suggested that the conclusions of [17] may not hold in general.

For the above mentioned reasons, we readdress the problem of quantum correlations in Remote State Preparation. Our basic aim is to find an answer to the question: can communication power of separable correlations exceed that of entanglement resource? We start by introducing the most general Remote State Preparation in Section 3.2 as we would like our findings not to depend on particular settings of the protocol. We impose only one restriction on the amount of classical communication between parties taking part in the protocol, to prevent the direct transmission of a state to be prepared. Subsequently, in Subsection 3.2.1 we discuss settings of the paper [17]. Then we address the problem of fidelity of the protocol and show that the quadratic one is not the correct figure of merit. This is the content of Section 3.3. Having settled the problem of fidelity, in Section 3.4 we provide a negative answer to the question about supremacy of separable over entangled states in Remote State preparation protocol. This could in principle end investigations in this Chapter. However, although the results of paper [17] are questionable, they point out a possibility that in some restricted cases the striking conclusion regarding relation of separable and entangled states may hold. To explore this possibility in Section 3.5 we perform optimization of the correct linear fidelity with the respect to Alice's operations. Subsequently, we study two case of restrictions that may be imposed on Bob's decoding operations in a natural way. We show that in these cases it is indeed possible that the quantum separable correlations can be better than entangled states. Finally, we conclude in Section 3.6. This Chapter is partially based on results form [71].

3.2 The most general Remote State Preparation protocol with one bit of forward communication

We begin our discussion by introducing the most general Remote State Preparation protocol and describing shortly the settings considered in [17].

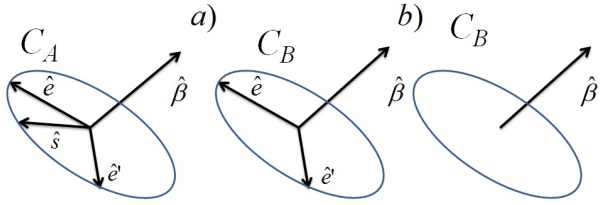

FIGURE 3.1: Initial data for Alice and Bob with a) or without b) shared reference frame on the $\hat{s}$ plane. The figure is reproduced from [71].

Before the beginning of the protocol Alice and Bob are given some classical data. The usual setting is that Alice is given description of the state that she aims at preparing, and Bob knows some characteristic of this state for example that its Bloch vector belongs to a particular plane. For our purpose, the description of the state is given in terms of a unit Bloch vector $\hat{s}$. Moreover, Alice and Bob know a vector $\hat{\beta}$ to which $\hat{s}$ is perpendicular. This determines the plane to which $\hat{s}$ belongs. Although it is not explicitly stated, usually they share also a common reference frame in that plane. However, this does not need to be the case. The possible structure of initial data is presented in Figure 3.1. To prevent direct classical transmission of $\hat{s}$, one should put the restriction on the classical channel. The natural choice, compatible with the original scheme of Remote State Preparation protocol, is to allow for one bit of classical communication from sender to the receiver.

Furthermore, Alice and Bob share a bipartite qubit state ρ_{AB}. It can be parametrized in terms of i) Bloch vectors of reduced states ρ_A, ρ_B , ii) correlation tensor T as

$$\rho = \rho(\vec{x}, \vec{y}; T) = \frac{1}{4}[I \otimes I + \vec{x}\vec{\sigma} \otimes I + I \otimes \vec{y}\vec{\sigma} + \sum_{ij} T_{ij}[\sigma_i \otimes \sigma_j]. \tag{3.1}$$

We note, that one can always choose a local reference frame on Alice's and Bob's sides such that the correlation tensor becomes a diagonal matrix in the Schmidt canonical form $T = \text{diag}[t_1, t_2, t_3]$, where t_i^2 are the eigenvalues of $T^T T$ [72].

In the present analysis Alice is allowed to perform any generalized quantum measurement – POVM, while Bob is authorized to apply any general quantum operation represented by quantum channel. The most general form of Alice binary POVM must be a function of the following family of parameters $\mathcal{A} = \{\vec{a}, a_+, a_-\}$ and is defined by the formula $M_\pm = a_\pm I \pm \vec{a}\vec{\sigma}$ with the probability-like parameters $a_\pm$ and vector $\vec{a}$ satisfying the conditions

$$a_+ + a_- = 1,\ 0 \leq a_\pm \leq 1, ||\vec{a}|| \leq min[a_+, a_-] \leq \frac{1}{2}, \tag{3.2}$$

where in general both $a_\pm$ and $\vec{a}$ are functions of the unit vector $\hat{s}$ perpendicular to $\hat{\beta}$ which has a fixed orientation during the protocol. Finally the payoff function of the protocol is minimized over $\hat{\beta}$.

The resulting probabilities of the Alice outcomes on the state (3.1) and the resulting states $\rho_\pm$ on Bob side are defined by the relations

$$\begin{aligned} p_\pm &\equiv Tr_{AB}[M_\pm \otimes I\rho] = (a_\pm \pm \vec{a}\vec{x}), \\ p_\pm\rho_\pm &\equiv Tr_A[M_\pm \otimes I\rho] = \frac{1}{2}[(a_\pm \pm \vec{a}\vec{x})I + (\pm T\vec{a} + a_\pm\vec{y})\vec{\sigma}]. \end{aligned} \tag{3.3}$$

Bob is allowed to perform channels $\Lambda_\pm$ which depend upon the result $\pm$ of the Alice measurement and act on any qubit state $\rho(\vec{u}) = \frac{1}{2}(I + \vec{u}\vec{\sigma})$ as

$$\Lambda_\pm[\rho(\vec{u})] = \frac{1}{2}[I + (T_\pm\vec{u} + \vec{v}_\pm)\vec{\sigma}]. \tag{3.4}$$

The range of parameters $\mathcal{T}$ is determined by the structure of the extremal one-qubit channels

$$T_\pm = \mathcal{O}_\pm^{(1)} T_\pm^0 (\mathcal{O}_\pm^{(2)})^T, \vec{v}_\pm = \mathcal{O}_\pm^{(1)}\vec{v}_\pm^0, \tag{3.5}$$

where $\mathcal{O}_\pm^{(1)}, \mathcal{O}_\pm^{(2)}$ are arbitrary rotations combined with representation of completely positive trace preserving maps. Here we use a family given by

$$\begin{aligned} \vec{v}_\pm^0 &= [0, 0, \sin u_\pm \sin w_\pm], \\ T_+^0 &= [\cos u_+, \cos w_+, \cos u_+ \cos w_+] \\ T_-^0 &= [cosu_-, \cos w_-, \cos u_- \cos w_-], \end{aligned} \tag{3.6}$$

with $u_\pm \in [0, 2\pi)$, $w_\pm \in [0, \pi)$ [73]. This is the most general form of any one-qubit channel belonging to the closure of the set of extreme one-qubit channels and the simple convexity argument allows one to restrict considerations only them. After the action of $\Lambda_\pm$ the final Bob state is

$$\tilde{\rho}_B = \sum_{r=\pm} p_r \Lambda_r(\rho_B^{(r)}) = \frac{1}{2}(I + \vec{r}\vec{\sigma}), \tag{3.7}$$

with the final Bob Bloch vector

$$\vec{r} = \sum_{r=\pm}[T_r(a_r\vec{y} + rT\vec{a}) + (a_r + r\vec{a}\vec{x})\vec{v}_r]. \tag{3.8}$$

The transmission fidelity is averaged over the unit circle constituted by all vectors on the plane perpendicular to $\hat{\beta}$. The above local operations and classical communication (LOCC) scheme with (i) known local Bloch coordinates and (ii) 1 bit of forward (form Alice to Bob) communication allowed is an example of one-way LOCC with one classical bit of information introduced in Section 2.3 and accordingly to the notation used there we will refer to it as $LOCC^{\rightarrow,1}$. The general structure of the protocol is schematically depicted in Figure 3.2.

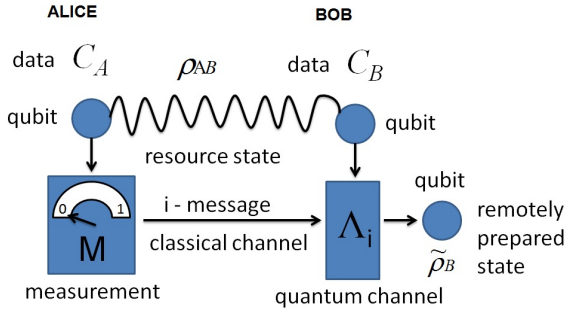

FIGURE 3.2: General scheme of RSP. For structure of initial data see Figure 3.1. The measurement M is a quantum POVM and Λ_i is the decoding channel. The decoding channels Λ_i are supposed to belong to a fixed class Γ. In this thesis we consider the most general class of all quantum channels $\Gamma_{general}$ – in Section 3.4 and restricted classes: channels invariant in the $\hat{s}$ plane $\Gamma_{invariant}$ and the bistochastic channels $\Gamma_{bistochastic}$ that are considered in Subsections 3.5.1, 3.5.2 respectively. The figure is reproduced from [71].

3.2.1 Overview of the recently proposed protocol

In [17] the authors consider the specific subclass of the protocols from Figure 3.2. In their work only projective (von Neumann) measurement M on Alice's side were considered. Moreover, only very specific unitary decodings $\Lambda_+ = I$, $\Lambda_- = -I$, which correspond to identity or reflection on the considered circle on the Bloch sphere, were allowed. Concerning the classical data, Alice knows the state to be prepared in terms of it's Bloch vector $\hat{s}$ and the direction $\hat{B}$ to which $\hat{s}$ is perpendicular and Bob also knows $\hat{B}$. Moreover, as there is no information about shared a reference frame, we assume that Bob does not posses knowledge about a reference frame of Alice. To evaluate the efficiency of the protocol the authors introduced the following pay-off function

$$\mathcal{P} = \int d\hat{s} (\hat{s}\vec{r})^2, \tag{3.9}$$

to which we refer as to quadratic fidelity. We note that (3.9) is a non-linear function of a fidelity between the desired state $\rho_{\hat{s}}$ to be prepared and the state that is obtained in the protocol $\tilde{\rho}_B$

$$F(\rho_{\hat{s}}, \tilde{\rho}_B) = \sqrt{\sqrt{\rho_{\hat{s}}}\tilde{\rho}_B\sqrt{\rho_{\hat{s}}}}, \tag{3.10}$$

which for qubits can be expressed in terms of corresponding Bloch vectors $\hat{s}$, $\vec{r}$ as

$$F(\rho_{\hat{s}}, \tilde{\rho}_B) = \frac{1}{2}\left(1 + \hat{s}\cdot\vec{r}\right). \tag{3.11}$$

Thus the relation between (3.9) and (3.11) is

$$\mathcal{P} = (2F(\rho_{\hat{s}}, \tilde{\rho}_B) - 1)^2 \tag{3.12}$$

Coming back to the protocol's description, for given shared state ρ_{AB} the fidelity (3.9) is first maximized over all von Neumann measurements on Alice's side. Bob's encoding operations are fixed and therefore there is no maximization process associated to them. Finally the fidelity is minimized with respect to the orientation of the vector $\hat{\beta}$ which gives for an initial state ρ_{AB} the optimal quadratic fidelity $\mathcal{P}_{opt}$. The result obtained in [17] is

$$\mathcal{P}_{opt} = \frac{1}{2}\left(t_2^2 + t_3^2\right), \tag{3.13}$$

where t_2^2, t_3^2 are the two lowest eigenvalues of $T^T T$. The expression for $\mathcal{P}_{opt}$ coincides with the value of geometric discord, which for states with maximally mixed marginals $\vec{x} = \vec{y} = 0$ or with isotropic correlation tensor $T = -\lambda I$ (where I is the 3x3 identity matrix) is

$$D(\rho) = \frac{1}{2}\left(t_2^2 + t_3^2\right). \tag{3.14}$$

Subsequently, the authors consider non-zero discord but non-entangled Werner state

$$\rho_{AB} = \rho(0, 0, -\lambda' I), \tag{3.15}$$

which is parametrized as in the formula (3.1), with $\lambda' = \frac{1}{3}$ for which $\mathcal{P}_{opt} = \frac{1}{9}$ is strictly larger than its value $\mathcal{P}_{opt} = \frac{1}{25}$ obtained for the following entangled state

$$\rho_{AB} = \rho(t\hat{z}, t\hat{z}, -\lambda I) \tag{3.16}$$

with $t = \frac{1}{5}$ and $\lambda' = \frac{2}{5}$. On that basis the conclusion of the paper [17] is made that quantum correlations beyond entanglement represented by non-zero discord of the separable state above make quantum correlations beyond entanglement better then entanglement itself in Remote State Preparation protocol. However, in the next Section we show that pay-off function (3.9) is in fact an incorrect tool for studying usefulnesses of different types of quantum correlations in the considered protocol.

3.3 Fidelity

3.3.1 Quadratic fidelity

The main problem with the quadratic fidelity is that this measure does not distinguish orthogonal states. This statement can be easily understood considering the original Remote State Protocol, in which, after the measurement of Alice, Bob is in possession of either the desired state or the state orthogonal to it. In the former case $F(|\varphi\rangle, |\varphi\rangle) = 1$, in the latter $F(|\varphi\rangle, |\varphi_\perp\rangle) = 0$ as for pure states fidelity reduces just to the module of the scalar product. However, there is no

difference in these two cases if one calculates the value of quadratic fidelity $\mathcal{P}_{|\varphi\rangle} = \mathcal{P}_{|\varphi_\perp\rangle}$

$$\begin{aligned} \mathcal{P}_{|\varphi\rangle} &= (2F(|\varphi\rangle, |\varphi\rangle) - 1)^2 = 1 \\ \mathcal{P}_{|\varphi_\perp\rangle} &= (2F(|\varphi\rangle, |\varphi_\perp\rangle) - 1)^2 = 1. \end{aligned} \tag{3.17}$$

This fact lead to a striking consequence. Namely, it turns out that there exist a *trivial* protocol which supersedes the one considered in [17]. Given any of the two-qubit states above Bob may ignore the Alice message and just take randomly chosen state $\tilde{\rho}_B$ with its Bloch vector randomly located on the circle perpendicular to $\hat{\beta}$ and get the fidelity $\frac{1}{2}$ which is much better than $\frac{1}{25}$ and $\frac{1}{9}$ discussed in the previous Section. Being more precise, let us consider a case of the protocol in which Bob, regardless of the Alice message, produces at random a pure state $|\varphi_R\rangle$ with a Bloch vector belonging to the $\hat{s}$ plane. Employing fidelity proposed in [17] we obtain

$$\mathcal{P}_{|\varphi_R\rangle} = \min_{\hat{\beta}} \left\langle (\hat{r}\hat{s})^2 \right\rangle = \left\langle (\hat{r}\hat{s})^2 \right\rangle = \int d\,\hat{s} (\hat{r}\hat{s})^2 = \frac{1}{2\pi} \int_0^{2\pi} d\,\varphi \cos^2\varphi = \frac{1}{2}, \tag{3.18}$$

where we used the invariance of the measure on the unit circle. Because this fidelity is higher than these considered in [17] ($\frac{1}{9}$ and $\frac{1}{25}$ for separable and entangled state respectively), it may seem that the random protocol is better choice than more sophisticated strategies. However, this is only because of misleading choice of the protocol's fidelity.

3.3.2 Linear fidelity

The analysis of the previous Subsection clearly shows that the only suitable choice for the pay-off function of the Remote State Preparation protocol is the linear fidelity (3.10). As we would like to arrive at a general conclusion, one should take into account different possible choices of initial state, expressed in terms of Bloch vectors $\hat{s}$. In such a case it is essential to average over $\hat{s}$, what lead to the final expression for fidelity

$$\bar{F} = \frac{1}{2}(1 + G), \tag{3.19}$$

where the fidelity parameter is

$$\begin{aligned} G = \quad & G(\rho; \hat{\beta}; \mathcal{A}, \mathcal{T}) = \int d\hat{s} (\vec{r}\hat{s}) = \\ & \int d\hat{s} [(T_+ - T_-) T\vec{a} + (\vec{v}_+ - \vec{v}_-)\vec{x}\vec{a} + a_+(T_+\vec{y} + \vec{v}_+) + a_-(T_-\vec{y} + \vec{v}_-)]\hat{s}. \end{aligned} \tag{3.20}$$

Here $\rho = \rho(\vec{x}, \vec{y}, T)$, $\hat{\beta}$ defines the plane to which the vector $\hat{s}$ belongs and the explicit dependence on the encoding $\mathcal{A} = \{\vec{a}, a_+, a_-\}$ and decoding strategy $\mathcal{T} = \{T_+, \vec{v}_+; T_-, \vec{v}_-\}$ is written.

The full range of parameters describing the encoding $\mathcal{A}$ is written explicitly in (3.2), whereas the decoding $\mathcal{T}$ in (3.6).

3.4 Optimal Remote State Preparation protocol for separable states

In this Subsection we derive the optimal Remote State Preparation protocol in the case when the shared state ρ_{AB} is separable. We still work under the assumption of $LOCC^{\rightarrow,1}$ in which Alice and Bob naturally share the reference frame on the Bloch sphere. We may choose the coordinates as $\left\{\hat{\beta}, \hat{e}, \hat{e}'\right\}$ where $\hat{\beta} \times \hat{e} = \hat{e}'$ and $\{\hat{e}, \hat{e}'\}$ represent the coordinates system in the $\hat{s}$ plane.

For separable states we can restrict our considerations to pure states since in this case fidelity is the convex function. For pure states one finds that $p_{\pm} = a_{\pm}(\hat{s}) + \vec{a}(\hat{s})\hat{\xi}$, where $\hat{\xi}$ is Alice Bloch vector. The reduced state of Bob is $\rho_{\pm} = \frac{1}{2}\left(I + \vec{n}_{\pm}\hat{\sigma}\right)$, where $\vec{n}_{\pm}$ is Bob Bloch vector transformed by respective channel. Then (3.21) is of a form

$$G = \frac{1}{2}\int d\hat{s} p_{+}(\hat{s})\left(\vec{n}_{+}(\hat{s}) - \vec{n}_{-}(\hat{s})\right)\hat{s}. \tag{3.21}$$

The bracket $\left(\vec{n}_{+}(\hat{s}) - \vec{n}_{-}(\hat{s})\right)\hat{s}$ attains maximal value for $\vec{n}_{+} = \hat{e}, \vec{n}_{-} = -\hat{e}$ ($\vec{n}_{+} = -\hat{e}, \vec{n}_{-} = \hat{e}$) such that $\hat{e}\hat{s} > 0$ ($\hat{e}\hat{s} < 0$), where $\hat{e}$ is an a priori known unit vector of the shared coordinates frame. Then setting $p_{+}(\hat{s}) = 1$ is optimal. In this case Alice POVM reduces to identity and Bob prepares vector $\pm\hat{e}$ depending on the sign of $\hat{e}\hat{s}$. Note that this protocol is independent of an input state and its fidelity is

$$\bar{F} = \frac{1}{2}\left(1 + \frac{2}{\pi}\int_{0}^{\frac{\pi}{2}} d\theta \cos\theta\right) = \frac{1}{2}\left(1 + \frac{2}{\pi}\right). \tag{3.22}$$

As a result, separable states cannot lead to better fidelity than entangled ones ($\bar{F}(\rho_{ent}) \geq \bar{F}(\rho_{sep})$). In the case, when for an entangled state there is no better strategy, one can always use the presented protocol that is in fact independent of the shared state.

This result shows that in general quantum correlations beyond entanglement manifested by non-zero quantum discord cannot be regarded as a better resource than entangled ones for Remote State Preparation protocol.

However, there is still an interesting open question, namely if there are scenarios with additional restrictions, in which separable states can have advantage over entangled states? In order to find an answer, we need to perform optimization of the general protocol over Alice POVMs

3.5 Optimization of the protocol

In this section we optimize the quantity

$$G = \int d\hat{s}[(T_+ - T_-)T\vec{a} + (\vec{v}_+ - \vec{v}_-)\vec{x}\vec{a} + a_+(T_+\vec{y} + \vec{v}_+) + a_-(T_-\vec{y} + \vec{v}_-)]\hat{s} \quad (3.23)$$

with respect to $\mathcal{A}$ (for the sake of clarity we omit all the arguments in its notation). We start by defining the matrix $M = (T_+ - T_-)T + (|\vec{v}_+\rangle - |\vec{v}_-\rangle)\langle\vec{x}|$, and $\vec{V}_+ = (T_+\vec{y} + \vec{v}_+)$, $\vec{V}_- = (T_-\vec{y} + \vec{v}_-)$. Then the above function is of the form

$$G = \int d\hat{s}[M\vec{a} + a_+\vec{V}_+ + a_-\vec{V}_-]\hat{s}, \quad (3.24)$$

where the vector $\vec{a}$ and the scalars $a_\pm$ depend in general on $\hat{s}$ and satisfy the conditions (3.2). Let us put $\vec{a} = a\hat{a}$, where $0 \leq a = ||\vec{a}|| \leq a_\pm$. Clearly the best choice to maximise the value of G is to put $\hat{a}$ parallel to the vector $M^T\hat{s}$ or, in other words, $\hat{a} = \frac{M^T\hat{s}}{||M^T\hat{s}||}$. Then the value of the integral becomes $G = \int d\hat{s}a[||M^T\hat{s}|| + a_+\vec{V}_+ + a_-\vec{V}_-]\hat{s}$, which may be further optimised with respect to a by taking its maximal allowed value $a = min[a_+, a_-]$.

Eventually, this gives the function optimised over $\vec{a}$ for fixed $a_\pm$ and all the other parameters:

$$G = \int d\hat{s}||[M^T\hat{s}||min[a_+, a_-] + a_+\vec{V}_+ + a_-\vec{V}_-]\hat{s}. \quad (3.25)$$

Using notation $M' = ||[M^T\hat{s}|| \geq 0$, $A_\pm = \vec{V}_\pm\hat{s}$, we may carefully consider the maximum of

$$f(p) = M'min[p, 1-p] + pA_+ + (1-p)A_- \quad (3.26)$$

over the interval $p \in [0, 1]$, where we put $p = a_+$ and $1 - p = a_-$ for conciseness. The above function has the following maxima:

(a) if $M' \geq |A_+ - A_-|$, then $max_{p\in[0,1]}f(p) = \frac{M+A_++A_-}{2}$ achieved at $p = \frac{1}{2}$;

(b) if $M' < |A_+ - A_-|$, then either (i) $max_{p\in[0,1]}f(p) = A_+$ for $A_+ - A_- > 0$ (achieved at $p = 1$) or (ii) $max_{p\in[0,1]}f(p) = A_-$ for $A_- - A_+ > 0$ (achieved at $p = 1$).

In case (a) the strategy of Alice is naturally the one of Ref. [17]; she performs the von Neumann measurement with the projections $P_{\pm\hat{a}} = \frac{1}{2}(I \pm \hat{a}\vec{\sigma})$. An intriguing strategy of Alice in case (b) is that she just does *nothing* (since then the POVM is the identity) and puts the message r to Bob depending on the sign of $(A_+ - A_-) = (\vec{V}_+ - \vec{V}_-)\hat{s}$. Quite remarkably this strategy gives *always nonnegative* contribution form the part of the integral (3.25) involving the vectors $\vec{V}_\pm$.

We have then the three sets Ω_0, $\Omega_\pm$ in the unit circle on the $\hat{s}$ plane, which are also presented in the Figure 3.3, defined as

$$\begin{aligned}\Omega_0 &= \{\hat{s} : \hat{s}\hat{\beta} = 0, ||M^T\hat{s}|| \geq (\vec{V}_+ - \vec{V}_-)\hat{s}\};\\ \Omega_+ &= \{\hat{s} : \hat{s}\hat{\beta} = 0, ||M^T\hat{s}|| < (\vec{V}_+ - \vec{V}_-)\hat{s}\};\\ \Omega_- &= \{\hat{s} : \hat{s}\hat{\beta} = 0, ||M^T\hat{s}|| < (\vec{V}_- - \vec{V}_+)\hat{s}\}.\end{aligned} \tag{3.27}$$

The formula optimized over $\mathcal{A}$ is of the form

$$max_{\mathcal{A}} G(\rho(\vec{0},\vec{0},T);\hat{\beta};\mathcal{A},\mathcal{T}) = \int_{\Omega_0} d\hat{s}\frac{||M^T\hat{s}|| + \vec{V}_+\hat{s} + \vec{V}_-\hat{s}}{2} + \int_{\Omega_+} d\hat{s}\vec{V}_+\hat{s} + \int_{\Omega_-} d\hat{s}\vec{V}_-\hat{s}. \tag{3.28}$$

We can further simplify the above formula by noting that the set Ω_0 is symmetrical: $\Omega_0 = -\Omega_0$, and that after the reflection the sets are equal $\Omega_+ = -\Omega_-$. From the former we get that

$$\int_{\Omega_0} d\hat{s}\frac{||M^T\hat{s}|| + \vec{V}_+\hat{s} + \vec{V}_-\hat{s}}{2} = \int_{\Omega_0} d\hat{s}\frac{||M^T\hat{s}||}{2}, \tag{3.29}$$

and from the latter

$$\int_{\Omega_+} d\hat{s}\vec{V}_+\hat{s} + \int_{\Omega_-} d\hat{s}\vec{V}_-\hat{s} = \int_{\Omega_+} d\hat{s}(\vec{V}_+ - \vec{V}_-)\hat{s}. \tag{3.30}$$

Introducing definitions $\Omega_0^+ = -\Omega_0^-$ (relations between different sets are presented in Figure 3.3) as any of two subsets of original Ω_0 such that $\Omega_0 = \Omega_0^+ \cup \Omega_0^-$ we arrive at the final formula

$$max_{\mathcal{A}} G(\rho;\hat{\beta};\mathcal{A},\mathcal{T}) = \int_{\Omega_0^+} d\hat{s}||M^T\hat{s}|| + \int_{\Omega_+} d\hat{s}(\vec{V}_+ - \vec{V}_-)\hat{s}. \tag{3.31}$$

where $\mathcal{A}^*$ denotes optimal Alice measurement (either von Neumann or trivial one).

3.5.1 Optimization in the case of $\Gamma_{invariant}$

In this Section we will investigate a case of the protocol, in which Bob's decoding strategy does not depend on a Alice's reference frame in the plane perpendicular to $\hat{\beta}$.

There are several possible reasons justifying this assumption. Alice and Bob may not be able to establish a common reference frame. Another is that Alice, after establishing decoding strategy with Bob, can change type of input state by choosing different angle φ or her coordinates system in the plane orthogonal to $\hat{\beta}$ and Bob's decoding should remain optimal. As a consequence, Bob's strategy cannot depend on the parametrization of the input Bloch vector.

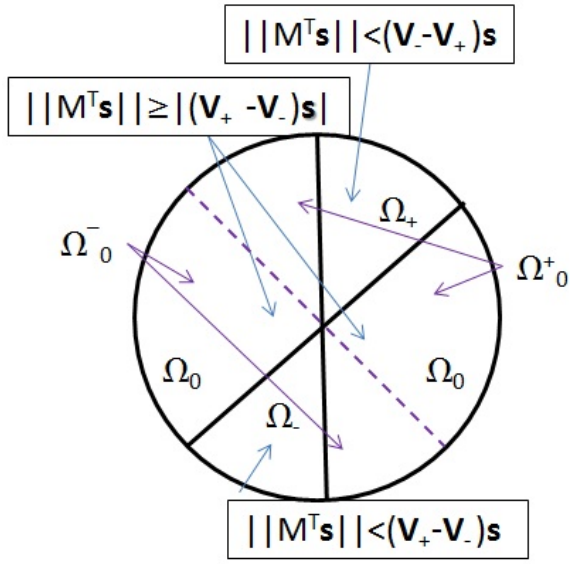

FIGURE 3.3: The sets Ω_0, $\Omega_\pm$ on the $\hat{s}$ plane, defined in equation (3.27). Additionally the subsets Ω_0^+, Ω_0^- forming the set Ω_0 ($\Omega_0 = \Omega_0^+ \cup \Omega_0^-$) are depicted.

Technically, in this case decoding operations should be restricted to the class, which is invariant under averaging in the plane orthogonal to $\hat{\beta}$ or always look the same after any rotation in that plane. We will denote this class as $\Gamma_{invariant}$. For operations belonging to $\Gamma_{invariant}$ we have that

$$\mathcal{T}\left(\{T_\pm\},\{v_\pm\}\right) = \tilde{\mathcal{T}}\left(\left\{\tilde{T}_\pm\right\},\{\tilde{v}_\pm\}\right) \tag{3.32}$$
$$\tilde{T}_\pm = \frac{1}{2\pi}\int_0^{2\pi} d\varphi O_{\hat{s}}(\varphi) T_\pm O_{\hat{s}}^T(\varphi), \tilde{\vec{v}}_\pm = \frac{1}{2\pi}\int_0^{2\pi} d\varphi O_{\hat{s}}(\varphi)\vec{v}_\pm,$$

where $O_{\hat{s}}(\varphi)$ denotes rotation in the $\hat{s}$ plane. As a result of averaging $\tilde{T}_\pm = \mathrm{diag}[t_\pm, \tilde{T}_\pm^{(1)}]$, where $|t_\pm| \leq 1$, $\left\|\tilde{T}_\pm^{(1)}\right\| \leq 1$ and $\tilde{T}_\pm^{(1)}$ are 2x2 matrices acting in the $\hat{s}$ plane that are invariant under any rotation $\tilde{T}_\pm^{(1)} = O\tilde{T}_\pm^{(1)}O^T$. The use of this class is natural also from game-like perspective: let us allow Bob to use arbitrary channel $\mathcal{T}$. Since he does not know the coordinates he must average his decoding strategy over all possible orientations of reference frame on the $\hat{s}$ plane. This results a in decoding from $\Gamma_{invariant}$. As a consequence we get that $\tilde{\vec{v}}_\pm$ have no components parallel to $\hat{s}$:

$$\vec{r}\hat{s} = \sum_{r=\pm}[\tilde{T}_r^{(1)}(a_r\vec{y} + rT\vec{a})]\hat{s}. \tag{3.33}$$

By setting $M = (\tilde{T}_+^{(1)} - \tilde{T}_-^{(1)})T$ and $\vec{V}_\pm = \tilde{T}_\pm^{(1)}\vec{y}$ and inserting it into (3.31), we obtain optimized formula for $max_{\mathcal{A}}G(\rho(\vec{x},\vec{y},T);\hat{\beta};\mathcal{A},\tilde{\mathcal{T}})$. In the case of an isotropic correlations $T = -\lambda I$ there

are two facts that allow to obtain the final result. We start by presenting and proving Fact 1 and subsequently we do the same with Fact 2.

Fact 1

We can always decompose $\vec{y}$ as $\vec{y} = \|\hat{y}\| \left[\alpha\hat{u} + (1-\alpha)\hat{\beta}\right]$. Then the formula $max_{\mathcal{A}} G(\rho(\vec{x}, \vec{y}, -\lambda I); \hat{\beta}; \mathcal{A}, \tilde{\mathcal{T}})$ is monotonic function of parameter $\alpha = |\vec{y}\hat{u}|$.

Proof of Fact 1

Let us consider $\alpha' > \alpha$, where $\alpha = |\vec{y}\hat{u}|$. Parameters α, α' correspond to two different orientations of $\vec{y}$ with respect to $\hat{s}$ plane, this is $\vec{y} = \|\hat{y}\| \left[\alpha\hat{u} + (1-\alpha)\hat{\beta}\right]$ and $\vec{y'} = \|\hat{y}\| \left[\alpha'\hat{u} + (1-\alpha')\hat{\beta}\right]$. For α' (α) we will denote solutions of inequalities defining the sets as $\Omega_0^{+'}$, $\Omega_+^{'}$, (Ω_0^{+}, Ω_+), similarly $||M^T\hat{s}|| = f'$ $(\vec{V'}_+ - \vec{V'}_-)\hat{s} = g'$ ($||M^T\hat{s}|| = f$ $(\vec{V}_+ - \vec{V}_-)\hat{s} = g$). Let us recall that here we consider only the restricted class of the invariant (equivalently averaged) decodings $\tilde{\mathcal{T}}$. It follows from the definition of the sets that $\Omega_0^{+'} < \Omega_0^{+}$ and $\Omega_+^{'} > \Omega_+$ as well as $f' = f = \lambda||(\tilde{T}_+^{(1)} - \tilde{T}_-^{(1)})^T\hat{s}||$. We can rewrite g' as $g' = (\tilde{T}_+^{(1)} - \tilde{T}_-^{(1)})\vec{y'}\hat{s} = \vec{y'}(\tilde{T}_+^{(1)} - \tilde{T}_-^{(1)})^T\hat{s} = \vec{y'}\vec{w}(\hat{s})$ and as a consequence the following relation holds $g' = \vec{y'}\vec{w}(\hat{s}) = \left\|\vec{y'}\right\| \alpha'\hat{u}\vec{w}(\hat{s}) = \|\vec{y}\| \alpha'\hat{u}\vec{w}(\hat{s}) > \|\vec{y}\| \alpha\hat{u}\vec{w}(\hat{s}) = g$. Thus we can write

$$\max_{\mathcal{A}} G(\rho; \hat{\beta}'; \mathcal{A}, \tilde{\mathcal{T}}) = \int_{\Omega_0^{+'}} d\hat{s} f' + \int_{\Omega_+^{'}} d\hat{s} g' = \tag{3.34}$$
$$\int_{\Omega_0^{+'}} d\hat{s} f + \int_{\Omega_+^{'} \setminus \Omega_+} d\hat{s} g' + \int_{\Omega_+} d\hat{s} g' \geq \int_{\Omega_0^{+'}} d\hat{s} f + \int_{\Omega_+^{'} \setminus \Omega_+} d\hat{s} f + \int_{\Omega_+} d\hat{s} g =$$
$$\int_{\Omega_0^{+}} d\hat{s} f + \int_{\Omega_+} d\hat{s} g = \max_{\mathcal{A}} G(\rho; \hat{\beta}; \mathcal{A}, \tilde{\mathcal{T}}).$$

As a result, for $\alpha' > \alpha$ it holds that $\max_{\mathcal{A}} G(\rho; \hat{\beta}'; \mathcal{A}, \tilde{\mathcal{T}}) \geq \max_{\mathcal{A}} G(\rho; \hat{\beta}; \mathcal{A}, \tilde{\mathcal{T}})$.

Fact 2

The optimization over $\Gamma_{invariant}$ class, which naturally corresponds to the situation with an unknown coordinates system, yields $min_{\hat{\beta}} max_{\mathcal{A}, \tilde{\mathcal{T}}} G(\rho(\vec{x}, \vec{y}, -\lambda I); \hat{\beta}; \mathcal{A}, \tilde{\mathcal{T}}) = \lambda$ and then consequently

$$\bar{F}_{invariant}(\rho(\vec{x}, \vec{y}, -\lambda I)) = \frac{1}{2}(1 + \lambda). \tag{3.35}$$

Proof of Fact 2 It follows from Fact 1 that $max_{\mathcal{A}} G(\rho(\vec{x}, \vec{y}, -\lambda I); \hat{\beta}; \mathcal{A}, \tilde{\mathcal{T}})$ is monotonic in α parameter, where $\alpha = |\vec{y}\hat{u}|$. Let us consider and prove a simple Lemma.

Lemma Let $f(a, x)$ be a function with $a \in [a_0, a_1]$ and $x \in \Omega \subset R^n$ where Ω is compact. Suppose that (i) for any $a \leq a'$ and for any x one has $f(a, x) \leq f(a', x)$; (ii) the $x(a)$ is some (may be not unique) point realising maximum of $f(a, x)$ over x for fixed a, i.e. $f(a, x(a)) = max_x f(a, x)$. Then the function $f(a, x(a))$ is monotonic in a. As a result

$min_{a\in[a_0,a_1]}max_{x\in\Omega}f(a,x) = max_{x\in\Omega}f(a_0,x)$.

Proof of Lemma

Consider any $a \leq a'$. Then we have $f(a,x(a)) \leq f(a',x(a)) \leq f(a',x(a'))$, where the first inequality follows from (i) and the second one from (ii).

Coming back to the proof of the Fact 2 we may put in place of $a \in [a_0,a_1]$ in the Lemma above the parameter $\alpha \in [0,1]$ and in place of x all the other parameters contained in the sets $\mathcal{A}, \tilde{\mathcal{T}}$ getting the desired monotonicity in Fact 2.

As a result of the Fact 2 we can set $\alpha = 0$ which implies $\hat{\beta}^* = \hat{y}$, $\Omega_0^+ = (0,\pi)$, $\Omega_+ = \emptyset$,what corresponds to von Neumann measurement of Alice

$$min_{\hat{\beta}}max_{\mathcal{A},\tilde{\mathcal{T}}}G(\rho(\vec{x},\vec{y},-\lambda I);\hat{\beta};\mathcal{A},\tilde{\mathcal{T}}) = min_{\hat{\beta}}max_{\tilde{\mathcal{T}}}G(\rho(\vec{x},\vec{y},-\lambda I);\hat{\beta};\mathcal{A}^*,\tilde{\mathcal{T}}) = \quad (3.36)$$
$$max_{\tilde{\mathcal{T}}}G(\rho(\vec{x},\vec{y},-\lambda I);\hat{\beta}^* = \hat{y};\mathcal{A}^*,\tilde{\mathcal{T}}) = max_{\tilde{T}_+^{(1)},\tilde{T}_-^{(1)}}\int_{\Omega_0^+} d\hat{s}\lambda||(\tilde{T}_+^{(1)} - \tilde{T}_-^{(1)})^T\hat{s}|| = \lambda.$$

To arrive at the above expression we exploited the fact that $\alpha = 0$, which implies $\vec{y}||\hat{\beta}$. Moreover the triangle inequality $||(\tilde{T}_+^{(1)} - \tilde{T}_-^{(1)})^T\hat{s}|| \leq ||(\tilde{T}_+^{(1)}\hat{s}|| + ||\tilde{T}_-^{(1)}\hat{s}|| \leq 2$ is saturated for $\tilde{T}_\pm^{(1)} = \pm I$ and $d\hat{s}$ represents the measure on the plane $d\hat{s} = \frac{d\varphi}{2\pi}$. Alice measurement is determined by $\hat{a} = \frac{M^T\hat{s}}{||M^T\hat{s}||}$. The choice of $\tilde{T}_\pm^{(1)} = \pm I$ implies that $M = 2\lambda I$ acts on the circle. This eventually determines the Alice von Neumann measurement $\hat{a} = \hat{s}$. The latter together with $\tilde{T}_\pm^{(1)} = \pm I$ shows that the protocol optimal under quadratic fidelity in [17] is also optimal in the case of $\Gamma_{invariant}$.

Now, following [17], consider the following class: $\rho(t\hat{z},t\hat{z},-\lambda I)$; or in other words the states with parameters: $T = -\lambda I$, $\vec{x} = \vec{y} = t\hat{z}$ where the positivity condition determines the following range of parameter t: $|t| \leq \frac{1-\lambda}{2}$. For any fixed non-zero λ there are entangled states in that class namely the ones satisfying in addition the inequality $|t| > \frac{1}{2}\sqrt{1-2\lambda-3\lambda^2}$. All of these entangled states $\rho(\vec{x},\vec{y},-\lambda I)$ with $\lambda < \frac{1}{3}$ will – due to Fact 2 – have worse fidelity in Remote State Preparation protocol (under the restriction of unknown coordinate system) than the separable states $\rho(\vec{0},\vec{0},-\lambda' I)$ with $\lambda' \in (\lambda,\frac{1}{3})$. This comprises as special cases considered in [17]: the separable case $\lambda' = \frac{1}{3}$, $t = 0$ and an entangled one with $\lambda = \frac{1}{5}$, $t = \frac{2}{5}$. The overall conclusion is that whenever Bob does not know the coordinates of Alice in the $\hat{s}$ plane then entanglement may be less useful than quantum correlations beyond it, this is the ones contained in separable states.

3.5.2 Optimal Remote State Preparation in the case of bistochastic channels for Bell diagonal states

Another possible situation leading to restrictions on Bob's decoding operations takes place when temperature of Bob's environment is infinite. Then he can use only bistochastic channels,

this is the ones for which $\vec{v}_{\pm} = 0$ in (3.4), what leads to allowed decodings of a from

$$\Lambda_{\pm}[\rho(\vec{u})] = \frac{1}{2}[I + (T_{\pm}\vec{u})\vec{\sigma}]. \tag{3.37}$$

For Bell diagonal states the formula (3.31) can be fully optimized. Here by Bell diagonal states we mean all the states that are local unitary (this is $U_1 \otimes U_2$ type) rotations of the states diagonal in the standard Bell basis $|\Psi_{\pm}\rangle = \frac{1}{\sqrt{2}}(|00\rangle \pm |11\rangle)$ and $|\Phi_{\pm}\rangle = \frac{1}{\sqrt{2}}(|01\rangle \pm |10\rangle)$. It is known that [72] all such states can be represented by $\rho(\vec{0}, \vec{0}, T)$.

Now we present details of the optimization. The first step it to maximize $\left\|M^T\hat{s}\right\|$ over bistochastic decoding strategies $\check{\mathcal{T}}$ and one obtains $\check{T}_+ = I$ and $\check{T}_- = -I$ – rotation about $\hat{\beta}$ direction. From the definition of sets 3.27 we see, that as in the case of $LOCC^{\rightarrow,1}$ the optimal von Neumann measurement is determined by $\hat{a} = \hat{s}$. Again, for fixed $\hat{\beta}$, the protocol from [17] turns out to be optimal. Now we should show that the minimization of the protocol fidelity over $\hat{\beta}$ is provided for circle Ω, which contains all versors $\hat{s}$ orthogonal to the eigenvector corresponding to the largest eigenvalue of TT^T. This means that Remote State Preparation of pure states with Bloch vectors $\hat{s}$ from that circle is the worst from the point of view of transfer fidelity. For Bell states $TT^T = \mathrm{diag}[t_1^2, t_2^2, t_3^2],\ t_3^2 \geq t_2^2 \geq t_1^2$. Let us parametrize all $\hat{s} \in \Omega$ (and hence orthogonal to the eigenvector corresponding to the largest eigenvalue of TT^T) by φ angle. Let us denote $max_{\mathcal{A},\check{\mathcal{T}}} G(\rho(0,0,T); \hat{\beta}; \mathcal{A}, \check{\mathcal{T}}) = \frac{1}{2\pi}\int_0^{2\pi} d\varphi g(\hat{s}(\varphi, \theta(\varphi)))$, where in this case $\theta(\varphi)$ is trivial, this is $\theta(\varphi) = 0$. In this setting we have

$$\max_{\mathcal{A},\check{\mathcal{T}}} G(\rho(0,0,T); \hat{\beta}; \mathcal{A}, \check{\mathcal{T}}) = \int d\hat{s} \left\| \left[(\check{T}_+ - \check{T}_-)T\right]^T \hat{s} \right\| = 2\int d\hat{s} \left\|T^T\hat{s}\right\| = \tag{3.38}$$
$$2\int d\hat{s} \left(\langle\hat{s}| TT^T |\hat{s}\rangle\right)^{\frac{1}{2}} = \frac{1}{2\pi}\int_0^{2\pi} d\varphi g(\hat{s}(\varphi, 0)) = \frac{1}{\pi}\int_0^{\pi} d\varphi \left(t_1^2\cos^2\varphi + t_2^2\sin^2\varphi\right)^{\frac{1}{2}}.$$

Let us now consider a rotation of $\hat{s}$. We can decompose any rotation into rotation about y axis in a plane perpendicular to $\hat{\beta}$ by η angle followed by rotation about $\hat{\beta}$ by μ angle. Then $\hat{s}$ is transformed into $\hat{s}'$, what corresponds to the change of parametrization $(\varphi, \theta(\varphi)) \rightarrow (\varphi'(\varphi), \theta'(\varphi))$ (this transformation is schematically depicted in Figure 3.4). In the rotated frame $max_{\mathcal{A},\mathcal{T}} G(\rho(0,0,T); \hat{\beta}'; \mathcal{A}, \check{\mathcal{T}}) = \int d\hat{s}' g(\hat{s}') = \frac{1}{2\pi}\int_0^{2\pi} d\varphi g(\hat{s}'(\varphi'(\varphi), \theta'(\varphi)))$ (for the explicit form of $g(\hat{s}'(\phi'(\varphi), \theta'(\varphi)))$ see (3.40) below). We will need the following

Lemma The function $f(x) = \int_0^{2\pi} d\varphi\sqrt{A - B\sin^2\varphi + x\sin 2\varphi}$ is decreasing function of x.

Proof We have

$$\frac{\partial}{\partial x} f(x) = \int_0^{2\pi} d\varphi \frac{\sin\varphi\cos\varphi}{\sqrt{A - B\sin^2\varphi + x\sin 2\varphi}} = \tag{3.39}$$
$$2\int_0^{\frac{\pi}{2}} d\varphi \sin\varphi\cos\varphi \left(\frac{1}{\sqrt{A - B\sin^2\varphi + x\sin 2\varphi}} - \frac{1}{\sqrt{A - B\sin^2\varphi - x\sin 2\varphi}}\right) < 0.$$

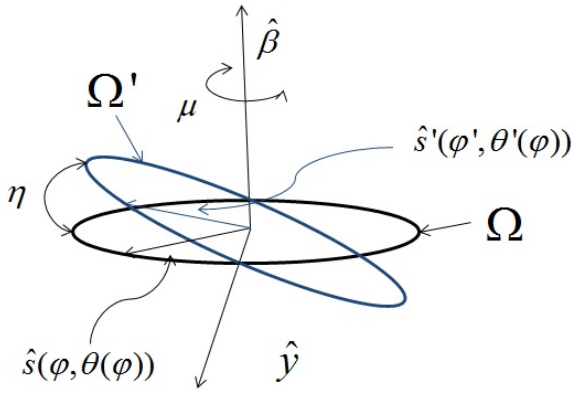

FIGURE 3.4: Relation between two coordinates systems. Plane containing circle Ω is orthogonal to $\hat{\beta}$. In this plane the unit versor $\hat{s}$ is parametrized be φ angle and $g(\hat{s}(\varphi,0))) = \left(\langle \hat{s}(\varphi,0)| TT^T |\hat{s}(\varphi,0)\rangle\right)^{\frac{1}{2}}$. Plane containing Ω' is rotated with respect to that containing Ω. Versor $\hat{s}'$ in the plane containing Ω' can be again parametrized by φ and we have $g(\hat{s}'(\varphi'(\varphi))) = \left(\langle R_\beta(\mu)R_y(\eta)\hat{s}(\varphi,0)| TT^T |R_\beta(\mu)R_y(\eta)\hat{s}(\varphi,0)\rangle\right)^{\frac{1}{2}}$. The figure is reproduced from [71].

To get the desired result, we consider the function $g(\hat{s}'(\varphi'(\varphi), \theta'(\varphi)))$ which can be explicitly written as

$$g(\hat{s}'(\varphi'(\phi), \theta'(\varphi))) = \left(\langle R_\beta(\mu)R_y(\eta)\hat{s}| TT^T |R_\beta(\mu)R_y(\eta)\hat{s}\rangle\right)^{\frac{1}{2}} = \tag{3.40}$$
$$\Bigg(\cos^2\varphi\left[\cos^2\eta(t_1^2\cos^2\mu + t_2^2\sin^2\mu) + \sin^2\eta t_3^2\right] + \frac{1}{2}\sin 2\varphi \sin 2\mu \cos\eta(t_2^2 - t_1^2) +$$
$$\sin^2\varphi(\sin^2\mu t_1^2 + \cos^2\mu t_2^2)\Bigg)^{\frac{1}{2}}.$$

Now the following relation holds

$$\int_0^{2\pi} d\varphi g(\hat{s}'(\varphi'(\phi), \theta'(\varphi))) = \tag{3.41}$$
$$\int_0^{2\pi} d\varphi \Bigg(\cos^2\varphi\left[\cos^2\eta(t_1^2\cos^2\mu + t_2^2\sin^2\mu) + \sin^2\eta t_3^2\right] + \frac{1}{2}\sin 2\varphi \sin 2\mu \cos\eta(t_2^2 - t_1^2) +$$
$$\sin^2\varphi(\sin^2\mu t_1^2 + \cos^2\mu t_2^2)\Bigg)^{\frac{1}{2}} =$$
$$\int_0^{2\pi} d\varphi \Bigg((1 - \sin^2\varphi)\left[\cos^2\eta(t_1^2\cos^2\mu + t_2^2\sin^2\mu) + \sin^2\eta t_3^2\right] + \frac{1}{2}\sin 2\varphi \sin 2\mu \cos\eta(t_2^2 - t_1^2) +$$
$$\sin^2\varphi(\sin^2\mu t_1^2 + \cos^2\mu t_2^2)\Bigg)^{\frac{1}{2}} \geq$$
$$\int_0^{2\pi} d\varphi \Bigg(\cos^2\varphi\left[\cos^2\eta(t_1^2\cos^2\mu + t_2^2\sin^2\mu) + \sin^2\eta t_3^2\right] + \frac{1}{2}\sin 2\varphi \sin 2\mu(t_2^2 - t_1^2) +$$

$$\sin^2\varphi(\sin^2\mu t_1^2+\cos^2\mu t_2^2)\Big)^{\frac{1}{2}}\geq$$
$$\int_0^{2\pi}d\varphi\left(\cos^2\varphi(t_1^2\cos^2\mu+t_2^2\sin^2\mu)+\frac{1}{2}\sin 2\varphi\sin 2\mu(t_2^2-t_1^2)+\sin^2\varphi(\sin^2\mu t_1^2+\cos^2\mu t_2^2)\right)^{\frac{1}{2}}=$$
$$\int_0^{2\pi}d\varphi\left(t_1^2\cos^2\varphi+t_2^2\sin^2\varphi\right)^{\frac{1}{2}}=\int_0^{2\pi}d\varphi g(\hat{s}(\varphi,0)).$$

The first inequality follows from Lemma with $A=\cos^2\eta(t_1^2\cos^2\mu+t_2^2\sin^2\mu)+\sin^2\eta t_3^2$, $B=\cos^2\eta(t_1^2\cos^2\mu+t_2^2\sin^2\mu)+\sin^2\eta t_3^2-\sin^2\mu t_1^2+\cos^2\mu t_2^2$ and $x=\frac{1}{2}\sin 2\varphi\sin 2\mu\cos\eta(t_2^2-t_1^2)$. We increased x by setting $\cos\eta=1$. The second inequality follows from the fact that $t_3^2\geq\sin^2\mu t_1^2+\cos^2\mu t_2^2$, the last equality from the fact that rotation about $\hat{\beta}$ direction by the angle μ does not change the value of the function.

Because $\int_0^{2\pi}d\phi g(\hat{s}(\varphi,0))\leq\int_0^{2\pi}d\phi g(\hat{s}'(\varphi',\theta'(\varphi)))$, minimum over $\hat{\beta}$ provides $\hat{s}$ orthogonal to the largest eigenvalue of TT^T. Taking this into account we have

$$\min_{\beta}\max_{\mathcal{A},\check{\mathcal{T}}}G(\rho(0,0,T);\hat{\beta};\mathcal{A},\check{\mathcal{T}})=\quad\frac{1}{2\pi}\int_0^{2\pi}d\phi g(\hat{s}(\varphi,0))=\quad\frac{1}{\pi}\int_0^{\pi}d\varphi\left(t_1^2\cos^2\varphi+t_2^2\sin^2\varphi\right)^{\frac{1}{2}}. \tag{3.42}$$

Let us recall the definition of the complete elliptic integral of the second kind [74]

$$E(k)=\int_0^{\frac{\pi}{2}}d\varphi\sqrt{1-k^2\sin^2\varphi}. \tag{3.43}$$

Using it we get

$$\min_{\beta}\max_{\mathcal{A},\check{\mathcal{T}}}G(\rho(0,0,T);\hat{\beta};\mathcal{A},\check{\mathcal{T}})=\frac{2|t_2|}{\pi}E\left(\sqrt{1-\frac{t_1^2}{t_2^2}}\right). \tag{3.44}$$

$$\bar{F}_{bistochastic}=\frac{1}{2}\left[1+\frac{2|t_2|}{\pi}E\left(\sqrt{1-\frac{t_1^2}{t_2^2}}\right)\right], \tag{3.45}$$

where t_1^2,t_2^2 are two lowest eigenvalues of T^TT, $E(x)$ is complete elliptic integral of the second kind [74] and $\check{\mathcal{T}}$ denotes Bob bistochastic decoding. In this case it is also possible to show that there exist separable states leading to higher fidelity of RSP protocol than entangled ones. To this end we consider two Bell diagonal states with the following correlation tensors: $T_1=\left[-\frac{1}{3},-\frac{1}{3},-\frac{1}{3}\right]$, $T_2=\left[-\frac{1}{3}-2\epsilon,-\frac{1}{3}+\frac{\epsilon}{2},-\frac{1}{3}+\frac{\epsilon}{2}\right]$, where $\epsilon>0$. The set of separable Bell diagonal states is specified by condition $|t_1|+|t_2|+|t_3|\leq 1$. Clearly the state corresponding to T_1 is

separable whereas that corresponding to T_2 is not. Using (3.45) one immediately obtains that

$$\bar{F}_{bistochastic}(\rho(\vec{0},\vec{0},T_1)) = \frac{2}{3} > \frac{2}{3} - \frac{\epsilon}{4} = \bar{F}_{bistochastic}(\rho(\vec{0},\vec{0},T_2)). \tag{3.46}$$

Interestingly (3.45) depends only on the two smallest eigenvalues of TT^T. Since the geometric discord is in this case of the form $D(\rho(\vec{0},\vec{0},T)) = \frac{1}{4}(t_1^2+t_2^2)$ the optimized fidelity depends on the same parameters like the one used in [17]. This shows that in the case of bistochastic decoding the presented result based on standard fidelity and the one based on quadratic fidelity are consistent in the sense that the qualitative behavior of optimized linear and quadratic fidelity is similar. This statement is illustrated in Figure 3.5

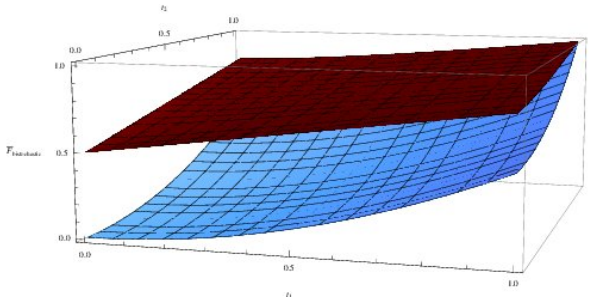

FIGURE 3.5: The comparison of optimized linear $\bar{F}_{bistochastic}$ (3.45) – upper surface and quadratic $\mathcal{P}_{opt}$ (3.13) – lower surface fidelity for bistochastic decodings.

3.6 Concluding remarks

In this Chapter we studied the usefulness of quantum entanglement and quantum separable correlations as the resource in the Remote State Preparation protocol. Our main motivation were the recent result from literature [17], in which it was claimed that the quantum correlations beyond entanglement are the crucial resource for the protocol in question. Although it is known that this type of quantum correlations, contained in separable states, may be useful in quantum information processing, the basic issue is whether they may outperform entanglement in any case.

The analysis performed in this chapter shown that one should be careful in comparison of the two resources. In fact two-qubit separable states cannot outperform two-qubit entanglement in the process of Remote State Preparation of quantum bit under the most general assumptions on the allowed operations. We assumed that the most natural setting is that provided by LOCC class, where additionally the classical communication is restricted to one bit of forward communication (to prevent the direct transition of the state to be prepared). This lies in the heart of the balance of quantum resources within LOCC scenario: whenever initial entanglement is too weak, it may be removed and an optimal separable state can be prepared

(as this can be achieved by LOCC operations). In such a case, the efficiency of the protocol is equal to the best efficiency provided by all separable correlations based protocols. Thus any protocol with initial entanglement cannot be worse than the one with separable state.

The apparent contradictions to the above may only take place if one use nonstandard figure of merit. It has been shown here that it is indeed the case when one uses the quadratic fidelity. As the latter is not able to make a difference between the orthogonal states, it is an incorrect tool for quantifying different resources in Remote State Preparation protocol. The standard linear fidelity works well from that perspective.

However, our analysis shows that all the above does not exclude the advantage of separable quantum correlations in the cases when there are additional restrictions on the set of allowed operations. As a result, in such cases the optimal protocol for separable states derived in this Chapter cannot be performed. Therefore, in principle, it could be no longer true that entangled states are in the worst case as useful as the separable ones. In this Chapter we have shown that if in the Remote State Preparation protocol of a qubit state the receiver is restricted to the decoding class, which reflects his lack of knowledge about the coordinates in the $\hat{s}$ plane, then separable correlated states can work better than entanglement. The second scenario when the latter may happen is the one when the receiver is forced to use bistochastic decodings. Then, whenever the parties share Bell diagonal quantum state, the linear fidelity of the protocol depends on the same set of parameters as geometric quantum discord.

The latter result is even more intriguing, when one realizes that the restriction of bistochastic character of the decoding may be interpreted as a presence of "thermodynamically unsuitable" anciallas, namely those of infinite temperature. Note that in this case quantum correlations beyond entanglement can work better than entanglement itself and that one option to discriminate those correlations form classical ones is just the thermodynamical picture of local engines (see [75, 76]). This suggests that possible thermodynamical perspective of the discussed protocol (and also practical aspects of other protocols aimed in using quantum correlations beyond entanglement) should be examined more in future.

The results of this section show also that one should carefully define notion of classical correlation structures in Quantum Theory. As has been mentioned in Section 2.2, some authors consider correlations that can be found in separable quantum states to be classical. Here we proved that there exists scenarios, in which such correlations can outperform entangled states in Remote State Preparation protocol. We would not expect classical resource to behave in this way.

Chapter 4

Spectrum Broadcast Structures for environments of harmonic oscillators

4.1 Introduction

The aim of this Chapter is to prepare tools that will be used to investigate formation of Spectrum Broadcast Structures in physical models, in particular those in Chapter 5. As has been discussed in Subsection 2.4.3, one method of checking the formation of Spectral Broadcast Structures is to study the behavior of two indicator functions – decoherence factor governing the disappearance of coherences in the partially reduced system-environment state and generalized overlap measuring the information content of the observed fragments of the environment. The indicator functions in general depend on the considered physical model – an interaction between a system and an environment and an initial state of the environment. Here our objective is to derive expressions for indicator functions that will be as general as possible. Therefore, instead of invoking a particular system-environment model, we assume that we deal with a situation in which environment consists of N quantum harmonic oscillators. The central system at the moment is not specified. This setting encompass two canonical models of decoherence: Quantum Brownian Motion and spin – boson model [12]. This Chapter is partially based on results published in [77].

4.2 Derivation of the evolution operator

For the purpose of this Chapter we assume that the relevant Hamiltonian is

$$\hat{H}_{S:E} = \sum_{k=1}^{N} \left(\frac{\hat{p}_k^2}{2m_k} + \frac{m_k \omega_k^2 \hat{x}_k^2}{2} \right) + \sum_O f(O,t)|O\rangle\langle O| \otimes \sum_{k=1}^{N} (C_k \hat{x}_k + G_k \hat{p}_k), \tag{4.1}$$

where $f(O,t)$ is some function depending in general on O,t. Here we assume that the system operator is finite-dimensional to keep notation simple. However, extension to infinite-dimensional case is (at least from notational point of view) straightforward. The Hamiltonian is far from being the most general one: we assume that the coupling is linear in position and momentum of the environmental oscillators and it is of a product form, given by tensor product of system's and environments' operators. Moreover, there is no system's self-Hamiltonian and the system enters the problem only via the interaction term given by some function of operator $\hat{O} = \sum_O O|O\rangle\langle O|$. However, this is the most general form of a Hamiltonian, for which we are able to derive formulas for functions indicating Spectrum Broadcast Structure formation. In the case when both $[\hat{H}_S, \hat{H}_{INT}] \neq 0$ and $[\hat{H}_E, \hat{H}_{INT}] \neq 0$ there is no general method of checking if the Spectrum Broadcast Structure is formed and each such situation requires a separate treatment (one of such cases will be presented in Chapter 5). Although the choice of the Hamiltonian may to some extend seem to be artificial, in fact there are situations, relevant from the physical point of view, in which the dynamics is governed by (4.1). The above Hamiltonian arises for example in the mentioned canonical models of decoherence where the environment is described as a set of quantum harmonic oscillators – so called boson-boson and spin-boson models – in (at least) two cases. The first one corresponds to a situation in which the system's self-Hamiltonian commutes with the interaction Hamiltonian. Usually it is achieved by neglecting the non-commuting part of the self-Hamiltonian like in simplified spin-boson or simplified Quantum Brownian Motion model. Alternatively one can arrive at Hamiltonian (4.1) by invoking an approximation that separates the dynamics of the system and environment (similar to Born-Oppenheimer approximation). We use this approach to study Quantum Brownian Motion model in Chapter 5.

To solve the dynamics, we pass to interaction picture with respect to the environment (as we assume that, in some sense, the dynamics of the system is already taken into consideration by $f(O,t)$ function) $\hat{H}^I(t) = e^{i\hat{H}_{0E}t/\hbar}\hat{H}e^{-i\hat{H}_{0E}t/\hbar}$ to get

$$\hat{H}^I(t)_{S:E} = \sum_O |O\rangle\langle O| \otimes f(O,t)\sum_{k=1}^{N}(C_k\hat{x}_k(t) + G_k\hat{p}_k(t)) \equiv \sum_O |O\rangle\langle O| \otimes \sum_{k=1}^{N}\hat{H}_k^I(f(O,t);t). \quad (4.2)$$

To calculate the evolution operator $\hat{U}^I(t) = \mathcal{T}\exp\left[-\frac{i}{\hbar}\int_0^t d\tau \hat{H}^I(f(O,\tau);\tau)\right]$ we use the standard decomposition

$$\hat{U}^I(t) = \lim_{n\to\infty}\left(\prod_{r=1}^{n}\exp\left[-\frac{i}{\hbar}\hat{H}^I(f(O,t_r);t_r)\Delta t\right]\right), \quad (4.3)$$

where $\Delta t \equiv t/n$, $t_r \equiv r\Delta t$. Direct calculation of the exponent series for each infinitesimal time step Δt gives:

$$\exp\left[-\frac{i}{\hbar}\hat{H}^I(f(O,t_r);t_r)\Delta t\right] = \sum_O |O\rangle\langle O| \otimes \bigotimes_{k=1}^{N} e^{-\frac{i}{\hbar}\hat{H}_k^I(f(O,t_r);t_r)\Delta t}. \tag{4.4}$$

Now we use the expressions for evolution of position and momentum operators under Hamiltonian of quantum harmonic oscillator $\hat{H}_k = \hat{p}_k^2/(2m_k) + m_k\omega_k\hat{x}_k^2/2$

$$\hat{x}_k(t) \equiv e^{it\hat{H}_k/\hbar}\hat{x}_k e^{-it\hat{H}_k/\hbar} = \sqrt{\frac{\hbar}{2m_k\omega_k}}(\hat{a}_k e^{-i\omega_k t} + \hat{a}^\dagger e^{i\omega_k t}) \tag{4.5}$$

$$\hat{p}_k(t) \equiv e^{it\hat{H}_k/\hbar}\hat{p}_k e^{-it\hat{H}_k/\hbar} = -i\sqrt{\frac{\hbar m_k\omega_k}{2}}(\hat{a}_k e^{-i\omega_k t} - \hat{a}^\dagger e^{i\omega_k t}) \tag{4.6}$$

, with $\hat{a}^\dagger, \hat{a}$ being the creation and annihilation operators for the k-th environmental oscillator, we further obtain:

$$e^{-\frac{i}{\hbar}\hat{H}_k^I(f(O,t);t)\Delta t} = \exp\left[-\frac{f(O,t)\Delta t}{\sqrt{2\hbar m_k\omega_k}}\left(ie^{i\omega_k t}\left(C_k + iG_k m_k\omega_k\right)\hat{a}^\dagger - \left(ie^{i\omega_k t}\left(C_k + iG_k m_k\omega_k\right)\right)^*\hat{a}\right)\right] =$$
$$\hat{D}\left(\alpha_k'(t)f(O,t)\Delta t\right), \tag{4.7}$$

where $\hat{D}(\alpha) = \exp(\alpha\hat{a}_k^\dagger - \alpha^*\hat{a}_k)$ is displacement operator and

$$\alpha_k'(t) = -\frac{i\left(C_k + iG_k m_k\omega_k\right)}{\sqrt{2\hbar m_k\omega_k}}e^{i\omega_k t}. \tag{4.8}$$

Inserting (4.7) into (4.3) gives:

$$\prod_{r=1}^{n}\exp\left[-\frac{i}{\hbar}\hat{H}^I(f(O,t_r);t_r)\Delta t\right] = \tag{4.9}$$
$$\sum_O |O\rangle\langle O| \otimes \bigotimes_{k=1}^{N}\hat{D}\left(\alpha_k'(t_n)f(O,t_n)\Delta t\right)\cdots\hat{D}\left(\alpha_k'(t_1)f(O,t_1)\Delta t\right).$$

To calculate the string of the displacement operators we use repetitively the composition law:

$$\hat{D}(\alpha)\hat{D}(\beta) = e^{\frac{1}{2}(\alpha\beta^* - \alpha^*\beta)}\hat{D}(\alpha+\beta), \tag{4.10}$$

and obtain:

$$\prod_{r=1}^{n}\hat{D}\left(\alpha_k'(t_r)f(O,t_r)\Delta t\right) = \hat{D}\left(\sum_{r=1}^{n}\alpha_k'(t_r)f(O,t_r)\Delta t\right)\times \tag{4.11}$$

$$\times \exp\left[i\frac{C_k^2+G_k^2m_k^2\omega_k^2}{2\hbar m_k\omega_k}\mathrm{Im}\Delta t^2\sum_{r'=1}^{n}e^{i\omega_k t_{r'}}f(O,t_{r'})\sum_{r''=1}^{r'}e^{-i\omega_k t_{r''}}f(O,t_{r''})\right].$$

Now we are ready to take the limit $n\to\infty$, resulting in $\Delta t\to 0$, $n\Delta t = const = t$. For the displacement operator the limit can be moved inside the argument so that:

$$\lim_{n\to\infty}\hat{D}\left(\sum_{r=1}^{n}\alpha_k'(t_r)f(O,t_r)\Delta t\right)=\hat{D}\left(\int_0^t\alpha_k'(\tau)f(O,\tau)d\tau\right)\equiv\hat{D}(\eta_k(O,t)). \tag{4.12}$$

For the phase factor (4.11) we again move the limit inside the argument of the exponent to obtain:

$$\begin{aligned}&\frac{C_k^2+G_k^2m_k^2\omega_k^2}{2\hbar m_k\omega_k}\lim_{n\to\infty}\mathrm{Im}\sum_{r'=1}^{n}f(O,t_{r'})e^{i\omega_k t_{r'}}\Delta t\sum_{r''=1}^{r'}f(O,t_{r''})e^{-i\omega_k t_{r''}}\Delta t \\ &=\frac{C_k^2+G_k^2m_k^2\omega_k^2}{2\hbar m_k\omega_k}\int_0^t dt'\int_0^{t'}dt''f(O,t')f(O,t'')\sin\left[\omega_k(t'-t'')\right]\equiv\xi_t(O,t).\end{aligned} \tag{4.13}$$

Thus, restoring the free evolution of the environment, we arrive at the final form of the evolution operator

$$\hat{U}_{S:E}(t)=\sum_O|O\rangle\langle O|\otimes\bigotimes_{k=1}^{N}\hat{e}^{i\xi_k(O,t)}e^{-i\hat{H}_kt/\hbar}\hat{D}_k(\eta_k(O,t))\equiv\sum_O|O\rangle\langle O|\otimes\bigotimes_{k=1}^{N}\hat{U}_k(O,t). \tag{4.14}$$

This is the main result of this Subsection. We see that the above dynamics is of the so-called control type – the evolution of the environment depends on the central system.

4.3 Analytical derivation of functions indicating Spectrum Broadcast Structure formation

In this section we derive expressions for functions indicating Spectrum Broadcast Structure formation – the decoherence factor and generalized overlap and calculate them explicitly for initial thermal states of the environment in the case of the evolution operator given by equation (4.14). In the following considerations we refer to those functions as indicator functions. We begin by specifying the type of system-environment initial state.

Usually in the treatment of open quantum systems one assumes that initial system-environment state factorizes

$$\rho_{S:E}(0)=\rho_{0S}\otimes\bigotimes_{k=1}^{N}\rho_{0k}. \tag{4.15}$$

This means that there are no correlation between the system and the environment. Such a statement should be considered as an idealization. In fact, this case corresponds to a situation in which the system and the environment is initially uncoupled and then the interaction is "switched on" instantly. This assumption may lead to some unexpected results concerning quantities considered in the context of open quantum systems (for example diffusion coefficient in low temperature Quantum Brownian motion with Ohmic environment [78]). However, the approximation does not affect in a significant way results concerning decoherence. Moreover, as we are interested in system-environment correlations created dynamically during evolution, the above approximation is convenient also from technical point of view. For these reasons we adopt it in our considerations. As a result of the evolution at time t the system-environment state is

$$\rho(t)_{S:E} = \sum_{O} \langle O|\rho_{0S}\,|O\rangle |O\rangle\langle O| \otimes \bigotimes_{k=1}^{N} \hat{U}_k(O,t)\rho_{0k}\hat{U}_k^{\dagger}(O,t) + \sum_{O,O',O\neq O'} \langle O|\rho_{0S}\,|O'\rangle |O\rangle\langle O'| \otimes \bigotimes_{k=1}^{N} e^{i(\xi_k(O,t)-\xi_k(O',t))}\hat{U}_k(O,t)\rho_{0k}\hat{U}_k^{\dagger}(O',t). \tag{4.16}$$

Subsequently some fragment of the environment needs to pass unobserved. As has been explained previously, this requirement is crucial for the decoherence process to happen. Due to the interaction an initial coherence of the state of the central system becomes a property of the global system-environment state and it may no longer be observed at the level of partially reduced state. The unobserved fragment of the environment is denoted as $(1-f)$, where $0 \leq f \leq 1$. After performing the trace the partially reduced state is

$$\rho(t)_{S:fE} = \sum_{O} \langle O|\rho_{0S}\,|O\rangle |O\rangle\langle O| \otimes \bigotimes_{k=1}^{fN} \hat{U}_k(O,t)\rho_{0k}\hat{U}_k^{\dagger}(O,t) + \sum_{O,O',O\neq O'} \Gamma_{O,O'}(t)\langle O|\rho_{0S}\,|O'\rangle |O\rangle\langle O'| \otimes \bigotimes_{k=1}^{fN} e^{i(\xi_k(O,t)-\xi_k(O',t))}\hat{U}_k(O,t)\rho_{0k}\hat{U}_k^{\dagger}(O',t). \tag{4.17}$$

where $\Gamma_{O,O'}(t)$ is the decoherence factor that reads

$$\Gamma_{O,O'}(t) = \prod_{k\in(1-f)E} Tr\left[e^{i(\xi_k(O,t)-\xi_k(O',t))}\hat{D}_k(\eta_k(O,t))\rho_{0k}\hat{D}_k^{\dagger}(\eta_k(O',t))\right], \tag{4.18}$$

where the free evolution terms dropped out due to the cyclic property of the trace. We note that, since the evolution of the environment is in this case given by the displacement operators (4.14), the decoherence factor (4.18) is in fact a characteristic function (refereed sometimes to as zero-order or Wigner characteristic function) of the unobserved fragment of initial state of

the environment (or more precisely, due to the presence of the phase factor $e^{i\xi_k(O,t)}$ is a non-commutative characteristic function on the Heisenberg group [79]).

We proceed accordingly to steps outlined in Section 2.4: to show Spectrum Broadcast Structure we must firstly investigate the decoherence process – disappearance of off-diagonal terms in equation (4.17) and then the transfer of classical information to the environment.

4.3.1 Decoherence factor

In fact, to show that the off-diagonal coherent part vanishes it is sufficient to consider modulus of the decoherence factor

$$\left|\Gamma_{O,O'}(t)\right| = \left| \prod_{k\in(1-f)E} Tr\left[e^{i(\xi_k(O,t)-\xi_k(O',t))} \hat{D}_k(\eta_k(O,t))\rho_{0k}\hat{D}_k^\dagger(\eta_k(O',t))\right]\right|. \tag{4.19}$$

We immediately see that the dynamical phase factor drops out due to the modulus and therefore will not contribute to the decoherence process. The decoherence factor consists of a product of individual decoherence factors for each environmental subsystem that is not observed. We focus on a single term in the product and for a moment drop the explicit dependence on the environmental index k, value of O and t. At this point we do not specify the state of the environment, we assume only that it can be written in terms of Glauber–Sudarshan P-representation [80, 81]:

$$\varrho_0 = \int \frac{d^2\gamma}{\pi} P(\gamma)|\gamma\rangle\langle\gamma| \tag{4.20}$$

where P is in general a distribution [82] and $|\gamma\rangle \equiv \hat{D}(\gamma)|0\rangle$ are the standard coherent states [83]. We insert this into (4.18) and perform formal calculations

$$\begin{aligned} &tr\left[\int \frac{d^2\gamma}{\pi} P(\gamma)\hat{D}\left(\eta\right)|\gamma\rangle\langle\gamma|\hat{D}\left(\eta'\right)\right] = \\ &\int \frac{d^2\gamma}{\pi} P(\gamma)\left\langle\gamma+|\gamma+(\eta-\eta')\right\rangle e^{\frac{1}{2}[(\eta\eta'^*-\eta^*\eta')+(\eta-\eta')\gamma^*-(\eta-\eta')^*\gamma]} = \\ &= \int \frac{d^2\gamma}{\pi} P(\gamma)\exp\left[-\frac{|\gamma|^2}{2} - \frac{|\gamma+(\eta-\eta')|^2}{2} + \gamma^*(\gamma+(\eta-\eta')) + \right. \\ &\left.\frac{1}{2}(\eta\eta'^*-\eta^*\eta') + (\eta-\eta')\gamma^* - (\eta-\eta')^*\gamma\right], \end{aligned} \tag{4.21}$$

where we used twice the composition law (4.10). Performing the simple algebra in (4.21), we finally obtain:

$$\left|\Gamma_{O,O'}(t)\right| = \prod_{k\in(1-f)E} e^{-\frac{1}{2}|\eta_k(O,t)-\eta_k(O',t)|^2} \times \tag{4.22}$$

$$\times \quad \left| \int \frac{d^2\gamma}{\pi} P(\gamma) \exp\left[-\left((\eta_k(O,t) - \eta_k(O',t))^* \gamma - (\eta_k(O,t) - \eta_k(O',t))\gamma^* \right) \right] \right|.$$

As a result, we see that the decoherence factor for an individual environmental subsystem consists of a modulus of a Fourier transform of the P function with respect to a complex variable $\eta_k(O,t) - \eta_k(O',t)$ smoothed with a Gaussian function $e^{-\frac{1}{2}|\eta_k(O,t)-\eta_k(O',t)|^2}$.

To proceed further we need to specify the initial state of the environment. We begin with a natural assumption, namely that the environment is initially in a thermal state. Although well justified from physical perspective, this is still a restriction and we overcome it later by investigating general single mode Gaussian states. The P-representation of a thermal state is

$$\rho_{0k} = \frac{1}{\bar{n}_k} \int \frac{d^2\gamma_k}{\pi} e^{-\frac{|\gamma_k|^2}{\bar{n}_k}} |\gamma_k\rangle\langle\gamma_k|, \tag{4.23}$$

where $\bar{n} = 1/(e^{\tau_T \omega_k} - 1)$ is the mean photon number and we introduced thermal time parameter

$$\tau_T = \frac{\hbar}{k_B T}, \tag{4.24}$$

to keep equations concise. The formula for the decoherence factor takes the form

$$\left|\Gamma_{O,O'}(t)\right| = \exp\left[-\frac{1}{2} \sum_{k \in (1-f)E} |\eta_k(O,t) - \eta_k(O',t)|^2 \coth\left(\frac{\tau_T \omega_k}{2}\right) \right], \tag{4.25}$$

where ω_k is frequency of k^{th} oscillator. This is the final result of the present Subsection that will be used in further parts of the thesis to study particular physical models.

4.3.2 The generalized overlap for thermal states

In this Subsection we investigate information content of the environmental states

$$\varrho_k(O,t) \equiv \hat{U}_k(O,t) \rho_{0k} \hat{U}_k^\dagger(O,t), \tag{4.26}$$

which form the diagonal part of (4.17), by we calculating the generalized overlap

$$B^{mac}_{O,O'}(t) \equiv B\Big(\varrho_{mac}(O,t), \varrho_{mac}(O',t) \Big), \tag{4.27}$$

where

$$\varrho_{mac}(O,t) \equiv \bigotimes_{k \in mac} \varrho_k(O,t) \tag{4.28}$$

and

$$B(\varrho_1, \varrho_2) \equiv tr\sqrt{\sqrt{\varrho_1}\varrho_2\sqrt{\varrho_1}}. \tag{4.29}$$

As has been mentioned generalized overlap measures distinguishability of two states that in our case are parametrized by functions $\eta_k(O,t)$, $\eta_k(O',t)$. In other words, if the two states are perfectly distinguishable one should be, in principle, able to extract some information about O (or even about the function $\eta_k(O,t)$). Generalized overlap scales conveniently with a tensor product in (4.28):

$$B\Big(\bigotimes_k \varrho_k(O,t), \bigotimes_k \varrho_k(O',t)\Big) = \prod_k B\Big(\varrho_k(O,t), \varrho_k(O',t)\Big). \tag{4.30}$$

As has been pointed out, this is especially important in the case, when the single environmental subsystem is merely affected by the interaction with the central system. Then states evolving accordingly to O and O' are almost indistinguishable since the interaction is to week to imprint a significant piece of information about the central system on the single subsystem of the environment. However, it may happen that a group of subsystems allows to extract information about the central system since the joint states of the group, called macrofractions, become distinguishable. To check if this is indeed the case, it is enough to calculate the generalized overlap for a single environment (if there are no initial correlations between subsystems forming environment, what is our assumption) and then take the product over all subsystems forming macrofraction.

We work under the same assumptions as in the previous Section. We consider that the initial state is uncorrelated – equation (4.15). Coming back to calculations, for the sake of clarity, we drop the explicit dependence on the environmental index k denote a single-system overlap by $B^{mic}_{O,O'}(t)$. As a result we get

$$B^{mic}_{O,O'}(t) = Tr\sqrt{\sqrt{\varrho_0}\hat{U}^\dagger(O',t)\hat{U}(O,t)\varrho_0\hat{U}^\dagger(O,t)\hat{U}(O',t)\sqrt{\varrho_0}}. \tag{4.31}$$

To arrive at the above equation we used the fact that

$$Tr\sqrt{\hat{U}\hat{A}\hat{U}^\dagger} = Tr\hat{U}\left(\sqrt{\hat{A}}\right)\hat{U}^\dagger = Tr\sqrt{A}, \tag{4.32}$$

where $\hat{U}$ is some unitary and $\hat{A}$ some hermitian operator. Then the first equality follows from the fact that unitary does not change the spectrum, the second from cyclic property of the trace. Similarly, in equation (4.31) we firstly pulled the extreme left and right unitary operators out of the both square roots and used the cyclic property of the trace to cancel them out. Note that the free evolutions $e^{-i\hat{H}_k t/\hbar}$ and the dynamical phases from (4.1) cancel out as both unitary

operators under the square root are Hermitian conjugates of each other. The same applies to the phase factors arising from the composition law of displacement operators (4.10), when calculating $D^\dagger(\eta')\hat{D}(\eta))$. Thus, modulo phase factors (from now we drop dependence on value of O and t):

$$\hat{U}^\dagger(O',t)\hat{U}(O,t) \simeq \hat{D}^\dagger(\eta')\hat{D}_k(\eta) = \hat{D}(-\eta')\hat{D}(\eta) \simeq \hat{D}\left(\eta - \eta'\right) \equiv \hat{D}(\chi), \tag{4.33}$$

where we used $\hat{D}^\dagger(\alpha) = \hat{D}(-\alpha)$. Next, assuming all the initial states ϱ_{0k} are thermal, we use the corresponding P-representation for the middle ϱ_0 under the square root in (4.31) $\varrho_0 = \frac{1}{\bar{n}}\int \frac{d^2\gamma}{\pi} e^{-\frac{|\gamma|^2}{\bar{n}}}|\gamma\rangle\langle\gamma|$. This choice is motivated by the fact that the displacement operator acts in a simple way on coherent states. Denoting the Hermitian operator under the square root in (4.31) by $\hat{A}_t$ we obtain:

$$\hat{A}_t = \int \frac{d^2\gamma}{\pi\bar{n}} e^{-\frac{|\gamma|^2}{\bar{n}}} \sqrt{\varrho_0}\hat{D}(\chi)|\gamma\rangle\langle\gamma|\hat{D}^\dagger(\chi)\sqrt{\varrho_0} = \int \frac{d^2\gamma}{\pi\bar{n}} e^{-\frac{|\gamma|^2}{\bar{n}}} \sqrt{\varrho_0}|\gamma+\chi\rangle\langle\gamma+\chi|\sqrt{\varrho_0}. \tag{4.34}$$

To perform the square roots above we represent the thermal state using Fock basis

$$\varrho_0 = \sum_n \frac{\bar{n}^n}{(\bar{n}+1)^{n+1}}|n\rangle\langle n|. \tag{4.35}$$

As this density operator is diagonal in orthonormal Fock basis we immediately can perform the square root. Inserting the representation into (4.34) gives:

$$\hat{A}_t \;=\; \int \frac{d^2\gamma}{\pi\bar{n}} e^{-\frac{|\gamma|^2}{\bar{n}}} \sum_{m,n} \sqrt{\frac{\bar{n}^{m+n}}{(\bar{n}+1)^{m+n+2}}}\langle n|\gamma+\eta_t\rangle\langle\gamma+\eta_t|m\rangle|n\rangle\langle m|. \tag{4.36}$$

Now we calculate the scalar products in the above equation. To this end we use the Fock basis representation of coherent states

$$|\alpha\rangle = e^{-\frac{|\alpha|^2}{2}} \sum_n \frac{\alpha^n}{\sqrt{n!}}|n\rangle. \tag{4.37}$$

Then the scalar products above read:

$$\langle n|\gamma+\chi\rangle = e^{-\frac{1}{2}|\gamma+\chi|^2}\frac{(\gamma+\chi)^n}{\sqrt{n!}}. \tag{4.38}$$

There is still the square root to be taken and the present form of expression does not allow to perform it directly. As the square root can be conveniently calculated for operators that are diagonal is some orthonormal basis, or strategy is now to use the above relation and rewrite each sum in (4.36) as a coherent state but with a rescaled argument, and then try to rewrite

(4.36) as a single operator diagonal in Fock basis. To this end we note that:

$$e^{-\frac{1}{2}|\gamma+\chi|^2}\sum_n\left(\frac{\bar{n}}{\bar{n}+1}\right)^{\frac{n}{2}}\frac{(\gamma+\chi)^n}{\sqrt{n!}}|n\rangle = e^{-\frac{1}{2}\frac{|\gamma+\chi|^2}{\bar{n}+1}}\left|\sqrt{\frac{\bar{n}}{\bar{n}+1}}(\gamma+\chi)\right\rangle, \tag{4.39}$$

where we have again used (4.37) to rewrite the sum. Substituting this into (4.36) and performing reordering in the exponentials gives expression diagonal in coherent state basis:

$$\begin{aligned}\hat{A}_t &= \frac{1}{\bar{n}+1}\int\frac{d^2\gamma}{\pi\bar{n}}e^{-\frac{|\gamma|^2}{\bar{n}}-\frac{|\gamma+\chi|^2}{\bar{n}+1}}\left|\sqrt{\frac{\bar{n}}{\bar{n}+1}}(\gamma+\chi)\right\rangle\left\langle\sqrt{\frac{\bar{n}}{\bar{n}+1}}(\gamma+\chi)\right| \\ &= \frac{1}{\bar{n}+1}e^{-\frac{|\chi|^2}{1+2\bar{n}}}\int\frac{d^2\gamma}{\pi\bar{n}}e^{-\frac{1+2\bar{n}}{\bar{n}(\bar{n}+1)}\left|\gamma+\frac{\bar{n}}{1+2\bar{n}}\chi\right|^2}\left|\sqrt{\frac{\bar{n}}{\bar{n}+1}}(\gamma+\chi)\right\rangle\left\langle\sqrt{\frac{\bar{n}}{\bar{n}+1}}(\gamma+\chi)\right|.\end{aligned} \tag{4.40}$$

We now show that (4.41) although not equal to, is equivalent to some operator diagonal in the Fock basis. We use the same argument as at the beginning of the subsection: since we are interested in $Tr\sqrt{\hat{A}_t}$ rather than $\hat{A}_t$ itself, there is a freedom of rotating $\hat{A}_t$ by an unitary operator, in particular by a displacement, as: $Tr\sqrt{\hat{D}\hat{A}_t\hat{D}^\dagger} = Tr\left[\hat{D}\sqrt{\hat{A}_t}\hat{D}^\dagger\right] = Tr\sqrt{\hat{A}_t}$. We now find such a displacement as to turn (4.41) into the Fock diagonal form. Comparing the exponential under the integral in (4.41) with the form (4.23), we see that the argument of the subsequent coherent states should be proportional to $\gamma + \frac{\bar{n}}{1+2\bar{n}}\chi$. Simple algebra gives the desired displacement:

$$\left|\sqrt{\frac{\bar{n}}{\bar{n}+1}}(\gamma+\chi)\right\rangle \simeq \hat{D}\left(\sqrt{\frac{\bar{n}}{\bar{n}+1}}\frac{\bar{n}+1}{1+2\bar{n}}\chi\right)\left|\sqrt{\frac{\bar{n}}{\bar{n}+1}}\left(\gamma+\frac{\bar{n}}{1+2\bar{n}}\chi\right)\right\rangle, \tag{4.41}$$

where we have omitted the irrelevant phase factor arising from the action of the displacement as in the final expression it cancels out (the conjugated phase stems from the fact that we need to act with two conjugated displacement operators on both sides of equation (4.40)). Inserting the above relation into (4.41), dropping the displacements due to unitary freedom, and changing the integration variable:

$$\gamma \to \sqrt{\frac{\bar{n}}{\bar{n}+1}}\left(\gamma+\frac{\bar{n}}{1+2\bar{n}}\chi\right) \tag{4.42}$$

gives:

$$B^{mic}_{O,O'}(t) = e^{-\frac{1}{2}\frac{|\chi|^2}{1+2\bar{n}}}\frac{1}{\sqrt{1+2\bar{n}}}Tr\sqrt{\varrho_{th}\left(\frac{\bar{n}^2}{1+2\bar{n}}\right)}, \tag{4.43}$$

where $\varrho_{th}(\bar{n})$ denotes a thermal state with the mean photon number $\bar{n}$. To perform the square root and the trace we again use the Fock expansion for $\varrho_{th}\left(\frac{\bar{n}^2}{1+2\bar{n}}\right)$:

$$B^{mic}_{O,O'}(t) = e^{-\frac{|\chi|^2}{2+4\bar{n}}} \frac{1}{\sqrt{1+2\bar{n}}} \left(1+\frac{\bar{n}^2}{1+2\bar{n}}\right)^{-\frac{1}{2}} \sum_n \left(\frac{\bar{n}^2/(1+2\bar{n})}{1+\bar{n}^2/(1+2\bar{n})}\right)^{\frac{n}{2}} \tag{4.44}$$
$$= \exp\left[-\frac{1}{2+4\bar{n}}|\eta-\eta'|^2\right] = \exp\left[-\frac{1}{2}|\eta-\eta'|^2 \tanh\left(\frac{\tau_T\omega}{2}\right)\right],$$

where we have used the definition of χ (4.33) and $\bar{n} = 1/(e^{\tau_T\omega}-1)$. Coming back to the generalized overlap for macro-fraction states (4.27) with a help of (4.30), we finally obtain the desired result:

$$B^{mac}_{O,O'}(t) = \exp\left[-\frac{1}{2}\sum_{k\in mac}|\eta_k(O,t)-\eta_k(O',t)|^2 \tanh\left(\frac{\tau_T\omega_k}{2}\right)\right]. \tag{4.45}$$

This is the main result of this Subsection. Note, that only difference between the above expression for generalized overlap and that for decoherence factor (4.25), apart from the fact that both quantities are calculated with respect to different environmental degrees of freedom, is the temperature dependence. We will elaborate on this fact in Section 4.4.

4.3.3 Generalization to the case of arbitrary single mode Gaussian states of the environment

The above results can be generalized to the case, in which the initial state of the environment is given by a product of arbitrary single mode Gaussian states. To this end, we use the fact that an arbitrary single-mode Gaussian state can be parametrized as follows [84]:

$$\varrho = e^{i\psi\hat{a}^\dagger a}\hat{D}(\beta)\hat{S}(\xi)\varrho_T\hat{S}^\dagger(\xi)\hat{D}^\dagger(\beta)e^{-i\psi\hat{a}^\dagger a}, \tag{4.46}$$

where $\hat{S}(\xi) \equiv e^{\frac{1}{2}(\xi^*\hat{a}^2-\xi\hat{a}^{\dagger 2})}$ is the squeezing operator, $\xi \equiv re^{i\theta}$, and ϱ_T is some thermal state.

We begin with an analysis of changes that need to be introduced to the decoherence factor by simply plugging the above formula to the equation (4.19)

$$\left|\Gamma_{O,O'}(t)\right| = \tag{4.47}$$
$$\prod_{k\in(1-f)E}\left|Tr\left[\hat{D}_k(\eta_k(O,t)-\eta_k(O',t))e^{i\psi\hat{a}^\dagger a}\hat{D}(\beta)\hat{S}(\xi)\varrho_T\hat{S}^\dagger(\xi)\hat{D}^\dagger(\beta)e^{-i\psi\hat{a}^\dagger a}\right]\right|,$$

where we dropped unimportant from our perspective phase factor steaming from the evolution. Now we focus on the modulus - we drop the dependence on k, again use the variable

$\chi = \eta_k(O,t) - \eta_k(O',t)$ and subsequently exploit the cyclic property of trace

$$\begin{aligned}
&\left|Tr\left[\hat{D}_k(\chi)e^{i\psi\hat{a}^\dagger a}\hat{D}(\beta)\hat{S}(\xi)\varrho_T\hat{S}^\dagger(\xi)\hat{D}^\dagger(\beta)e^{-i\psi\hat{a}^\dagger a}\right]\right| = \\
&\left|Tr\left[\hat{S}^\dagger(\xi)\hat{D}^\dagger(\beta)e^{-i\psi\hat{a}^\dagger a}\hat{D}_k(\chi)e^{i\psi\hat{a}^\dagger a}\hat{D}(\beta)\hat{S}(\xi)\varrho_T\right]\right| = \\
&\left|Tr\left[\hat{S}^\dagger(\xi)\hat{D}^\dagger(\beta)\hat{D}_k(e^{-i\psi}\chi)\hat{D}(\beta)\hat{S}(\xi)\varrho_T\right]\right| = \left|Tr\left[\hat{S}^\dagger(\xi)\hat{D}_k(e^{-i\psi}\chi)\hat{S}(\xi)\varrho_T\right]\right| = \\
&\left|Tr\left[\hat{D}_k\left(\coth r\left(e^{-i\psi}\chi - e^{i(\psi+\theta)}\chi^*\tanh r\right)\right)\rho_T\right]\right|.
\end{aligned} \tag{4.48}$$

The equality in the third line is a consequence of the fact that we are interested in the modulus only, so the phase steaming from composition of displacement operators can be neglected. As a result of the calculation we see that consideration of a single mode Gaussian state lead to the modification of the displacement operator parameter, so for the decoherence factor one just needs to modify its modulus. The same conclusion should hold for the generalized overlap and now we show that this is indeed the case.

We start as previously, exploiting the fact that we can pool out of the square root unitary operators and then cancel them with the help of the trace. The relevant expression is

$$B^{mic}_{O,O'}(t) = Tr\sqrt{\sqrt{\varrho_T}\hat{R}\varrho_T\hat{R}^\dagger\sqrt{\varrho_T}}, \tag{4.49}$$

where for the sake of the clarity we introduced an unitary operator

$$\hat{R} = S^\dagger(\xi)\hat{D}^\dagger(\beta)e^{-i\psi\hat{a}^\dagger a}\hat{D}(\chi)e^{i\psi\hat{a}^\dagger a}\hat{D}^\dagger(\beta)\hat{S}^\dagger(\xi). \tag{4.50}$$

The calculations needed to obtain the final result are basically the same as in the case of decoherence. There is only one difference, namely there is no modulus to cancel the phases resulting from composition of displacement operators. However, as we deal with a pair of the conjugated unitary operators their phase must cancel, what allow us to conclude that all the previous steps in calculation of generalized overlap hold also for arbitrary single-mode Gaussian state if one modifies the parameter of the displacement according to

$$\chi \to \left(e^{-i\psi}\chi - e^{i(\psi+\theta)}\chi^*\tanh r\right)\coth r. \tag{4.51}$$

Finlay we can conclude that it is possible to consider a more general initial states of the environment, namely single-mode Gaussian states, and use the formulas derived in two previous Subsections. If one expresses the initial states in terms of parametrization given by equation (4.46), the only necessary modification in leads to the same expressions (4.25,4.45) but with the modulus $|\eta_k(O,t) - \eta_k(O',t)|^2 = |\chi|^2$ substituted by:

$$|\chi|^2 \to \left|\left(e^{-i\psi}\chi - e^{i(\psi+\theta)}\chi^*\tanh r\right)\coth r\right|^2 \tag{4.52}$$

4.4 Detailed discussion of the dependence of the indicator functions on the temperature

From now on we will refer to decoherence factor and generalized overlap as indicator function. The expressions for indicator functions differ only in the temperature dependence. From equations (4.25,4.45) one can easily see that $\lim_{T\to\infty}|\Gamma_{O,O'}(t)| = 0$, this is hot environments decohere the central system better, but as the temperature grows $\lim_{T\to\infty} B^{mac}_{O,O'}(t) = 1$ so they are unable to discriminate the parameter O, without a significant increase of the observed macro-fraction size. In other words, the level of thermal noise increases as the environments are hotter (the initial states ϱ_{0k} are getting closer to the maximally mixed state). As a result, the imprint and extraction of the information on and from such an environment (creating states with orthogonal supports for different values of O) is a very demanding task and in some cases can be even impossible. At this moment we are not able to identify which physical mechanism is responsible for the fact that high temperature environments decohere better than the cold ones. In our opinion this is an interesting open problem. Below we present remarks that can provide some insight into it.

We note that the expression $\coth\left(\frac{\tau_T\omega_k}{2}\right)$ appearing in the decoherence factor is related to the mean initial energy of the environmental oscillators at temperature T, $\coth\left(\frac{\tau_T\omega_k}{2}\right) = \langle E(\omega_k, T)\rangle / E_0(\omega_k)$, where $E_0(\omega) \equiv \hbar\omega/2$ is the zero-point energy of the quantum harmonic oscillator, while $\tanh(\frac{\tau_T\omega_k}{2})$, appearing in the generalized overlap, is nothing else but the purity $tr(\varrho_{0k}^2)$ of the initial thermal state ϱ_{0k}, which in turn is related to the linear entropy $S_{lin}(\varrho_{0k}) = 1 - tr(\varrho_{0k}^2)$. Thus, the effectiveness of the decoherence depends on the initial energy of the environment, while information accumulation on its purity.

One may wonder if the described dependence of decoherence on temperature holds for all non-trivial controlled unitary operators. To illustrate that this not the case we provide an example. For simplicity let us consider a case, in which the system and the environment are two-dimensional. The initial state of the environment is a thermal state

$$\rho_{0k} = \left(1 + e^{-\frac{E}{k_B T}}\right)^{-1} \left(|0\rangle\langle 0| + e^{-\frac{E}{k_B T}}|1\rangle\langle 1|\right) = (1 - q_T)|0\rangle\langle 0| + q_T|1\rangle\langle 1|. \tag{4.53}$$

Now we would like to compare formation of Spectrum Broadcast Structures under two time independent control-unitary operators

$$\hat{U}_{S:E} = |0\rangle\langle 0|_S \otimes \bigotimes_k I_k + |1\rangle\langle 1|_S \otimes \bigotimes_k \hat{Y}_k \quad \hat{U}'_{S:E} = |0\rangle\langle 0|_S \otimes \bigotimes_k I_k + |1\rangle\langle 1|_S \otimes \bigotimes_k \hat{V}_k, \tag{4.54}$$

where the action of $\hat{Y}, \hat{V}$ is given by

$$\begin{aligned} \hat{Y}|0\rangle \to |\tilde{0}\rangle &= \sqrt{1-\epsilon}|0\rangle + \sqrt{\epsilon}|1\rangle \\ \hat{Y}|1\rangle \to |\tilde{1}\rangle &= \sqrt{1-\epsilon}|1\rangle - \sqrt{\epsilon}|0\rangle \end{aligned} \tag{4.55}$$

and

$$\begin{aligned} \hat{V}|0\rangle \to |\bar{0}\rangle &= \sqrt{1-\epsilon}|0\rangle + \sqrt{\epsilon}|1\rangle \\ \hat{V}|1\rangle \to |\bar{1}\rangle &= -\sqrt{1-\epsilon}|1\rangle + \sqrt{\epsilon}|0\rangle \end{aligned} \tag{4.56}$$

respectively. It will prove useful to purify the environment, by introducing an artificial subsystem k' and state $|\phi\rangle_{kk'}$ such that for each k $\rho_k = Tr_{k'}|\phi\rangle\langle\phi|_{kk'}$. In particular we find that the purification of the initial state is

$$|\phi\rangle_{kk'} = \sqrt{1-q_T}|00\rangle_{kk'} + \sqrt{q_T}|11\rangle_{kk'}. \tag{4.57}$$

We initialize the state of the system in a superposed state

$$|\Psi\rangle = \sqrt{p}|0\rangle + \sqrt{1-p}|1\rangle. \tag{4.58}$$

The evolution is then

$$\begin{aligned} \hat{U}_{S:E} \otimes \bigotimes_{k'} I_{k'}|\Psi\rangle_S \otimes \bigotimes_{kk'} |\phi\rangle_{kk'} = \quad & \sqrt{p}|0\rangle_S \otimes \bigotimes_{kk'} \left(\sqrt{1-q_T}|00\rangle_{kk'} + \sqrt{q_T}|11\rangle_{kk'}\right) + \\ & \sqrt{1-p}|1\rangle_S \otimes \bigotimes_{kk'} \left(\sqrt{1-q}|\tilde{0}0\rangle_{kk'} + \sqrt{q_T}|\tilde{1}1\rangle_{kk'}\right) \end{aligned} \tag{4.59}$$

$$\begin{aligned} \hat{U}'_{S:E} \otimes \bigotimes_{k'} I_{k'}|\Psi\rangle_S \otimes \bigotimes_{kk'} |\phi\rangle_{kk'} = \quad & \sqrt{p}|0\rangle_S \otimes \bigotimes_{kk'} \left(\sqrt{1-q_T}|00\rangle_{kk'} + \sqrt{q_T}|11\rangle_{kk'}\right) + \\ & \sqrt{1-p}|1\rangle_S \otimes \bigotimes_{kk'} \left(\sqrt{1-q_T}|\bar{0}0\rangle_{kk'} + \sqrt{q_T}|\bar{1}1\rangle_{kk'}\right). \end{aligned} \tag{4.60}$$

The action of controlled unitary operation on pure system-environment states results in the so-called branch structure: each branch consists of environmental states evolving according to a given system's state. In our example there are two branches:the first one consists of the states that are not affected by the evolution (if the system's state is $|0\rangle$), whereas the second one of these transformed according to $\bigotimes_k \hat{Y}_k$ (or $\bigotimes_k \hat{V}_k$). Although we introduced purifying subsystems, we do not need to trace them out before performing the calculation of decoherence factor and we can simply calculate scalar product between states of different branches. This is

because for control-type unitary operators we have

$$\Gamma^k_{ij} = Tr_k(\hat{U}^k_i \rho_{0k} \hat{U}^{k\,\dagger}_j) = Tr_{kk'}(\hat{U}^k_i \otimes I_{k'} |\varphi\rangle\langle\varphi|_{kk'} \hat{U}^{k\,\dagger}_j \otimes I_{k'}) = \langle\varphi| U^{k\,\dagger}_j \hat{U}^k_i \otimes I_{k'} |\varphi\rangle_{kk'}, \quad (4.61)$$

Calculating decoherence factors (for single environmental subsystem) in the cases considered here we obtain

$$\Gamma^{k,\hat{Y}} = \sqrt{1-\epsilon} \quad (4.62)$$

$$\Gamma^{k,\hat{V}} = \sqrt{1-\epsilon}(1-2q_T). \quad (4.63)$$

From the above equations one can see that in the first case the decohering power of a single environment is constant and depend only on the interaction. However, in the second case the temperature (via parameter q_T) also influences the decoherence. In fact, as temperature grows $q_T \xrightarrow{T\to\infty} \frac{1}{2}$ so $\Gamma^{k,\hat{V}} \xrightarrow{T\to\infty} 0$. This means that in high temperatures not observing a single environment results in a significant decoherence process, just as it was in the previously discussed case of continuous variables.

As decoherence process is caused by the fact that the system correlates to the environment in a non-classical way, one could intuitively expect that the "correlating power" of unitary $\hat{U}'_{S:E}$ depends on the temperature of initial state of the environment. To support this claim we could investigate the entanglement between a single subsystem of environment and the system. However, as our physical subsystems k are initially in a mixed states, computing entanglement measures is not an easy task. For this reason it is more convenient to deal with the purified states and we compute entanglement between a chosen purified subsystem nn' and the rest of the system-environment state, so we introduce a partition $S\overline{nn'} : nn'$, where $\overline{nn'}$ denotes all environmental subsystems but for nn'. For pure bipartite states $\rho_{A:B} = |\Psi\rangle\langle\Psi|_{A:B}$ a good entanglement quantifier is entanglement entropy defined as a von Neumann entropy of the reduced state

$$S(\rho_{A:B}) = -Tr\left(\rho_A \log \rho_A\right) = -Tr\left(\rho_B \log \rho_B\right), \quad (4.64)$$

where ρ_A, ρ_B are respective reduced states. Non-zero value of entanglement entropy indicates that there is entanglement in a given cut. From equations (4.59, 4.60) we can easy obtain the reduced states of a single environmental subsystem $\rho^{\hat{Y}}_{kk'}$ and $\rho^{\hat{V}}_{kk'}$ respectively and calculate the entanglement entropy. The results are presented in Figure 4.1. It can be clearly seen that indeed in the second case, when the evolution is given by $\hat{U}'_{S:E}$, the value of entanglement entropy grows as a function of q_T (so also as a function of temperature) indicating growth of entanglement in partition $S\overline{nn'} : nn'$.

In the case of controlled unitary operators it is even possible to predict the behavior of

decoherence factor as a function of temperature without the need of performing detailed calculations. We assume that the controlled unitary is of a form $\sum_i |i\rangle\langle i| \otimes \bigotimes_k^N \hat{Y}_i^k$. We note that as the temperature grows the d dimensional initial thermal state of the environment approaches maximally mixed state

$$\rho_{0k} \xrightarrow{T\to\infty} \frac{1}{d}\sum_l |l\rangle\langle l|, \tag{4.65}$$

so

$$\Gamma_{ij}^k \xrightarrow{T\to\infty} \frac{1}{d} Tr\left(\hat{Y}_i^k \sum_l |l\rangle\langle l| \hat{Y}_j^{k\,\dagger}\right) = \frac{1}{d} Tr\left(\hat{Y}_i^k \hat{Y}_j^{k,\dagger}\right). \tag{4.66}$$

As a result, for the controlled unitary the condition guarantying the increased strength of decoherence process with growing temperature is

$$Tr\left(\hat{Y}_i^k \hat{Y}_j^{k,\dagger}\right) = 0. \tag{4.67}$$

We started this Chapter discussing a control unitary (4.14)

$$\hat{U}_{S:E} = \sum_O |O\rangle\langle O| \otimes \bigotimes_{k=1}^N \hat{e}^{i\xi_k(O,t)} e^{-i\hat{H}^k t/\hbar} \hat{D}_k(\eta_k(O,t)),$$

where the environment is collection of continuous variable systems – harmonic oscillators. As in this case the decoherence process also becomes stronger with growing temperature, it is tempting to directly apply condition (4.67) to see if the intuition from finite-dimensional systems can be adapted to infinite-dimensional ones. However, one should be more careful since the maximally mixed state is not well defined in the continuous setting. Yet, succumbing to the temptation, we note that for displacement operators it is known that $Tr(\hat{D}_k(\eta_k)\hat{D}_k^\dagger(\eta_{k'})) = \delta(\eta_k - \eta_{k'})$, where $= \delta(x)$ is Dirac's delta distribution. As a result, it seems plausible that after performing detailed analysis a rigorous statement similar to (4.67) could be made. We leave this as an open problem.

Now we turn our attention to the information content of the environment. It turns out that although evolutions $\hat{U}_{S:E}$, $\hat{U}'_{S:E}$ lead to decoherence processes that behave differently with temperature, there is no difference concerning the distinguishability of environmental subsystems. However, now one should be careful as the purifying subsystems may be highly misleading: observers have access only to the physical subsystems k, they deal with states $\rho_{0k}, \rho_k^{\hat{Y}} = \hat{Y}_k \rho_{0k} \hat{Y}_k^\dagger$ and $\rho_k^{\hat{Y}} = \hat{V}_k \rho_{0k} \hat{V}_k^\dagger$ so the distinguishability should be calculated accordingly to the definition (equation (4.29)) and it can be not expressed as scalar product of purifications

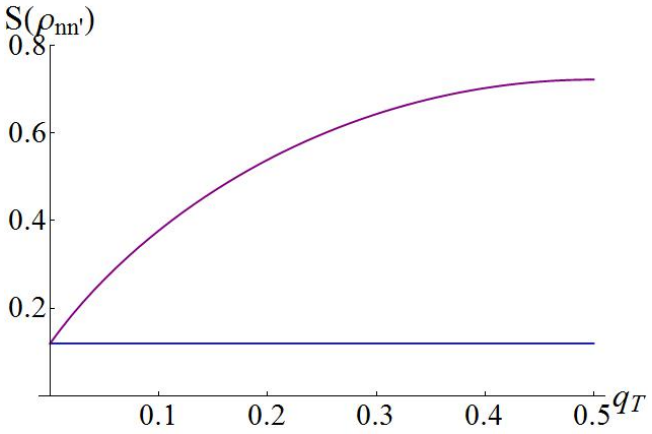

FIGURE 4.1: The entanglement entropy of $\rho^{\hat{Y}}_{kk'}$ (the lower trace) and $\rho^{\hat{V}}_{kk'}$ (the upper trace) as the function of the initial mixedness of the environment parametrized by q_T (for details see text). Only in the second case the amount of quantum entanglement changes with q_T. In this example $\epsilon = 0.1$.

that we introduced. In Figure 4.2 we present results of the correct procedure: generalized overlap $B(\rho_{0k}, \rho^{\hat{Y}}_k)$ as a function of parameter q_T. The results for $B(\rho_{0k}, \rho^{\hat{V}}_k)$ are the same what can be easily seen noting that $\hat{V} = \sigma_3\hat{Y}$ and $\rho_{0k} = \sigma_3\rho_{0k}\sigma_3$ so we can use the unitary invariance of generalized overlap

$$B\left(\rho_{0k}, \hat{V}_k\rho_{0k}\hat{V}_k^\dagger\right) = B\left(\sigma_3\rho_{0k}\sigma_3, \sigma_3\hat{Y}_k\rho_{0k}\hat{Y}_k^\dagger\sigma_3\right) = B\left(\rho_{0k}, \hat{Y}_k\rho_{0k}\hat{Y}_k^\dagger\right). \tag{4.68}$$

The behavior shown in Figure 4.2 is not of a big surprise. When $q_T = 0$ the initial state of the environment is pure and the value of generalized overlap coincides with the value of decoherence factor $\sqrt{1-\epsilon}$. For $q_T = \frac{1}{2}$ the state of the environment is maximally mixed, this implies in turn that

$$\rho^{\hat{Y}}_k = \hat{Y}_k\rho_{0k}\hat{Y}_k^\dagger = \hat{Y}_k I_k\hat{Y}_k^\dagger = I_k = \rho_{0k}. \tag{4.69}$$

The level of noise is too high to encode information, the two states remain indistinguishable and nothing can be learned from them about the state of the central system. This fact shows that the local records of classical information about the system are not necessary for decoherence process to happen. The individual environmental subsystem can carry vanishingly small amount of information about the system, yet causing a significant destruction of coherences at the level of partially-reduced state. From this example it can be seen that the nature of decoherence process is really a quantum one: the information about the coherences is delocalized and encoded at the level of the total state and can have no effect on states of individual subsystems.

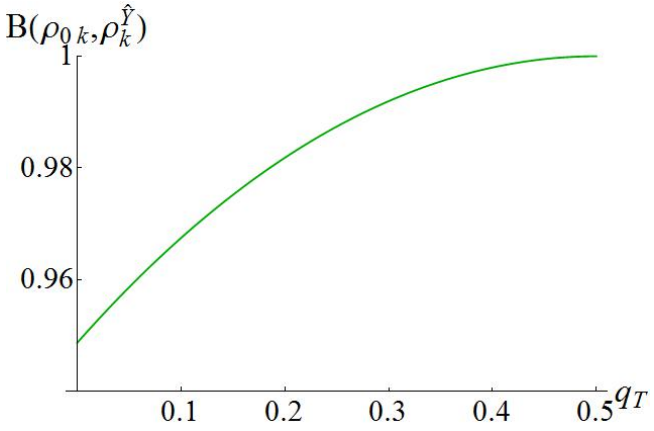

FIGURE 4.2: Distinguishability of environmental states $\rho_{0k}, \rho_k^{\hat{Y}}$ measured by generalized overlap as the function of the initial mixedness of the environment parametrized by q_T (for details see text). In this example $\epsilon = 0.1$.

4.5 Concluding remarks

Summarizing, in this chapter we considered the case when the environment consists of harmonic oscillators and the central system acts on it via displacement operator. We showed that this in true for broad class of Hamiltonians, when the environment couples to a central system via linear combination of position and momentum observables.

In this setting we derived expressions for functions indicating the Spectral Broadcast Structure formation – decoherence factor and generalized overlap. Initially the derivations were performed for thermal states of the environment and subsequently we generalized them to the case of arbitrary single mode Gaussian states.

We discussed also the dependence of the indicator functions on the temperature. For the considered case, the temperature growth enhances the decoherence process. The opposite is true for the generalized overlap – the hotter the environment gets the more noise there is making the imprint of information of the central system on the environment (and it's potential readout) hard to achieve.

We provided an explicit example showing that the decoherence behavior presented above is not general. The enhancement depends on the form of the interaction. We showed that in some cases the strength of the correlations between the system and the environment growths with temperature. For the case of the controlled unitary operators acting in finite dimensional Hilbert spaces we provided necessary condition for the discussed behavior and we conjectured that a similar one should hold for continuous variable scenarios. We showed also that the classical information deposited in the environment must decline with growing temperature.

Chapter 5

Spectrum Broadcast Structures in Quantum Brownian Motion model

5.1 Introduction

In this Chapter we focus on one of the mentioned canonical models of decoherence, namely on the Quantum Brownian Motion model. This is a one-dimensional model consisting of a particle interacting with an environment of harmonic oscillators in a linear way (although the non-linear extensions has also been considered [85]). Apart form decoherence theory, Quantum Brownian Motion has been also used as a toy model to explain the emergence of friction from the unitary dynamics of quantum theory (see for example [86]). Thus it is one of the most studied and important models not only for Quantum to Classical transition but also for quantum dissipative systems and numerous works has been devoted to study its properties. Therefore, this model is a natural candidate for the investigation of Spectrum Broadcast Structure formation, what had not been performed before we started working on the thesis. The results presented in this Chapter are partially based on [77, 87, 88].

5.2 The model

We specify the central system S to be a harmonic oscillator of a mass M and a frequency Ω, linearly coupled to the environment E—a bath of N oscillators, each of a mass m_k and a frequency ω_k, $k = 1, \ldots, N$. The total Hamiltonian is [8, 49]:

$$\hat{H}_{S:E} = \frac{\hat{P}^2}{2M} + \frac{M\Omega^2\hat{X}^2}{2} + \sum_{k=1}^{N}\left(\frac{\hat{p}_k^2}{2m_k} + \frac{m_k\omega_k^2\hat{x}_k^2}{2}\right) + \hat{X}\sum_{k=1}^{N} C_k\hat{x}_k, \tag{5.1}$$

where $\hat{X}, \hat{P}$ are the system's variables, $\hat{x}_k, \hat{p}_k$ describe the k-th environmental oscillator, and C_k are the coupling constants. We denote the system's self-Hamiltonian by $\hat{H}_S$, while the k-th environmental by $\hat{H}_k$.

As has been explained in previous Chapters we are interested in properties of a partially-reduced state describing the central system and some environmental degrees of freedom. Apart from the usual decoherence process caused by the non-observed fraction of the environment, we would like to focus on the transfer of classical information about the system to the environment. From perspective of our aims, effects that usually capture attention in studies of open systems, such as dissipation of the central system caused by the interaction with the environment, are of secondary importance. For this reason we will assume that the central system is very massive, so it is effectively macroscopic and will neglect all the back-reaction of the environment – this approximation in the literature concerning decoherence is known as recoilless limit [8, 49]. We note that this is exactly the opposite regime to that usually studied in open system's literature concerning Quantum Brownian Motion [8]. One of the most widely applied approximations in the latter is the so called Born approximation stating that the influence of the central system on the environment is small so that at all times t the description of the total system factorizes with respect to the central system-environment cut

$$\rho_{S:E}(t) \approx \rho_S(t) \otimes \rho_E. \tag{5.2}$$

In such a setting the transfer of information from the system to the environment is obviously not possible as one explicitly assumes that there are no correlations between the former and the latter. As a result, in our investigation we cannot use most techniques developed in studies of open quantum systems (more precisely try to adopt them as in open systems the main object of study is reduced state of the system alone, not the partially reduced system-environment state that we are interested in).

The Hamiltonian (5.1) is more complicated that the ones studied previously in the thesis, as it contains non-trivial self-Hamiltonian of the central system. Before addressing the full problem, to get better insights into the model, in the following Subsections we study two simplified cases using approximations known as Full and Partial Quantum Measurement limits. In the former one neglects the self-Hamiltonians of the system and the environment and in the latter the self-Hamiltonian of the environment is restored. Finally in Section 5.5 we deal with the full model in the mentioned recoilless limit.

In almost all considerations we will assume that initially the environment is in the thermal state of temperature T. The only exception is found in Section 5.5.7, where we investigate influence of squeezing of the initial state of the environment on the Spectrum Broadcast Structure formation. As in Chapter 4, to keep formulas concise, the temperature dependence of indicator functions (decoherence factor and generalized overlap) is expressed in terms of thermal time $\tau_T = \hbar/(k_B T)$.

5.2.1 Continuous versus discrete description of the environment

To proceed further with the analysis, we would like to make some comments on the environment.

While dealing with the model (or more generally with models of open quantum systems), the standard procedure [8, 12, 49, 56, 89, 90] is to pass to a continuum limit of frequencies ω_k and encode the properties of the environment in a specific continuous approximation to the spectral density function $J(\omega) = \sum_k C_k^2/(2m_k\omega_k)\delta(\omega - \omega_k)$. This approach usually allows one to arrive at closed expressions for quantities of interest, as the sums are transformed into integrals that are easier to handle.

Although the discussed choice is considered to be the standard one, it is obviously not the only one. One can always decide to work with the discrete spectrum environmental subsystems. Let us comment on advantages and disadvantages of this approach.

From technical side, discrete set of random frequencies implies that the functions indicating Spectrum Broadcast Structure formation are almost periodic functions of time. Although the theory of such functions has been developed for some time [91], the questions that we would like to answer are harder to deal with than in the continuous spectral density approach. In the case of simplified Quantum Brownian Motion models presented in Sections 5.3 and 5.4 we overcome the difficulties using the known results from the theory of almost periodic functions. The situation is more complicated while dealing with the full model in Section 5.5 as there we were not able to find techniques that can be straightforwardly applied to investigate the indicator functions. Of course, nothing prevents us from plotting the indicator functions for a chosen set of frequencies and analyze their properties with respect to parameters such as temperature, the initial state of the environment or number of oscillators forming observed or unobserved fractions of the environment. Indeed, we do so in Subsection 5.5.3 and show that it allows to gain insights into and draw conclusions about the process of Spectrum Broadcast Structure formation in Quantum Brownian Motion model. However, some readers (as well as the author of the thesis) may not consider this way to be the most satisfactory one. Adapting the remark made by Philip W. Anderson in his Nobel speech to our (much more humbler) problem, the analysis relying on numerical plots leave us with the impression that "it has yet to receive adequate mathematical treatment" as "the one has to resort to the indignity of numerical simulations to settle even the simplest questions about" the process (quotations from Nobel Lecture [92]). To address the problem in a more mathematically rigorous way in Subsection 5.5.8 we perform an analytical analysis based on Law of Large Numbers.

The fact that the functions indicating the Spectrum Broadcast Structure formation are almost periodic functions of time has one more important consequence. In principle it implies that the Spectrum Broadcast Structure, if formed, will be destroyed at some time since there is a recurrence time in which the indicator functions – decoherence factor and generalized overlap

– will come back to their initial values. This could be seen as the "reversal" of the objectification process as the non-classical correlations between system and the observed fragment of the environment will be restored. However, the recurrence time is inversely proportional to the minimal difference of the two frequencies of the environmental degrees of freedom [89]. As a result it could be, in principle, arbitrarily large (some author claim that in some cases it is longer that the estimated age of the Universe) and it does not influence our investigation.

On the other hand, the discrete set of the environmental frequencies is not only the source of technical problems as it has an interpretative advantage that, in opinion of the author, overwhelms all the mentioned drawbacks of the approach. In the case of Spectrum Broadcast formation it is very interesting to find numbers of environmental subsystems needed to achieve the process in question, this is the number of subsystems that need to pass unobserved to decohere the central system and the number of subsystems needed to extract the information about it. This is a clear motivation of our approach to keep the spectrum discreet, although, as has been mentioned, this is not the standard treatment.

In most cases we will work in a setting, in which frequencies ω_k are chosen randomly from some given ensemble. For definiteness' sake we study here the simplest case, where the frequencies ω_k are independently, identically distributed (i.i.d.) with a uniform distribution over a finite interval $[\omega_L, \omega_U]$. This choice of the environment may be considered as a direct, "mechanstic", as opposed to the usual field treatment of the environment. The bath is a collection of identical mechanical oscillators with masses m_k and random frequencies ω_k.

Unless stated otherwise, for the sake of simplicity we assume a symmetric situation, in which the observed and unobserved groups of the environment contain the same number of degrees of freedom. We call these groups macro-fractions. As a result, the size of the traced macro-fraction $(1-f)E$ will be the same as the size of the observed one mac. One can argue that such a choice does not fulfill the conditions of Definition 2.6 since it does not allow to encompass "many observers". However, we do not make any assumptions on the total number of remaining environmental subsystems that are accessible to the observers.

5.3 Full Quantum Measurement limit and exact timescales

We first consider a highly simplified model, with dominating interaction term, and completely neglect self-Hamiltonians of both the system and the environment:

$$\hat{H}_{S:E} = \hat{X} \otimes \sum_{k=1}^{N} C_k \hat{x}_k. \tag{5.3}$$

In the decoherence literature, this is called Quantum Measurement Limit due to the fact that the Hamiltonian represents an ideal von Neumann measurement of the system observable $\hat{X}$

by the environments [93]. Such a simplified model allows us to obtain the character and the timescales of the Spectrum Broadcast Structure formation. As the Hamiltonian (5.3) is time independent it is easy to solve the dynamics. The corresponding evolution is of the controlled unitary type with X as the control parameter:

$$\hat{U}(t) = \int dX |X\rangle\langle X| \otimes \bigotimes_{k=1}^{N} \hat{D}_k \left(-\frac{iC_k t}{\sqrt{2}} X \right), \tag{5.4}$$

where $\hat{D}(\alpha) = e^{\alpha a^\dagger - \alpha^* a}$ is the displacement operator and we have set the oscillators masses and the frequencies to unity. Since the evolution operator is just of the form (4.14), the expressions for decoherence factor and generalized overlap can be obtained (after suitable modification) from results of the previous Chapter. We assume that the environment is in the thermal state so

$$\left|\Gamma_{X,X'}(t)\right| = \exp\left[-\frac{|X-X'|^2}{2} t^2 \coth\left(\frac{\tau_T}{2}\right) \sum_{k\in(1-f)E} C_k^2 \right], \tag{5.5}$$

$$B^{mac}_{X,X'}(t) = \exp\left[-\frac{|X-X'|^2}{2} t^2 \tanh\left(\frac{\tau_T}{2}\right) \sum_{k\in mac} C_k^2 \right], \tag{5.6}$$

where $\tau_T = \hbar/(k_B T)$ is thermal time. One immediately sees that in the Quantum Measurement limit there is always a formation of the spectrum broadcast structure, and hence objectivisation of the system's position X, described by the Gaussian decay in time of $\left|\Gamma_{X,X'}(t)\right|$, $B^{mac}_{X,X'}(t)$. Quite surprisingly, one does not even have to assume random coupling constants C_k as for example in the spin systems [7]. If, however, one assumes random that coupling constants C_k's are independent and identically distributed random variables with a finite average $\overline{C^2} < \infty$, the Law of Large Numbers [94] can give new insight into the problem. It states (in its strong form) that the averages $\sum_{k\in(1-f)N} C_k^2$, $\sum_{k\in mac} C_k^2$ converge almost surely, this is with probability one, to their expectation values (rescaled by the number of terms entering the sums: $(1-f)N$ and N_{mac}). By $(1-f)N$ with $f \in (0,1)$ and N_{mac} we denoted sizes of the unobserved macrofraction and (one of the) observed one respectively. As a result we have

$$\left|\Gamma_{X,X'}(t)\right| \underset{N\to\infty}{\approx} \exp\left[-(1-f)N \frac{|X-X'|^2}{2} \overline{C^2} t^2 \coth\left(\frac{\tau_T}{2}\right) \right] = e^{-(1-f)N\left(\frac{t}{\tau_D}\right)^2}, \tag{5.7}$$

$$B^{mac}_{X,X'}(t) \underset{N\to\infty}{\approx} \exp\left[-N_{mac} \frac{|X-X'|^2}{2} \overline{C^2} t^2 \tanh\left(\frac{\tau_T}{2}\right) \right] = e^{-N_{mac}\left(\frac{t}{\tau_B}\right)^2}, \tag{5.8}$$

The characteristic timescales of the processes are given by, respectively:

$$\frac{1}{\tau_D} = |X-X'| \sqrt{\frac{\coth(\tau_T/2)}{2} \overline{C^2}}, \tag{5.9}$$

$$\frac{1}{\tau_B} = \left|X - X'\right| \sqrt{\frac{\tanh(\tau_T/2)}{2}\overline{C^2}}, \tag{5.10}$$

with the second being in general larger than the first for a given temperature T. This is the effect of noise—it obviously slows down the accumulation of information in environmental macrofractions.

5.4 Partial Quantum Measurement Limit

Inclusion of the self-Hamiltonians of the environment lead to the Hamiltonian:

$$\hat{H}_{S:E} = \sum_{k=1}^{N}\left(\frac{\hat{p}_k^2}{2m_k} + \frac{m_k\omega_k^2\hat{x}_k^2}{2}\right) + \hat{X}\otimes\sum_{k=1}^{N} C_k\hat{x}_k, \tag{5.11}$$

which still allows for an exact solution.

Using the results of Chapter 4, we find that the evolution operator is given by

$$\hat{U}(t) = \int dX|X\rangle\langle X| \otimes \bigotimes_{k=1}^{N} e^{i\xi_k(t)X^2} e^{-i\hat{H}^k t/\hbar}\hat{D}_k\left(\alpha_k(t)X\right), \tag{5.12}$$

$$\alpha_k(t) = -\frac{C_k}{\sqrt{2\hbar\hbar m_k\omega_k^3}}\left(e^{i\omega_k t} - 1\right),\ \xi_k(t) = \frac{C_k^2}{2\hbar m_k\omega_k^3}\left(\omega_k t - \sin(\omega_k t)\right). \tag{5.13}$$

As in the case of full quantum measurement limit, assuming that the environment is initially in the thermal state, the expressions for decoherence factor and generalized overlap are readily obtained from (4.25) and (4.45) respectively. For random ω_k's, the decoherence factor and generalized overlap become almost periodic functions of time:

$$\left|\Gamma_{X,X'}\right| = \exp\left[\frac{|X-X'|^2}{2}\sum_{k\in(1-f)E}\coth\left(\frac{\tau_T\omega_k}{2}\right)\frac{C_k^2\left(\cos\omega_k t - 1\right)}{\hbar m_k\omega_k^3}\right], \tag{5.14}$$

$$B_{X,X'}^{mac}(t) = \exp\left[\frac{|X-X'|^2}{2}\sum_{k\in mac}\tanh\left(\frac{\tau_T\omega_k}{2}\right)\frac{C_k^2\left(\cos\omega_k t - 1\right)}{\hbar m_k\omega_k^3}\right], \tag{5.15}$$

where $\tau_T = \hbar/(k_B T)$. The functions are too complicated for an immediate analytical studies. As we will show for the full model, the useful tool is again the Law of Large Numbers. However, it turns out that using the theorem from the theory of almost periodic functions [95] one can evaluated the time averages $\left\langle|\Gamma_{X,X'}|\right\rangle = \lim_{\tau\to\infty}\frac{1}{\tau}\int_0^\tau dt|\Gamma_{X,X'}(t)|$, $\left\langle B_{X,X'}^{mac}\right\rangle = \lim_{\tau\to\infty}\frac{1}{\tau}\int_0^\tau dt B_{X,X'}^{mac}(t)$, noting that the amplitudes of the cosine functions in (5.14,5.15) are all non-negative. This approach allows to obtain the results in an easier way in comparison to the Law of Large Numbers. We believe that this is an interesting (and to the best of our knowledge

novel) application of the theory of almost periodic functions in context of decoherence and information transfer studies thus we present the derivation and the results in next Subsection.

5.4.1 Time averages of almost periodic functions with positive coefficients

We evaluate the time average:

$$\lim_{\tau\to\infty}\frac{1}{\tau}\int_0^\tau dt\exp\left[\frac{|X-X'|^2}{2}\sum_{k\in(1-f)E}\frac{C_k^2\cos\omega_k t}{m_k\omega_k^3}\coth\left(\frac{\tau_T\omega_k}{2}\right)\right]. \tag{5.16}$$

The crucial step is to use one of the results from [95], which states a form of ergodicity for such functions. Namely, due to the positive amplitudes of the trigonometric functions, the time average can be substituted with the ensemble average (average over the angles in this case). This gives:

$$\begin{aligned}
&\lim_{\tau\to\infty}\frac{1}{\tau}\int_0^\tau dt\prod_{k\in(1-f)E}\exp\left[\frac{|X-X'|^2}{2}\frac{C_k^2\cos\omega_k t}{m_k\omega_k^3}\coth\left(\frac{\tau_T\omega_k}{2}\right)\right] \qquad (5.17)\\
&=\prod_{k\in(1-f)E}\frac{1}{2\pi}\int_0^{2\pi}d\theta_k\exp\left[\frac{|X-X'|^2}{2}\frac{C_k^2}{m_k\omega_k^3}\coth\left(\frac{\tau_T\omega_k}{2}\right)\cos\theta_k\right]\\
&=\prod_{k\in(1-f)E}\mathrm{I}_0\left[\frac{|X-X'|^2}{2}\frac{C_k^2}{m_k\omega_k^3}\coth\left(\frac{\tau_T\omega_k}{2}\right)\right],
\end{aligned}$$

where the last step we used the definition of the Bessel integral, giving the modified Bessel function of the first kind: $\mathrm{I}_0(z)=(1/\pi)\int_0^\pi d\theta e^{z\cos\theta}$.

As a result the time averages of (5.14,5.15) are

$$\begin{aligned}
\left\langle|\Gamma_{X,X'}|\right\rangle = \quad & \exp\left[-\frac{|X-X'|^2}{2}\sum_{k\in(1-f)E}\frac{C_k^2\coth(\tau_T\omega_k/2)}{m_k\omega_k^3}\right]\times \qquad (5.18)\\
& \prod_{k\in(1-f)E}\mathrm{I}_0\left[\frac{|X-X'|^2C_k^2\coth(\tau_T\omega_k/2)}{2m_k\omega_k^3}\right],\\
\left\langle B_{X,X'}^{mac}\right\rangle = \quad & \exp\left[-\frac{|X-X'|^2}{2}\sum_{k\in mac}\frac{C_k^2\mathrm{th}(\beta\omega_k/2)}{m_k\omega_k^3}\right]\times \qquad (5.19)\\
& \prod_{k\in mac}\mathrm{I}_0\left[\frac{|X-X'|^2C_k^2\tanh(\tau_T\omega_k/2)}{2m_k\omega_k^3}\right],
\end{aligned}$$

The rationale behind studying time averages is that since the functions themselves are non-negative, vanishing of the time averages is a good measure of the functions being practically zero. We are again interested in the scaling of the averages with the macrofraction sizes, for

simplicity assuming them here to be equal: $(1-f)E = N_{mac}$. We also assume C_k's to be only mass-dependent (and not random), $C_k = \sqrt{\frac{M m_k \tilde{\gamma}_0}{\pi}}$, with M the mass of the central system and $\tilde{\gamma}_0$ some constant. The scaling of the indicator functions with respect to the macrofraction size can be evaluated in the large separation limit:

$$\frac{\sqrt{M\tilde{\gamma}_0}|X-X'|}{\omega_k^{3/2}} \gg 1 \text{ for every } k, \tag{5.20}$$

which allows one to use the asymptotic expansion $\mathrm{I}_0(x) \approx e^x/\sqrt{2\pi x}$. Assuming further low temperature limit, $\tau_T \to \infty$ (from (5.15) $B^{mac}_{X,X'}$ rises with T), one obtains:

$$\left\langle \left| \Gamma_{X,X'} \right| \right\rangle \approx \prod_{k=1}^{N_{mac}} \frac{\omega_k^{3/2}}{\sqrt{M\tilde{\gamma}_0}|X-X'|}, \tag{5.21}$$

and the same for $\left\langle B^{mac}_{X,X'} \right\rangle$, as $\tanh(\tau_T\omega_k/2) \approx 1 \approx \coth(\tau_T\omega_k/2)$ in (5.19,5.20). We perform further averaging over the random frequencies ω_k, assuming they are i.i.d. with a uniform distribution over a spectrum interval Δ, centered at some $\bar{\omega} \gg \Delta$. This gives:

$$\overline{\left\langle \left| \Gamma_{X,X'} \right| \right\rangle} = \int_{\bar{\omega}-\frac{\Delta}{2}}^{\bar{\omega}+\frac{\Delta}{2}} \prod_j \frac{d\omega_j}{\Delta} \left\langle \left| \Gamma_{X,X'} \right| \right\rangle \approx e^{-N_{mac}\left(\log \frac{\sqrt{M\tilde{\gamma}_0}|X-X'|}{\bar{\omega}^{3/2}}\right)} \tag{5.22}$$

and the same for the generalized overlap, due to the assumed low temperature limit:

$$\overline{\left\langle B^{mac}_{X,X'} \right\rangle} = \int_{\bar{\omega}-\frac{\Delta}{2}}^{\bar{\omega}+\frac{\Delta}{2}} \prod_j \frac{d\omega_j}{\Delta} \left\langle \left| B^{mac}_{X,X'} \right| \right\rangle \approx e^{-N_{mac}\left(\log \frac{\sqrt{M\tilde{\gamma}_0}|X-X'|}{\bar{\omega}^{3/2}}\right)}. \tag{5.23}$$

This is the desired scaling. One sees that whenever (5.20) holds, for low temperatures, both averages exponentially decay in the thermodynamic limit $N \to \infty$, indicating formation of the spectrum broadcast state.

5.5 The full model

After presenting simplified cases we are ready to restore the system's self Hamiltonian and discuss the full model in the recoilless limit.

5.5.1 The dynamics

As has been already mentioned, the full model can be in principle solved explicitly either directly [89] or using Wigner functions [96]. However, let us stress that because, unlike as in the standard treatments, we are interested here not merely in the reduced state of the central

oscillator alone but in the joint state of the central system and a part of bath oscillators, the mentioned exact methods do not produce manageable solutions or, at least at this moment, we were not able to use them for our purpose. Our main focus is on the decoherence process and the transfer of classical information about the system to the environment. Questions concerning for example dissipation are not of a crucial importance here so for the purpose of the study we will try to eliminate the dissipation caused by the non-observed fractions of the environment. This suggest a greatly simplifying assumption of a massive central system known as the recoilless limit [8, 49], which we will adopt. One can then use a non-adiabatic version of the Born-Oppenheimer approximation (see for example [97]), in which the motion of the central oscillator is separated from the motion of the environment.

We assume that, in the recoilless limit, the central system evolves unperturbed according to it's Hamiltonian $\hat{H}_S = \hat{P}^2/2M + M\Omega^2\hat{X}^2/2$ (with the renormalized frequency $\Omega^2 \equiv \Omega_0^2 - \sum_k C_k^2/(2m_k\omega_k^2)$). To see how this dynamics influences evolution of the environment we represent the central system free propagator

$$K_t(X; X_0) \equiv \langle X|e^{-i\hat{H}_S t/\hbar}|X_0\rangle, \tag{5.24}$$

with the help of the classical path $X(t; X_0)$, starting at $t = 0$ at X_0 and reaching X at time t. In our case (the oscillator) this semi-classical approximation is exact [98]. Now we parametrize the evolution of the environment along each classical trajectory. The motion of the central system, represented by path $X(t; X_0)$, acts on the environment as a external driving force via interaction Hamiltonian $\hat{H}_{INT}(X(t; X_0)) = X(t; X_0)\sum_{k=1}^N C_k\hat{x}_k$ (note that in the standard Born-Oppenheimer approximation such parametrization is performed with respect to a static quantity – position of a nucleus). As a result, for a fixed trajectory $X(t; X_0)$ the evolution of the environment is governed by

$$i\hbar\frac{\partial}{\partial t}|\psi_E(t)\rangle = \hat{H}_E\left(X(t; X_0)\right)|\psi_E(t)\rangle, \tag{5.25}$$

where $\hat{H}_E\left(X(t; X_0)\right) \equiv \sum_{k=1}^N \left[\hat{p}_k^2/(2m_k) + m_k\omega_k^2\hat{x}_k^2/2\right] + X(t; X_0)\sum_{k=1}^N C_k\hat{x}_k$. This means that we deal with forced Harmonic oscillator, a situation similar to this encountered in Chapter 4. The full system-environment state is constructed using the Born-Oppenheimer type of an ansatz, which takes into account all the possible trajectories of the central system:

$$\Psi_{S:E}^{NBO}(X, \mathbf{x}) = \int dX_0\phi_{S0}(X_0)\langle X|e^{-i\hat{H}_S t/\hbar}|X_0\rangle\langle \mathbf{x}|\hat{U}_E(X(t; X_0))|\psi_{E0}\rangle, \tag{5.26}$$

with $|\phi_{S0}\rangle, |\psi_{E0}\rangle$ being the initial states of the system and the environment respectively and $\hat{U}_E(X(t; X_0))$ is a solution of (5.25). Note that this is a similar reasoning to the path integral

techniques concerning open quantum systems, namely the Feynman-Vernon influence functional [99, 8].

From the type of the coupling in (5.1) and the analysis of the previous Section it could be anticipated that the candidates for the pointer states will be related to the position eigenstates. Hence, initial states of the system with large coherences in the position are of the greatest interest for the purpose of this study since we expect them to be affected by the coupling to a great extend. Therefore a good candidate is a momentum squeezed state due to its large coherences in the position. In the limit of large squeezing we may than assume that the initial velocity of each trajectory is zero so that $X(t;X_0) = X_0\cos(\Omega t)$. We will perform also the analysis for initial position squeezed state, which initially does not posses coherences in position eigenbasis but they are created due to the dynamics of the central system (position squeezed state evolves into momentum squeezed one). In this case $X_0 = 0$ and $X(t;X_0) = X_0\sin(\Omega t)$. As a result the classical trajectories to be considered are $X(t;X_0) = X_0\cos(\Omega t)$, $X(t;X_0) = X_0\sin(\Omega t)$ for momentum and position squeezed states respectively. A similar choice was made in context of Quantum Darwinism studies [56, 90].

The driven evolution of the environment is solved in an analogous steps to those presented in Section 4.2. Once again the Hamiltonian governing the evolution of a single environmental degree of freedom (equation (5.25)) is that of the forced quantum harmonic oscillator, where the driving force is provided by the central system. Adopting the notation of Section 4.2 we have

$$\alpha_k'(t) \equiv -\frac{iC_k}{\sqrt{2\hbar m_k\omega_k}}e^{i\omega_k t} \qquad f(X_0,t) \equiv X(t;X_0). \tag{5.27}$$

Finally, for the considered cases of squeezed states we consider following trajectories $X(t;X_0) = X_0\cos(\Omega t)$ for momentum squeezed states and $X(t;X_0) = X_0\sin(\Omega t)$ for the position squeezed states. As a result the driven evolution is of a form

$$\hat{U}_E(X_0\cos\Omega t) = \bigotimes_{k=1}^{N} e^{i\xi_k(X_0,t)}e^{-i\hat{H}_k t/\hbar}\hat{D}\left(\eta_k(X_0,t)\right) \equiv \bigotimes_{k=1}^{N}\hat{U}_k(X_0,t), \tag{5.28}$$

$$\eta_k(X_0,t) = \int_0^t d\tau\alpha_k'(\tau)X_0\cos(\Omega\tau) = -\frac{C_k}{2\sqrt{2\hbar m_k\omega_k}}\left[\frac{e^{i(\omega_k+\Omega)t}-1}{\omega_k+\Omega} + \frac{e^{i(\omega_k-\Omega)t}-1}{\omega_k-\Omega}\right]$$
$$\equiv \alpha_k(t)X_0, \tag{5.29}$$

$$\xi_k(X_0,t) \equiv \frac{C_k^2}{4m_k(\omega_k^2-\Omega^2)}\left[t + \frac{\sin(2\Omega t)}{2\Omega} - \frac{\sin(\omega_k+\Omega)t}{\omega_k+\Omega} - \frac{\sin(\omega_k-\Omega)t}{\omega_k-\Omega}\right]X_0^2. \tag{5.30}$$

for momentum squeezed states and

$$\hat{U}_E(X_0\sin\Omega t) = \bigotimes_{k=1}^{N} e^{i\xi_k(X_0,t)}e^{-i\hat{H}_k t/\hbar}\hat{D}\left(\eta_k(X_0,t)\right) \equiv \bigotimes_{k=1}^{N}\hat{U}_k(X_0,t), \tag{5.31}$$

$$\eta_k(X_0,t)=\int_0^t d\tau\alpha_k'(\tau)X_0\sin(\Omega\tau)=-\frac{C_k}{2i\sqrt{2m_k\omega_k}}\left[\frac{e^{i(\omega_k+\Omega)t}-1}{\omega_k+\Omega}-\frac{e^{i(\omega_k-\Omega)t}-1}{\omega_k-\Omega}\right]$$
$$\equiv\alpha_k(t)X_0. \tag{5.32}$$
$$\xi_k(X_0,t)\equiv\frac{C_k^2}{4m_k(\omega_k^2-\Omega^2)}\left[t-\frac{\sin(2\Omega t)}{2\Omega}+\frac{\Omega\sin(\omega_k+\Omega)t}{\omega_k(\omega_k+\Omega)}-\frac{\Omega\sin(\omega_k-\Omega)t}{\omega_k(\omega_k-\Omega)}\right]X_0^2 \tag{5.33}$$

for position squeezed states. By $\hat{H}_k\equiv\hat{p}_k^2/(2m_k)+m_k\omega_k^2\hat{x}_k^2/2$ we denoted the self Hamiltonian of the single environmental degree of freedom and $\hat{D}(\alpha)\equiv e^{\alpha\hat{a}^\dagger-\alpha^*\hat{a}}$ is the displacement operator. We stress that the expressions are valid in the large squeezing limit. As we have seen in the previous Chapter, the phase factors $\xi_k(X,t)$ are unimportant for our considerations.

Since for the initial squeezed states the trajectories of the central oscillator are functions of the initial position only, we can formally write the evolution operator as

$$\hat{U}_{S:E}(t)=\int dX_0 e^{-i\hat{H}_S t/\hbar}|X_0\rangle\langle X_0|\otimes\hat{U}_E(X_0\cos\Omega t) \tag{5.34}$$
$$\hat{U}_{S:E}(t)=\int dX_0 e^{-i\hat{H}_S t/\hbar}|X_0\rangle\langle X_0|\otimes\hat{U}_E(X_0\sin\Omega t). \tag{5.35}$$

The evolution operators (5.34, 5.35) are formally a controlled-unitary type (2.30,4.14), in which the environment evolves accordingly to the trajectory of the central oscillator (more precisely to functional of it).

In what follows we aim to show that in Quantum Brownian Motion in the recoilless limit there is a regime of parameters, in which the Spectrum Broadcast Structure is formed. Therefore our central object of interest is the partially reduced state describing the system and an observed fragment of environment. Since we deal with continuous rather than discrete spectrum one should be careful with the integral in (5.34, 5.35). We rewrite the integral using a finite division of the real line of X_0 into intervals $\{\Delta_i\}$ with $|X_0\rangle\langle X_0|$ replaced by orthogonal projectors $\hat{\Pi}_\Delta$ on the intervals Δ (continuous distribution of X_0 is recovered in the limit of these divisions [18, 19]). The partially traced state then reads:

$$\varrho_{S:fE}(t)=\sum_\Delta e^{-i\hat{H}_S t/\hbar}\hat{\Pi}_\Delta|\phi_0\rangle\langle\phi_0|\hat{\Pi}_\Delta e^{i\hat{H}_S t/\hbar}\bigotimes_{k=1}^{fN}\varrho_k(X_\Delta,t) \tag{5.36}$$
$$+\sum_{\Delta\neq\Delta'}\Gamma_{X_\Delta,X_{\Delta'}}(t)e^{-i\hat{H}_S t/\hbar}\hat{\Pi}_\Delta|\phi_0\rangle\langle\phi_0|\hat{\Pi}_{\Delta'}e^{i\hat{H}_S t/\hbar}\otimes\bigotimes_{k=1}^{fN}\hat{U}_k(X_\Delta,t)\varrho_{0k}\hat{U}_k^\dagger(X_{\Delta'},t),$$

where X_Δ is some position within an interval Δ,

$$\varrho_k(X_\Delta;t)\equiv\hat{U}_k(X_\Delta,t)\varrho_{0k}\hat{U}_k^\dagger(X_\Delta,t) \tag{5.37}$$

are the system-dependent states of the environment and

$$\Gamma_{X_\Delta,X'_\Delta}(t) \equiv \prod_{k\in(1-f)E} Tr\left[\hat{U}_k(X_\Delta,t)\varrho_{0k}\hat{U}_k^\dagger(X'_\Delta,t)\right] \equiv \prod_{k\in(1-f)E} \Gamma^{(k)}_{X_\Delta,X'_\Delta}(t), \tag{5.38}$$

is the decoherence factor. To study the information content of the system dependent states of the environment we again use the generalized overlap

$$B^k_{X_\Delta,X'_\Delta} = \sqrt{\sqrt{\varrho_k(X_\Delta,t)}\varrho_k(X'_\Delta,t)\sqrt{\varrho_k(X_\Delta,t)}}. \tag{5.39}$$

Furthermore we assume that the environment in initially in the thermal state. As a result we can use the formulas derived in Chapter 4 to obtain the expressions for the decoherence factor and the generalized overlap (in what follows, to keep the notation simple, we will omit the subscript 0 and write X instead of X_0). The former is

$$\left|\Gamma_{X,X'}\right| = \prod_{k\in(1-f)E} \exp\left[\frac{|X-X'|^2}{2}\left|\alpha_k(t)\right|^2 \coth\left(\frac{\tau_T\omega_k}{2}\right)\right], \tag{5.40}$$

whereas the latter

$$B^{mac}_{X,X'} = \prod_{k\in mac} \exp\left[\frac{|X-X'|^2}{2}\left|\alpha_k(t)\right|^2 \tanh\left(\frac{\tau_T\omega_k}{2}\right)\right], \tag{5.41}$$

where

$$|\alpha_k(t)|^2 = \frac{C_k^2\omega_k}{2\hbar m_k(\omega_k^2-\Omega^2)^2}\left[(\cos\omega_k t-\cos\Omega t)^2+\left(\sin\omega_k t-\frac{\Omega}{\omega_k}\sin\Omega t\right)^2\right] \tag{5.42}$$

for an initial momentum squeezed state of S (equation (5.29)), while for a position squeezed (equation (5.32)):

$$|\alpha_k(t)|^2 = \frac{C_k^2\Omega^2}{2\hbar m_k\omega_k(\omega_k^2-\Omega^2)^2}\left[(\cos\omega_k t-\cos\Omega t)^2+\left(\sin\omega_k t-\frac{\omega_k}{\Omega}\sin\Omega t\right)^2\right]. \tag{5.43}$$

5.5.2 Continuous environmental spectrum – Caldeira Legget model

In the literature the properties of the environment are usually encoded in the spectral density function. It is defined as

$$J(\omega) \equiv \sum_k \delta(\omega-\omega_k)\frac{C_k^2}{2m_k\omega_k}. \tag{5.44}$$

As a result, relevant functions, in our case decoherence factor and generalized overlap, can be expressed in terms of the spectral density instead of parameters of individual environmental subsystems. To see how the spectral density enters the indicator functions under consideration, let us provide expressions for decoherence factor and generalized overlap in a different form than that derived in equations (5.40,5.41). It will prove more convenient to keep the argument of the displacement operator as an integral so our expression for decoherence factor is

$$\begin{aligned} &-\log\left|\Gamma_{X,X'}(t)\right| = \\ &\frac{1}{2}\sum_{k\in(1-f)E}\left|\int_0^t \alpha_k'(\tau)f(X,\tau)\,d\tau - \int_0^t \alpha_k'(\tau)f(X',\tau)\,d\tau\right|^2 \coth\left(\frac{\tau_T\omega_k}{2}\right). \end{aligned} \tag{5.45}$$

We focus on the single term in the sum

$$\begin{aligned} &\left|\int_0^t \alpha_k'(\tau)f(X,\tau)\,d\tau - \int_0^t \alpha_k'(\tau)f(X',\tau)\,d\tau\right|^2 = \int_0^t\int_0^t d\tau d\tau' \alpha_k'(\tau)\alpha_k'(\tau')^* \times \\ &\left[f(X,\tau)f(X,\tau')^* - f(X,\tau)f(X',\tau')^* + f(X,\tau)^*f(X',\tau') - f(X',\tau)f(X',\tau')^*\right] \\ &\equiv \int_0^t\int_0^t d\tau d\tau' \alpha_k'(\tau)\alpha_k'(\tau')^*\Delta(X,X',\tau,\tau') \end{aligned} \tag{5.46}$$

Taking into account that

$$\alpha_k'(\tau)\alpha_k'(\tau')^* = \frac{C_k^2}{2\hbar m_k\omega_k}e^{i\omega_k(\tau-\tau')} \tag{5.47}$$

we have

$$\begin{aligned} &-\log\left|\Gamma_{X,X'}(t)\right| = \\ &\frac{1}{2}\sum_{k\in(1-f)E}\int_0^t\int_0^t d\tau d\tau' \frac{C_k^2}{2\hbar m_k\omega_k}e^{i\omega_k(\tau-\tau')}\Delta(X,X',\tau,\tau')\coth\left(\frac{\tau_T\omega_k}{2}\right) = \\ &\frac{1}{2}\int d\omega\int_0^t\int_0^t d\tau d\tau' J(\omega)e^{i\omega(\tau-\tau')}\Delta(X,X',\tau,\tau')\coth\left(\frac{\tau_T\omega}{2}\right), \end{aligned} \tag{5.48}$$

where in the last line we used the definition of spectral density. Now we will assume that the unobserved fraction of the environment is large and consists of all possible frequencies of the environment so that we can integrate over whole spectrum. This choice can be questioned, however it has one undeniable advantage: it will allow us to perform the integral analytically. Before doing that we need to specify the form of the spectral density. One of the possible and frequent choices is an Ohmic (that is linear in ω for small frequencies) spectral density with the

Lorentz-Drude cutoff

$$J(\omega) = \frac{M\gamma}{\pi}\omega\frac{\Lambda^2}{\Lambda^2 - \omega^2}. \tag{5.49}$$

To compute the integral we need also the Matsubara representation of hyperbolic cotangent [100]:

$$\coth\left(\frac{\tau_T\omega}{2}\right) = \frac{2}{\tau_T\omega}\sum_{n=-\infty}^{\infty}\frac{1}{1+(v_n/\omega)^2}, \tag{5.50}$$

where v_n are the bosonic frequencies $v_n = 2\pi n/\tau_T$. Now the integral over frequencies can be calculated using the Cauchy's residue theorem. The result is

$$\frac{1}{2}\int_0^\infty d\omega J(\omega)\coth\left(\frac{\tau_T\omega}{2}\right)e^{i\omega(\tau-\tau')} = \frac{M\gamma\Lambda^2}{2\tau_T}\sum_{n=-\infty}^{\infty}\frac{\Lambda e^{-\Lambda|\tau-\tau'|} - |v_n|e^{-|v_n(\tau-\tau')|}}{\Lambda^2 - v_n^2}. \tag{5.51}$$

We are interested in evaluating this expression in a high temperature limit, in which the thermal energy of the bath in much larger than the cutoff energy and the energy of the central oscillator, such that $\tau_T^{-1} = \frac{k_BT}{\hbar} \gg \Lambda \gg \Omega$. This limit is widely used in the literature to study both decoherence and dissipation processes and is usually referred to as Caldeira-Leggett (since it was firstly used by Caldeira and Leggett to derive master equation [86]) or Fokker-Planck limit. Then one can approximate the above sum by the zeroth term only (in larger temperatures non-zero terms behave roughly as $\sim 1/v_n \sim 1/T$ so they can be approximated by 0):

$$\frac{M\gamma\Lambda^2}{2\tau_T}\sum_{n=-\infty}^{\infty}\frac{\Lambda e^{-\Lambda|\tau-\tau'|} - |v_n|e^{-|v_n(\tau-\tau')|}}{\Lambda^2 - v_n^2} \approx \frac{M\gamma\Lambda^2}{\tau_T}\frac{e^{-\Lambda|\tau-\tau'|}}{2/\Lambda}. \tag{5.52}$$

For large values of Λ the above expression approaches Dirac's delta distribution. This means that the process is Markovian – it does not depend on the past history of the system (there are no memory effects). In this case the equation (5.48) takes the form

$$\frac{1}{2}\int_0^\infty d\omega\int_0^t\int_0^t d\tau d\tau' J(\omega)e^{i\omega(\tau-\tau')}\Delta(X,X',\tau,\tau')\coth\left(\frac{\tau_T\omega}{2}\right) \approx \frac{M\gamma\Lambda^2}{\tau_T}\int_0^t d\tau\Delta(X,X',\tau,\tau) = \frac{M\gamma\Lambda^2}{\tau_T}\int_0^t d\tau\left|f(X,\tau) - f(X',\tau)\right|^2 = \frac{M\gamma\Lambda^2}{\tau_T}\int_0^t d\tau\left|f(X,\tau) - f(X',\tau)\right|^2. \tag{5.53}$$

Now we can evaluate the above expression for two types of trajectories that we are considering. For momentum squeezed states ($f(X,\tau) = X\cos(\Omega t)$) we get

$$-\log\left|\Gamma_{X,X'}(t)\right| = \frac{M\gamma\Lambda^2 k_BT}{2\hbar}|X-X'|^2\left(t + \frac{\sin(2\Omega t)}{2\Omega}\right), \tag{5.54}$$

whereas for position squeezed ones ($f(X,\tau) = X\sin(\Omega t)$)

$$-\log\left|\Gamma_{X,X'}(t)\right| = \frac{M\gamma\Lambda^2 k_B T}{2\hbar}|X-X'|^2\left(t - \frac{\sin(2\Omega t)}{2\Omega}\right). \tag{5.55}$$

In above equations the explicit dependence on temperature was restored. We see that in both cases the argument of the decoherence factor is non-decreasing function of time multiplied by the temperature. This is in agreement with results of Chapter 4, where we found that in such situations temperature enhances decoherence process. In the considered limit value of decoherence factor between every possible position eigenstates X, X' will drop below any chosen threshold provided that we wait sufficiently long. For position squeezed states the process is longer. To understand why this is the case let us present the expression for the modulus of the freely evolving squeezed wavefunction, which is [101]

$$|\Psi(X,t)|^2 = \left(\frac{M\Omega}{\pi\hbar r}\right)^{\frac{1}{2}}\left(1+\left(r^{-2}-1\right)\cos^2(\Omega t)\right)^{-\frac{1}{2}}\exp\left[-\frac{M\Omega/(\hbar r)(X-X_c\cos(\Omega t))^2}{1+(r^{-2}-1)\cos^2(\Omega t)}\right], \tag{5.56}$$

and the uncertainty in position that is given by

$$\Delta X(t) = \left(\frac{r\hbar}{2M\Omega}\right)^{\frac{1}{2}}\left[1+(r^{-2}-1)\cos^2(\Omega t)\right]^{\frac{1}{2}}. \tag{5.57}$$

Squeezing in position occurs when $r > 1$. From the above expressions we see that, in the regime of large position squeezing, states have almost no initial coherences in position basis but the free evolution transforms them into momentum squeezed states so the coherences are built due to the dynamics and the decoherence process starts later (in case of free evolution the uncertainty in position oscillates between minimal $\left(\frac{\hbar}{2rM\Omega}\right)^{\frac{1}{2}}$ and maximal $\left(\frac{2r\hbar}{M\Omega}\right)^{\frac{1}{2}}$ value indicating that the coherences in position also oscillate with time).

We would like to perform a similar analysis to check the information content of the environment. We work under the same assumptions as for decoherence process – the remaining part of the environment is sufficiently large to be described by the whole spectral density function, we study this process in the Caldeira-Leggett limit. From the computational point of view we need to deal now with hyperbolic tangent, with Matsubara representation given by [100]:

$$\tanh\left(\frac{\tau_T\omega}{2}\right) = \frac{4}{\tau_T\omega}\sum_{n=0}^{\infty}\frac{1}{1+(w_n/\omega)^2}, \tag{5.58}$$

with fermionic frequencies $w_n = (2n+1)\pi/\tau_T$. Again, using almost the same arguments that led to equation (5.53), we can approximate the sum by zeroth term only

$$\frac{1}{2}\int_0^\infty d\omega J(\omega)\coth\left(\frac{\tau_T\omega}{2}\right)e^{i\omega(\tau-\tau')} = \frac{M\gamma\Lambda^2}{\tau_T}\sum_{n=0}^{\infty}\frac{\Lambda e^{-\Lambda|\tau-\tau'|} - w_n e^{-|w_n(\tau-\tau')|}}{\Lambda^2 - w_n^2} \approx \frac{2M\gamma\Lambda^2\tau_T}{\pi^2}\frac{e^{-\left|\frac{(\tau-\tau')}{\tau_T/\pi}\right|}}{\tau_T/\pi}. \tag{5.59}$$

Now we repeat the reasoning that led to (5.53). This time we take into account that in the large temperature limit $\tau_T/\pi \to 0$ and the above expression tends to Dirac's delta distribution so again there are no memory effects and we are left with one time integral

$$\frac{1}{2}\int_0^\infty d\omega\int_0^t\int_0^t d\tau d\tau' J(\omega)e^{i\omega(\tau-\tau')}\Delta(X,X',\tau,\tau')\coth\left(\frac{\tau_T\omega}{2}\right) \approx \frac{2M\gamma\Lambda^2\tau_T}{\pi}\int_0^t d\tau\left|f(X,\tau)-f(X',\tau)\right|^2. \tag{5.60}$$

The only important difference between the above equation and equation (5.53) is the temperature dependence, with growing temperature the environment will slower acquire the information about the state of the central system, in the case of momentum squeezing ($f(X,\tau) = X\cos(\Omega t)$) we get

$$-\log B_{X,X'}(t) = \frac{2M\gamma\Lambda^2\hbar}{\pi k_B T}|X-X'|^2\left(t+\frac{\sin(2\Omega t)}{2\Omega}\right), \tag{5.61}$$

whereas for position squeezed ones ($f(X,\tau) = X\sin(\Omega t)$)

$$-\log B_{X,X'}(t) = \frac{2M\gamma\Lambda^2\hbar}{\pi k_B T}|X-X'|^2\left(t-\frac{\sin(2\Omega t)}{2\Omega}\right). \tag{5.62}$$

In above equations the explicit dependence on temperature was restored. Note that in the considered limit, when $\frac{k_B T}{\hbar} \gg \Lambda$ in a long period of time we have $B_{X,X'}(t) \approx 1$ for both initial states. This is in agreement with results obtained in Chapter 4 – high level of thermal noise makes it hard to create environmental states with non-overlapping supports for different values of the initial position X, which means that it could be impossible for the observers to extract information about the central system from the environment.

5.5.3 Discrete environmental spectrum – numerical analysis

In this subsection we investigate the functions indicating the Spectrum Broadcast Structure formation in the case when the spectrum of environmental frequencies is discrete.

In general, there are three possibilities of choosing the interval $[\omega_L, \omega_U]$, from which frequencies ω_k are chosen, with respect to the frequency of the central system Ω (note that we did not discuss this issue in case of simplified Quantum Brownian Motion models as there the self-Hamiltonian of the central system was neglected and as a consequence the system's frequency dropped out of the considerations):

$$\begin{aligned} &\omega_L, \omega_U \ll \Omega \quad \text{off-resonant, "slow"} \\ &\omega_L < \Omega < \omega_U \quad \text{resonant} \\ &\Omega \ll \omega_L, \omega_U \quad \text{off-resonant, "fast".} \end{aligned}$$

The meaning of the term off-resonant for our investigations becomes clear after inspecting equations (5.40,5.41) – the single subsystem of environment may not able to decohere or provide classical information about the system. As a result the choice of the regime, from which the environmental frequencies are sampled (resonant/off-resonant "slow"/off-resonant "fast"), influences strongly the results. We analyze all these regimes in the following discussion, but before doing so we choose other parameters of the model.

The parameters of the model

From now on, unless we state otherwise, to present the plots we set parameters of the central system as: $M = 10^{-5}$kg, $\Omega = 3 \times 10^8 \text{s}^{-1}$. We assume that coupling constants C_k depend only on the masses: $C_k \equiv 2\sqrt{(M m_k \tilde{\gamma}_0)/\pi}$, and $\tilde{\gamma}_0 = 0.33 \times 10^{18}$ s^{-4} is a constant. We choose the frequencies of the environmental degrees of freedom ω_k to be independently, identically and uniformly distributed in the intervals reflecting the three regimes discussed above (off-resonant "slow" and "fast", resonant). The masses of the environmental subsystems are chosen to be $m_k = 10^{-15}$ kg. We set the $|X - X'| = 10^{-9}$ m, this means that we investigate the decoherence process between eigenstates of position, which are 10^{-9} m away from each other. The same applies for the information content of the environment, we would like to know if an observer having access to some fragment of the environment will distinguish two states of the central system that are far apart at this distance.

5.5.4 Numerical analysis of discrete environmental spectrum – resonant case

In this subsection we assume frequencies ω_k to be independently, identically and uniformly distributed in the interval $3 \times 10^7 \text{s}^{-1} \ldots 6 \times 10^9 \text{s}^{-1}$. Intuitively, we can expect that in this case the decoherence as well as the transfer of information to the environment happens as from the formulas for the indicator functions (5.40, 5.41) and expressions for $|\alpha_k(t)|^2$ parameters (5.42, 5.43) we see that the subsystems with frequencies close to the system's frequency Ω will have a dominant influence on decoherence factor and generalized overlap. A closer inspection shows

that

$$\lim_{\omega\to\Omega}|\alpha(t)|^2=\frac{M\tilde{\gamma}_0}{4\pi\hbar\Omega^3}\left(1+2\Omega^2t^2-\cos\left(2\Omega t\right)\pm 2\Omega t\sin\left(2\Omega t\right)\right), \tag{5.63}$$

where in the last term sign $+$ corresponds to momentum squeezed states and $-$ to position squeezed ones. This result confirms our previous expectations: a single subsystems suffices to decohere the central system. Also, an observer needs access to just one subsystem to extract the information about the state of the central system. However, the sign difference between momentum and position squeezed states indicates that the timescales of discussed processes are different for discussed initial states, as the formation of Spectrum Broadcast Structure in the case of an initial position squeezed state takes longer time. Indeed, this is consistent with all the results that we have so far presented and the knowledge of squeezed states evolution. From the formulas for indicator functions we know that the decoherence process affects superpositions of position egienstates and that information about position is transfered to the environment. The initial state with large momentum squeezing poses large coherences in the mentioned basis so both processes begin to happen instantly. On the other hand, the initial position squeezed state has almost no coherences in the position eigenbasis. However, due to the evolution under self-Hamiltonian of the quantum harmonic oscillator it is transformed to the momentum squeezed state so the coherences in positions are built up due to the dynamics. Therefore one should expect that the discussed processes will happen also in this case but on a longer time scale.

This discussion is reflected in Figure 5.1, where we see that for momentum and position squeezed states both indicator functions (decoherence factor and generalized overlap) decay rapidly confirming formation of Spectrum Broadcast Structure formation. However, in the case of position squeezing the decay is slower. On the other hand, the differences in timescales between the decoherence and information transfer processes for a given initial squeezing of the initial state of the central system are caused by different temperature behavior of the indicator functions (5.40, 5.41), what is also visible in Figure 5.1.

5.5.5 Numerical analysis of discrete environmental spectrum – off-resonant "slow" case

Here we assume frequencies ω_k to be independently, identically and uniformly distributed in the interval $3\ldots 6\times 10^7$s. What we should expect in this case? For $\Omega\gg\omega_k$ the proportional constant in formulas (5.42, 5.43) is of the order

$$|\alpha_k(t)|^2\propto\frac{M\tilde{\gamma}_0}{\pi\omega_k\Omega^2}. \tag{5.64}$$

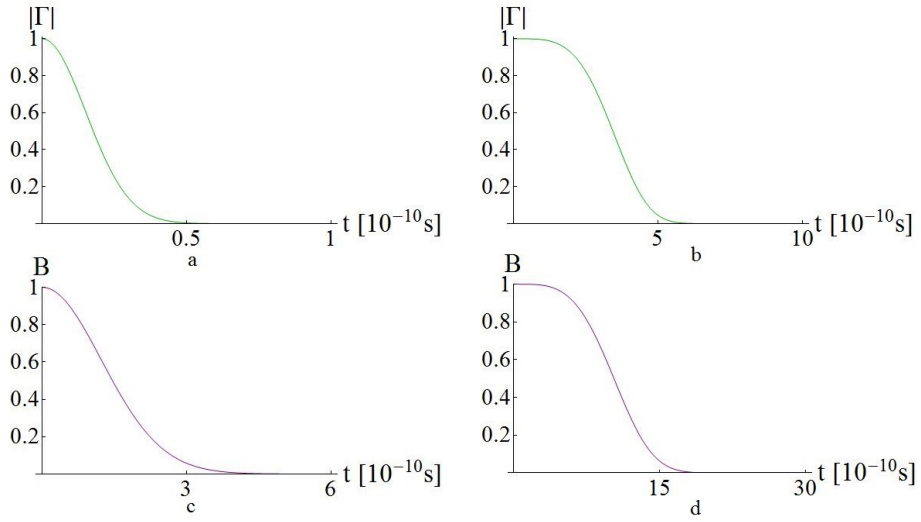

FIGURE 5.1: Time dependencies of $|\Gamma_{X,X'}(t)|$ a),b) and $B^{mac}_{X,X'}(t)$ c),d) for the system initially in a momentum squeezed state a), c) and position squeezed state b), d). The observed and unobserved macrofractions consists of 10 oscillators and the temperature is $T = 10^{-2}$K. The long time behavior is not shown in the plots as there are no revivals in relevant timescales.

If we compare this to the expression obtained in the resonance (5.63) in which $|\alpha_k(t)|^2 \propto \frac{M\tilde{\gamma}_0}{4\pi\Omega^3}$ we actually see that for off-resonant "slow" environment the proportional constant is of order of magnitude larger than in the resonant case. If there is enough randomness in the phases the decoherence process can happen even faster than in the resonant case. However, the difference between decoherence factor and generalized overlap should be also more visible in this case, as differences in values of hyperbolic tangent and cotangent are bigger in the small frequency regime. With regard to temperatures, the decoherence process will be enhanced in comparison to the resonant case but the opposite is true in case of information transfer to the environment. As a result, while we expect decoherence process to happen on a shorter timescale, the difference in the broadcasting information about the central system may not be so clear as there are two factors influencing it in opposite ways.

In the Figure 5.2 we can see that our conjectures discussed above were quite accurate, as the plots behave in the expected way.

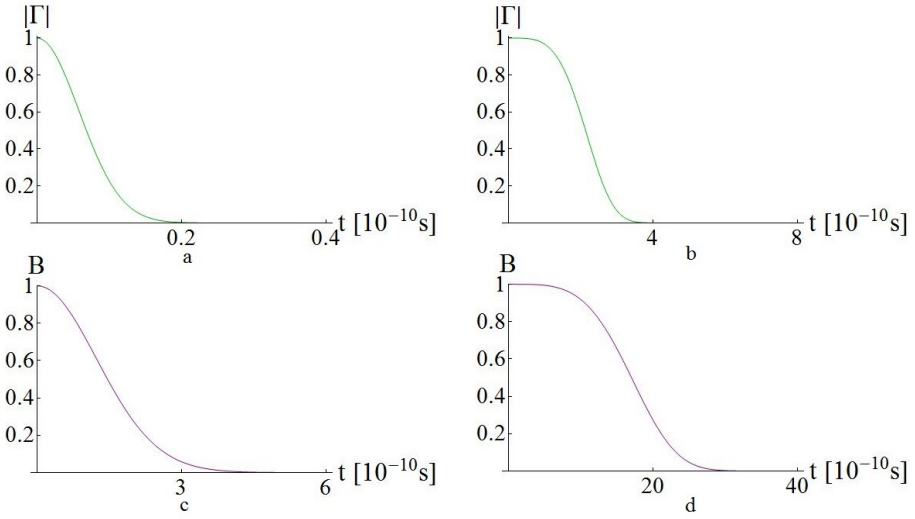

FIGURE 5.2: Time dependencies of $|\Gamma_{X,X'}(t)|$ (a),(b) and $B^{mac}_{X,X'}(t)$ (c),(d) for the system initially in a momentum squeezed state (a), (c) and position squeezed state (b), (d). The observed and unobserved macrofractions consists of 10 oscillators and the temperature is $T = 10^{-2}$K. The long time behavior is not shown in the plots as there are no revivals in relevant timescales.

5.5.6 Numerical analysis of discrete environmental spectrum – off-resonant "fast" case

The last case to be discussed is the "fast" off-resonant environment. We can perform a similar analysis to this presented in the previous Subsection, this time for $\Omega \ll \omega_k$ to see that proportional constant in formulas (5.42, 5.43) is of the order

$$|\alpha_k(t)|^2 \propto \frac{M\tilde{\gamma}_0}{\pi\omega_k^3}. \tag{5.65}$$

This constant is the smallest one from all that we have discussed so far, it is plausible to think that in this case the behavior of decoherence factor and generalized overlap will be different than those presented previously and one will need more random phases to cause decoherence and broadcast processes. For position squeezed states the situation may be even more involved, as the oscillatory term $\sin^2(\Omega t)$ in expression (5.43) can have a dominant role. Note that one could have expected a similar behavior for off-resonant "slow" environment and the momentum squeezed state as there also term $\sin^2(\Omega t)$ is orders of magnitude larger than other oscillatory functions. However, there the other oscillatory functions were multiplied by a large constant. As a consequence, for times when the term $\sin^2(\Omega t)$ was close to zero, due to the value of the other terms the expression (5.43) was still much larger than zero at each instant of time. Here, there is no such mechanism to "compensates" oscillations of the leading term.

We begin our analysis with momentum squeezed states. The above discussion is confirmed

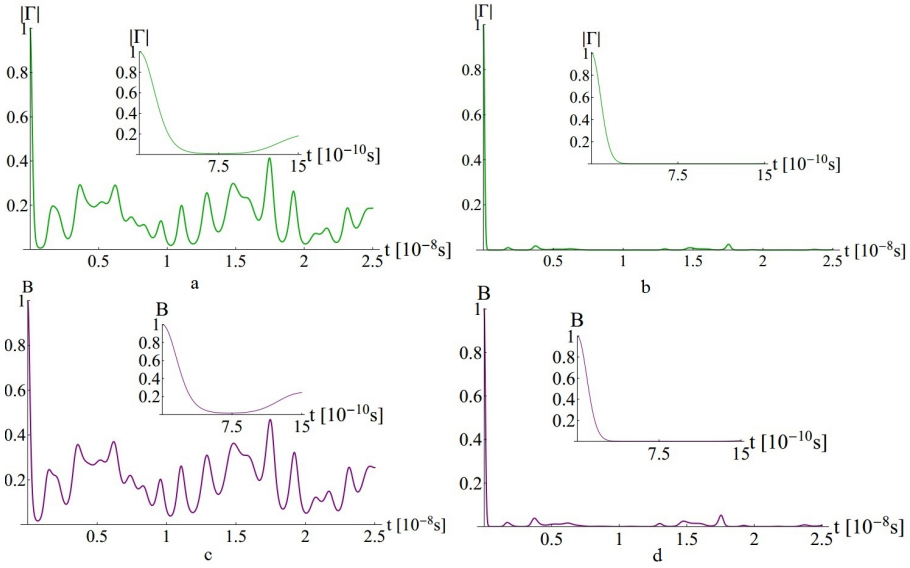

FIGURE 5.3: Time dependencies of $|\Gamma_{X,X'}(t)|$ a),b) and $B^{mac}_{X,X'}(t)$ c),d) for the system initially in a momentum squeezed state for different macro-fraction sizes: 10 oscillators – a) ,c); 30 oscillators – b), d) and $T = 10^{-2}$K. The inserts show short-time behavior. The figure is reproduced from [77].

in Figure 5.3. From Figure 5.3 b),d) we see that for 30 oscillators both functions decay rapidly, while for 10 oscillators they do not—the macro-fraction is too small for the given T. Note that in previously discussed cases this number of oscillators was enough to observe the formation of Spectrum Broadcast Structure. However, even for 30 oscillators of the environment we see that there are small fluctuations visible at the plots.

To study them, we further analyze the time averages $\left\langle |\Gamma_{X,X'}| \right\rangle = (1/\tau)\int_0^\tau dt|\Gamma_{X,X'}(t)|$, $\left\langle B^{mac}_{X,X'} \right\rangle = (1/\tau)\int_0^\tau dt B^{mac}_{X,X'}(t)$ as functions of the temperature T with τ taken large ($\sim 1s$). We present them in Figure 5.4. Since both functions are non-negative, vanishing of their time averages is a good indicator of the functions having small typical fluctuations above zero. From Figure 5.4 a) one sees that, in the chosen parameter range,there is no formation of the broadcast state for a macro-fraction of 10 oscillators: While $\left\langle |\Gamma_{X,X'}| \right\rangle \approx 0$ (the lower trace) for $T \approx 10^{-1}K$, $\left\langle B^{mac}_{X,X'} \right\rangle \approx 0.6$ (the upper trace). From Figure 5.4 we can deduce that in the recoilless limit for macrofraction size of 30 oscillators up to the temperature $T = 10^{-2}$ K the Spectrum Broadcast Structure in Quantum Brownian is formed. This is the main result of this subsection.

The situation with initial position squeezing is, as expected, quite different. Under exactly the same conditions as above there is no decoherenece neither orthogonalization for macrofractions of both 10 and 30 oscillators as Fig. 5.5 shows. The plots suggest that both functions are periodic in time, evolving almost at the central system frequency. This confirms our conjecture that in the expression (5.43) the term proportional to $\sin^2(\Omega t)$ plays a dominant role and there is no mechanism that can balance its influence on the indicator functions.

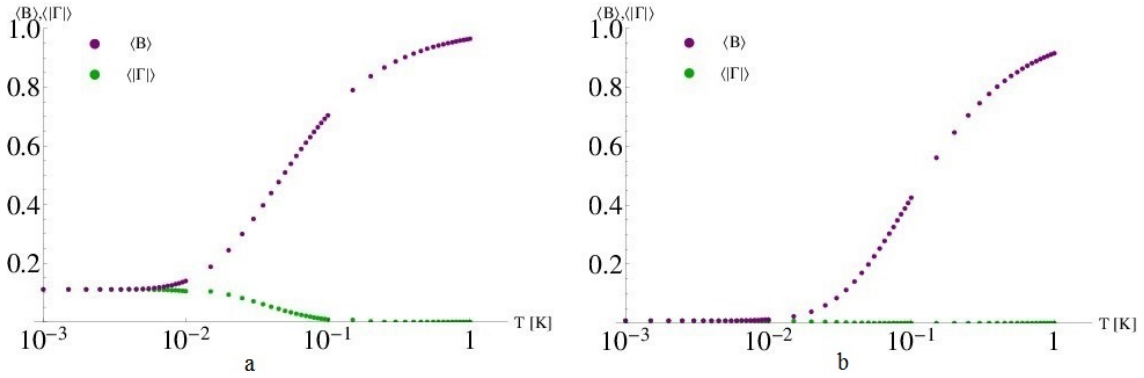

FIGURE 5.4: Time-averaged $|\Gamma_{X,X'}|$ (lower traces) and $B^{mac}_{X,X'}$ (upper traces) for the system initially in a momentum squeezed state as functions of the temperature (on the logarithmic scale) for different macrofraction sizes: 10 oscillators – a); 30 oscillators – b). Plot b) shows formation of the broadcast state for $T < 10^{-2}K$. The figure is reproduced form [77].

5.5.7 Numerical analysis of discrete environmental spectrum – squeezed thermal states

Due to the fact that the expressions for the indicator functions are valid also in the case of arbitrary single mode Gaussian states of the environment we are able to analyze the influence of the initial state of the environment on the formation of Spectrum Broadcast Structure. In fact, the most interesting parameter is the squeezing of the initial state. Intuitively, the larger the squeezing is the more efficient the formation should be in the sense that one needs smaller number of oscillators to decohere the central system and to extract information from it. We assume that the initial state is

$$\varrho_{0k} = \hat{S}(r)\varrho_{kT}\hat{S}(r)^{\dagger}, \tag{5.66}$$

where $\hat{S}(r) = e^{\frac{r}{2}(\hat{a}^2 - \hat{a}^{\dagger 2})}$ is the squeezing operator and ϱ_{kT} are the thermal oscillator states. A simple calculation combined with the results of Subsection 4.3.3 shows that it is enough to substitute in (5.40,5.41) $|\alpha_k(t)|^2$ for:

$$|\tilde{\alpha}_k(t)|^2 = \cosh(2r)\left[|\alpha_k(t)|^2 - \tanh(2r)\mathrm{Re}\alpha_k^2(t)\right], \tag{5.67}$$

$$\begin{aligned}\mathrm{Re}a_k(t)^2 = \frac{C_k^2}{4m_k\omega_k}\Bigg\{&\frac{1}{(\omega_k+\Omega)^2}\left\{\cos\left[2(\omega_k+\Omega)t\right] - 2\cos\left[(\omega_k+\Omega)t\right]\right\} \\ &+\frac{1}{(\omega_k-\Omega)^2}\left\{\cos\left[2(\omega_k-\Omega)t\right] - 2\cos\left[(\omega_k-\Omega)t\right]\right\} \\ &+\frac{1}{\omega_k^2-\Omega^2}\left\{\cos 2(\omega_k t) - \cos\left[(\omega_k-\Omega)\,t\right] - \cos\left[(\omega_k+\Omega)\,t\right]\right\} + \frac{3\omega_k^2+\Omega^2}{(\omega_k^2-\Omega^2)^2}\Bigg\}.\end{aligned} \tag{5.68}$$

From (5.67) one sees that for large squeezing, $|\tilde{\alpha}_k(t)|^2$ grows exponentially as e^{2r}, enabling a formation of the broadcast structure as the most problematic term in (5.41) decay as $\tanh(\tau_T\omega_k/2) \approx$

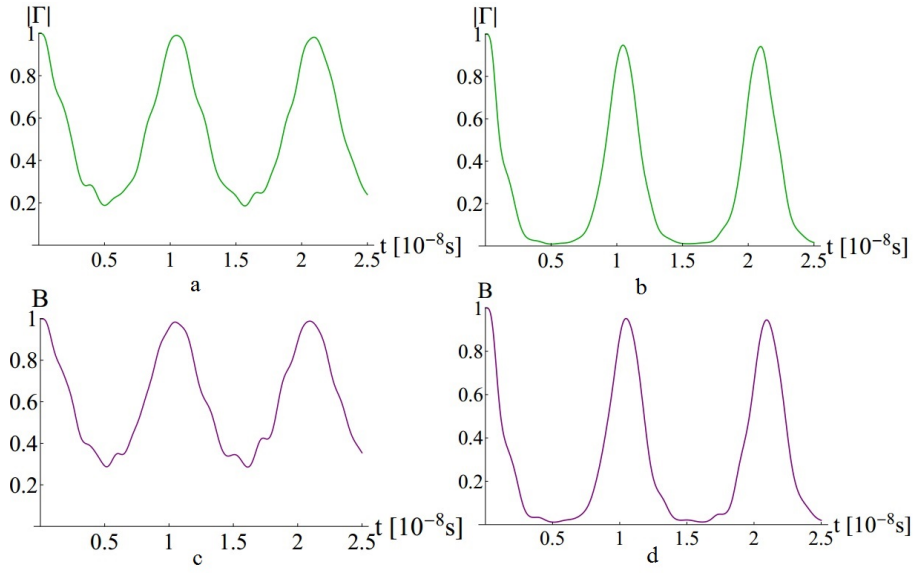

FIGURE 5.5: Time dependencies of $|\Gamma_{X,X'}(t)|$ a),b) and $B^{mac}_{X,X'}(t)$ (c),(d) for the system initially in a position squeezed state for different macro-fraction sizes and $T = 10^{-2}$K. The inserts show short-time behavior. The figure is reproduced from [77].

$\tau_T\omega_k/2$ for high temperatures. This reflects the fact that large squeezing decreases the noise, increasing the information capacity of the environment. To confirm this claim we investigate the case of off-resonant "fast" environment with the momentum squeezed state of the central system from the previous Subsection as we expect that the influence of initial squeezing of the environment will be the most visible here. The plots in Figure 5.6 confirm our analysis. From Figure 5.6 a) it can be seen that for a moderate macrofractions of 10 oscillators only with a help of a large squeezing $\log r > 0$ the negative effect of the temperature can be overcome, and both functions are damped indicating formation of the spectrum broadcast structure.

For 30 oscillators, Figure 5.6 b), the effect of random phases in (5.40,5.41) is much stronger, the functions are much more damped for the chosen parameters range, and hence the plateau of a broadcast structure formation is much larger. Quite surprisingly, there is a bump around $\log r = 0$ where the formation is suppressed, most probably due to a constructive interference in (5.67,5.69).

5.5.8 Discrete environmental spectrum – analytical estimates of the SBS formation

The numerical analysis of the previous Subsection clearly shows that Quantum Brownian Motion, in the recoilless limit, there is a regime of parameters in which the Spectrum Broadcast Structure is formed. However, this analysis is not as elegant and insightful as an analytical

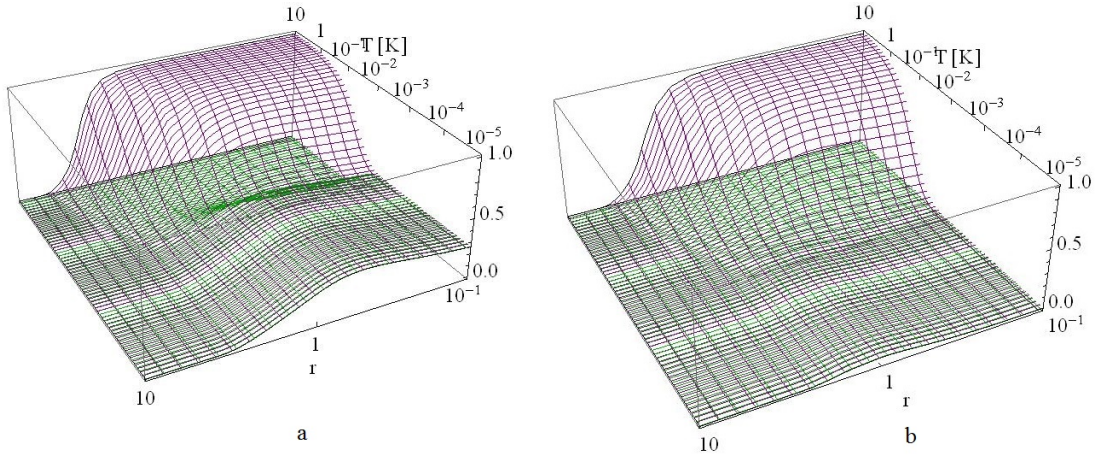

FIGURE 5.6: Time averaged decoherence $\langle|\Gamma_{X,X'}|\rangle$ (green; lower surfaces) and distinguishability $\langle B^{mac}_{X,X'}\rangle$ (magenta; upper surfaces) factors as functions of the temperature T and squeezing r (both on the logarithmic scale) of the environment. The set of random frequencies ω_k was generated once per plot. The traced over and observed macrofractions, $(1-f)E$ and mac, are assumed to be of the same size: 10 oscillators – a); 30 oscillators – b). Both plots simultaneously approaching zero indicates formation of the spectrum broadcast structure for a given (r,T). Averaging time was set to $1s$. The figure is reproduced from [87].

one and it does not allow to make a general statements about the Spectrum Broadcast Structures formation in the considered model. In particular, of great interest are the characteristic timescale of the deceherence process and the time that is needed to imprint the information about the central system on the remaining environment. From the plots they can be obtained only by a posteriori analysis. Moreover, it is impossible to predict accurately the long time behavior of the indicator functions before the numerical analysis is performed. In this Subsection we show that there exists an analytical method, which allows to overcome this drawbacks.

We restrict our analysis to momentum squeezed states of the central oscillator since from the previous analysis it follows that in this case the Spectrum Broadcast structure is formed in principle in all possible regimes of frequencies (at least for the considered choice of model parameters). In general our formulas are valid for resonant as well as off-resonant environments. However, as we have seen previously the case of off-resonant "fast" environment is the most involved and interesting one since the almost periodic nature of indicator functions is more visible there than in two other cases. Therefore, whenever we find it insightful to approximate the derived formulas we do it for the off-resonant "fast" environment (this means that in approximations we assume $\omega_U, \omega_L \gg \Omega$).

To perform the analysis we rewrite the decoherence factor for a single system of the environment as

$$-\log|\Gamma^{(k)}_{X,X'}(t)| = \frac{(X-X')^2}{2}|\alpha_k(t)|^2 \coth\left(\frac{\tau_T\omega_k}{2}\right) = \tag{5.69}$$

$$\frac{|X-X'|^2\, C_k^2 \omega_k \coth\left(\frac{\tau_T \omega_k}{2}\right)}{4\hbar m_k(\omega_k^2-\Omega^2)^2}\left[(\cos\omega_k t-\cos\Omega t)^2-\left(\sin\omega_k t-\frac{\Omega}{\omega_k}\sin\Omega t\right)^2\right]$$
$$\equiv \frac{|X-X'|^2}{2} f_T^{\Gamma}(t;\omega_k)$$

where $\tau_T \equiv \hbar/(k_B T)$ is the thermal time and we have introduced a function $f_T^{\Gamma}(t;\omega_k) \equiv |\alpha_k(t)|^2 \coth\left(\frac{\tau_T\omega_k}{2}\right)$ for a later convenience. The generalized overlap for the single environment is:

$$-\log B^{(k)}_{X,X'}(t) = \frac{(X-X')^2}{2}|\alpha_k(t)|^2 \tanh\left(\frac{\tau_T\omega_k}{2}\right) \equiv \frac{|X-X'|^2}{2} f_T^B(t;\omega_k). \tag{5.70}$$

The indicator functions for macrofractions then take the form

$$\left|\Gamma_{X,X'}(t)\right| = \exp\left[-\frac{|X-X'|^2}{2}\sum_{k\in(1-f)E} f_T^{\Gamma}(t;\omega_k)\right], \tag{5.71}$$

$$B_{X,X'}(t) = \exp\left[-\frac{|X-X'|^2}{2}\sum_{k\in mac} f_T^{B}(t;\omega_k)\right]. \tag{5.72}$$

As has been already mentioned, we are working with random environments with independent identically distributed (i.i.d.) frequencies ω_k with some distribution $P(\omega)$. As a consequence, the functions $f_T^B(t;\omega_k)$ and $f_T^{\Gamma}(t;\omega_k)$, appearing in the Spectrum Broadcast Structure indicator functions (5.71,5.72), also become i.i.d. random variables for a fixed time t and temperature T. Analytical study of their sums over a macrofraction $\sum_{k=1}^{N_{mac}} f_T^{\Gamma,B}(t;\omega_k)$ (we again assume for simplicity that both the unobserved macrofraction $(1-f)E$ as well as each of the observed ones have the same size N_{mac}) is possible in the limit of a large macrofraction size $N_{mac}\to\infty$ using the Law of Large Numbers [94]. This will be our main tool. It states (in its strong form) that the macrofraction averages $1/N_{mac}\sum_{k=1}^{N_{mac}} f_T^{\Gamma,B}(t;\omega_k)$ converge almost surely, this is with probability one, to their expectation values:

$$\frac{1}{N_{mac}}\sum_{k=1}^{N_{mac}} f_T(t;\omega_k) \overset{a.s.}{\to} \int d\omega P(\omega) f_T(t;\omega) \equiv \langle\langle f_T(t;\omega)\rangle\rangle \tag{5.73}$$

(we will neglect the superscripts Γ, B unless it leads to a confusion). This allows us to approximate the sums $\sum_{k=1}^{N_{mac}} f_T(t;\omega_k)$ with $N_{mac}\langle\langle f_T(t;\omega)\rangle\rangle$.

We note that the invocation of Law of Large Numbers is somehow a similar approach to this, in which one introduces the continuous limit for the macrofractions of the environment with $P(\omega)$ determining the spectral density. In other words, we divide the environment into fractions of such a size that the approximation obtained with the help of Law of Large Numbers may be applied. To bound the error of the approximation one can use Large Deviations Theory

stating that the probability of the sum $\sum_{k=1}^{N_{mac}} f_T(t;\omega_k)$ being grater than mean $\langle\langle f_T(t;\omega)\rangle\rangle$ by some value Z decays exponentially with growing N_{mac}, at a rate depending on Z (this result can be also used to bound the probability of the sum being smaller than the mean). Following our approach we will use here simple, uniform probability distribution over an interval $[\omega_L, \omega_U]$ due to an ease of analysis:

$$\langle\langle f_T(t;\omega)\rangle\rangle = \frac{1}{\Delta\omega}\int_{\omega_L}^{\omega_U} d\omega f_T(t;\omega), \tag{5.74}$$

where $\Delta\omega = \omega_U - \omega_L$. Let us remind that the coupling constants are $C_k = 2\sqrt{(Mm_k\bar{\gamma}_0)/\pi}$, with $\bar{\gamma}_0$ a constant. In what follows we analyze the short- and long-time behavior of this expression in the limits of high and low temperature. The latter approximation allows us to perform the relevant integrals analytically. This will enable us to estimate the macrofraction size N_{mac} needed in order for the functions (5.71,5.72) to attain asymptotically values close to zero within a given error as well as give the timescales of their initial decays, observed numerically in the previous Subsection. Before presenting the results, for the compactness sake, we introduce a notation for particular combinations of Sine- and Cosine-integral functions $\mathrm{Si}(z) = \int_0^z dz\frac{\sin z}{z}$, $\mathrm{Ci}(z) = \int_0^z dz\frac{\cos z}{z}$, which will appear in formulas:

$$\begin{aligned} &F_{\mathrm{Si}}(\pm,\pm,\pm,\pm) = [\pm1,\pm1,\pm1,\pm1]\cdot \\ &[\mathrm{Si}\left((\omega_L-\Omega)t\right),\mathrm{Si}\left((\omega_U-\Omega)t\right),\mathrm{Si}\left((\omega_L+\Omega)t\right),\mathrm{Si}\left((\omega_U+\Omega)t\right)]^T \end{aligned} \tag{5.75}$$

$$\begin{aligned} &F_{\mathrm{Ci}}(\pm,\pm,\pm,\pm) = [\pm1,\pm1,\pm1,\pm1]\cdot \\ &[\mathrm{Ci}\left((\omega_L-\Omega)t\right),\mathrm{Ci}\left((\omega_U-\Omega)t\right),\mathrm{Ci}\left((\omega_L+\Omega)t\right),\mathrm{Ci}\left((\omega_U+\Omega)t\right)]^T, \end{aligned} \tag{5.76}$$

where $[\pm1,\ldots\pm1]$ is a vector, $\cdot$ denotes vector product and T stands for transposition. The argument of $F_{\mathrm{Si}}(\pm,\pm,\pm,\pm)$, $F_{\mathrm{Ci}}(\pm,\pm,\pm,\pm)$ specifies pattern of signs, for example:

$$F_{\mathrm{Si}}(+,-,+,-) = \mathrm{Si}\left((\omega_L-\Omega)t\right) - \mathrm{Si}\left((\omega_U-\Omega)t\right) + \mathrm{Si}\left((\omega_L+\Omega)t\right) - \mathrm{Si}\left((\omega_U+\Omega)t\right). \tag{5.77}$$

As we will be interested in the short- and long-time behavior of the indicator functions, below we derive approximations for $F_{\mathrm{Si}}(\pm,\pm,\pm,\pm)$, $F_{\mathrm{Ci}}(\pm,\pm,\pm,\pm)$ relevant for the problem. In the short time regime, this is for $t \ll \omega_U^{-1}$ (off-resonant "fast environment"), we can approximate relevant functions as follows:

$$\begin{aligned} F_{\mathrm{Si}}(+,-,+,-) &= 2(\omega_L-\omega_U)t + \frac{t^3}{9}(\omega_U^3-\omega_L^3+3\Omega^2\omega_U-3\Omega^2\omega_L)+O(t^5) \\ F_{\mathrm{Si}}(+,-,-,+) &= \frac{t^3}{3}\Omega(\omega_L^2-\omega_U^2)+O(t^5) \\ F_{\mathrm{Ci}}(+,-,+,-) &= \log\frac{\omega_L^2-\omega^2}{\omega_U^2-\omega^2}+\frac{1}{2}(\omega_U^2-\omega_L^2)t^2+o(t^4) \end{aligned} \tag{5.78}$$

$$F_{\mathrm{Ci}}(+,-,-,+) = \log\frac{(\omega_L-\Omega)(\omega_U+\Omega)}{(\omega_L+\Omega)(\omega_U-\Omega)} + \Omega(\omega_L-\omega_U)t^2 + O(t^4).$$

On the other hand, the asymptotic is given by:

$$\begin{aligned}
tF_{\mathrm{Si}}(+,-,+,-) = \quad & 2\Bigg(\omega_U\frac{\cos(\omega_U t)}{\omega_U^2-\Omega^2}\cos(\Omega t) + \Omega\frac{\sin(\omega_U t)}{\omega_U^2-\Omega^2}\sin(\Omega t) - \\
& \omega_L\frac{\cos(\omega_L t)}{\omega_L^2-\Omega^2}\cos(\Omega t) - \Omega\frac{\sin(\omega_L t)}{\omega_L^2-\Omega^2}\sin(\Omega t)\Bigg) + O(t^{-1}) \\
tF_{\mathrm{Si}}(+,-,-,+) = \quad & 2\Bigg(\omega_U\frac{\sin(\omega_U t)}{\omega_U^2-\Omega^2}\sin(\Omega t) + \Omega\frac{\cos(\omega_U t)}{\omega_U^2-\Omega^2}\cos(\Omega t) - \\
& \omega_L\frac{\sin(\omega_L t)}{\omega_L^2-\Omega^2}\sin(\Omega t) - \Omega\frac{\cos(\omega_L t)}{\omega_L^2-\Omega^2}\cos(\Omega t)\Bigg) + O(t^{-1}) \\
tF_{\mathrm{Ci}}(+,-,+,-) = \quad & 2\Bigg(\omega_L\frac{\sin(\omega_L t)}{\omega_L^2-\Omega^2}\cos(\Omega t) - \Omega\frac{\sin(\omega_L t)}{\omega_L^2-\Omega^2}\sin(\Omega t) - \\
& \omega_U\frac{\sin(\omega_U t)}{\omega_U^2-\Omega^2}\cos(\Omega t) + \Omega\frac{\cos(\omega_U t)}{\omega_U^2-\Omega^2}\sin(\Omega t)\Bigg) + O(t^{-1}) \\
tF_{\mathrm{Ci}}(+,-,-,+) = \quad & 2\Bigg(\Omega\frac{\sin(\omega_L t)}{\omega_L^2-\Omega^2}\cos(\Omega t) - \omega_L\frac{\cos(\omega_L t)}{\omega_L^2-\Omega^2}\sin(\Omega t) + \\
& \omega_U\frac{\cos(\omega_U t)}{\omega_U^2-\Omega^2}\sin(\Omega t) - \Omega\frac{\sin(\omega_U t)}{\omega_U^2-\Omega^2}\cos(\Omega t)\Bigg) + O(t^{-1}).
\end{aligned} \tag{5.79}$$

Low temperature

Let us first assume that the temperature is so low, that the associated thermal energy is much lower than the lowest oscillator energy: $k_BT \ll \hbar\omega_L$. Then in the leading order the temperature dependence can be neglected $\coth(\hbar\omega_k/2k_BT) \approx \tanh(\hbar\omega_k/2k_BT) \approx 1$ and the behavior of decoherence and orthogonalization becomes identical:

$$f_T^{\Gamma}(t;\omega_k) \approx f_T^{B}(t;\omega_k) \approx |\alpha_k(t)|^2 \equiv f_0(t;\omega_k) \tag{5.80}$$

with $\alpha_k(t)$ given by (5.29). We need to compute the integral

$$\begin{aligned}
\langle\langle f_0(t;\omega)\rangle\rangle = \quad & \frac{2M\bar{\gamma}_0}{\hbar\pi\Delta\omega}\int_{\omega_L}^{\omega_U}\frac{\omega_k}{(\omega_k^2-\Omega^2)^2}\Bigg(\left(1-\cos^2\Omega t\right) + \frac{\Omega^2}{\omega^2}\left(1+\cos^2\Omega t\right) \\
& -2\cos(\Omega t)(\cos\omega t) - \frac{2\Omega}{\omega_k}\sin(\Omega t)\sin(\omega t)\Bigg) = \\
& \frac{2M\bar{\gamma}_0}{\hbar\pi\Delta\omega}\left(I_1+I_2-2I_3-2I_4\right),
\end{aligned} \tag{5.81}$$

which splits in four terms. Results of each integration are given by:

$$I_1 = \int_{\omega_L}^{\omega_U} \frac{\omega}{(\omega^2-\Omega^2)}(1+\cos^2(\Omega t)) = \frac{1}{2}\left(\frac{1}{\omega_L^2-\Omega^2} - \frac{1}{\omega_U^2-\Omega^2}\right)(1+\cos^2(\Omega t)) \tag{5.82}$$

$$I_2 = \int_{\omega_L}^{\omega_U} \frac{\Omega^2}{\omega(\omega^2-\Omega^2)}(1-\cos^2(\Omega t)) = \tag{5.83}$$
$$\left[\frac{1}{4\Omega^2}\left(4\log\frac{\omega_U}{\omega_L} - 2\log\frac{\omega_U^2-\Omega^2}{\omega_L^2-\Omega^2}\right) + \frac{1}{2(\omega_L^2-\Omega^2)} - \frac{1}{2(\omega_U^2-\Omega^2)}\right](1-\cos^2(\Omega t))$$

$$I_3 = \int_{\omega_L}^{\omega_U} d\omega \frac{\omega}{(\omega^2-\Omega^2)^2}\cos(\omega t)\cos(\Omega t) = \frac{1}{4\Omega}\cos(\Omega t)\left[\frac{2\Omega\cos(\omega_L t)}{\omega_L^2-\Omega^2} - \frac{2\Omega\cos(\omega_U t)}{\omega_U^2-\Omega^2} + \right. \tag{5.84}$$
$$\left. t\cos(\Omega t)F_{\text{Si}}(+,-,-,+) + t\sin(\Omega t)F_{\text{Ci}}(+,-,+,-)\right]$$

$$I_4 = \int_{\omega_L}^{\omega_U} d\omega \frac{\Omega}{(\omega^2-\Omega^2)^2}\sin(\omega t)(\sin\Omega t) = \frac{1}{4\Omega}\sin(\Omega t)\Big\{\frac{2\omega_L\sin(\omega_L t)}{\omega_L^2-\Omega^2} - \frac{2\omega_U\sin(\omega_U t)}{\omega_U^2-\Omega^2} + \tag{5.85}$$
$$t\left[\cos(\Omega t)F_{\text{Ci}}(-,+,-,+) + \sin(\Omega t)F_{\text{Si}}(+,-,-,+)\right] - \Omega^{-1}\left[F_{\text{Si}}(-,+,+,-) - F_{\text{Ci}}(-,+,-,+)\right]\Big\}.$$

First, we are interested in the short-time behavior, valid for times much shorter than the shortest timescale of the full Hamiltonian, which in this case is $t \ll \omega_U^{-1}$ (here we work in the off-resonant "fast" regime). By expanding the expression for $\langle\langle f_0(t;\omega)\rangle\rangle$ in power series with respect to time, we find after a tedious calculation that

$$I_1 = \tag{5.86}$$
$$\left[\frac{1}{4\Omega^2}\left(4\log\frac{\omega_U}{\omega_L} - 2\log\frac{\omega_U^2-\Omega^2}{\omega_L^2-\Omega^2}\right) + \frac{1}{2(\omega_L^2-\Omega^2)} - \frac{1}{2(\omega_U^2-\Omega^2)}\right]\Omega^2 t^2 + O(t^4)$$

$$I_2 = \left(\frac{1}{\omega_L^2-\Omega^2} - \frac{1}{\omega_U^2-\Omega^2}\right)\left(2-\Omega^2 t^2\right) + O(t^4) \tag{5.87}$$

$$I_3 = \tag{5.88}$$
$$\frac{1}{4\Omega}\left[\frac{2\Omega}{\omega_L^2-\Omega^2}\left(1-\frac{\omega_L^2 t^2}{2}-\frac{\Omega^2 t^2}{2}\right) - \frac{2\Omega}{\omega_U^2-\Omega^2}\left(1-\frac{\omega_U^2 t^2}{2}-\frac{\Omega^2 t^2}{2}\right) + \Omega t^2\log\frac{\omega_L^2-\Omega^2}{\omega_U^2-\Omega^2}\right] + O(t^4)$$

$$I_4 = \frac{1}{4\Omega}\left(\frac{2\omega_L\omega_L t}{\omega_L^2-\Omega^2}\Omega\omega_L t^2\ \frac{2\omega_U\omega_U t}{\omega_U^2-\Omega^2}\Omega\omega_U t^2\right) + O(t^4). \tag{5.89}$$

As a result, the expression for the mean valid in the short-time regime is

$$\langle\langle f_0(t;\omega)\rangle\rangle = \frac{2M\bar{\gamma}_0}{\hbar\pi\Delta\omega}\log\left(\frac{\omega_U}{\omega_L}\right)t^2 + O(t^4), \tag{5.90}$$

which immediately implies that the initial behavior of both the decoherence and the orthogonalization factors is a Gaussian decay (equations (5.69, 5.70)):

$$|\Gamma_{X,X'}(t)| \approx B_{X,X'}(t) \approx \exp\left[-N_{mac}\left(\frac{t}{\tau_0}\right)^2\right], \tag{5.91}$$

with a common timescale:

$$\frac{\tau_0}{\sqrt{N_{mac}}},\ \tau_0 = \frac{\hbar\pi\Delta\omega}{\Delta X M\bar{\gamma}_0}\log^{-1}\left(1+\frac{\Delta\omega}{\omega_L}\right). \tag{5.92}$$

We note that it depends on the macrofraction size and the separation through the product $\Delta X\sqrt{N_{mac}}$. Thus, in order to keep the same time-scale for small separations the macrofraction size should increase quadratically with decreasing separation.

The initial Gaussian decay (5.91) by no means guarantees that the functions will stay close to zero with negligible fluctuations—revivals are possible, as can be seen on the plots from the previous Section. Thus a long-time analysis is needed, governed in the case of off-resonant "fast" environment by the condition $t \gg 1/(\omega_L - \Omega) \approx 1/\omega_L$ as $\Omega \ll \omega_L$. The detailed calculation, basing on the equation (5.79), is tedious. The result reads:

$$\langle\langle f_0(t;\omega)\rangle\rangle = \frac{2M\bar{\gamma}_0}{\hbar\pi\Delta\omega}\left(A_0\cos^2(\Omega t) + B_0\right), \tag{5.93}$$

where:

$$A_0 \equiv -\frac{1}{2\Omega^2}\left(2\log\frac{\omega_U}{\omega_L} - \log\frac{\omega_U^2-\Omega^2}{\omega_L^2-\Omega^2}\right), \tag{5.94}$$

$$B_0 \equiv \frac{1}{\omega_L^2-\Omega^2} - \frac{1}{\omega_U^2-\Omega^2} - A_0. \tag{5.95}$$

Interestingly, for large times the mean has an oscillatory part with the system frequency Ω, but for "fast" environments this part is vanishingly small as $A_0 \approx 0$. The above formulas allow us to solve a very important problem in the context of Spectrum Broadcast Structures, namely how big should be macrofractions in order to get decoherence and orthogonalization with a prescribed error ϵ (common in the low T limit for both functions):

$$|\Gamma_{X,X'}(t)|, B_{X,X'}(t) < \epsilon. \tag{5.96}$$

This in turn will determine the trace norm distance of the actual state $\varrho_{S:fE}(t)$ to the spectrum broadcast form. By minimizing equation (5.93) we find the maximal value of the decoherence

factor and generalized overlap (5.71,5.72). This immediately leads to a conclusion that if:

$$\Delta X^2 N_{mac} > \frac{\hbar\pi\Delta\omega}{M\bar{\gamma}_0 B_0}\log\frac{1}{\epsilon} \approx \frac{\hbar\pi\omega_U^2\omega_L^2}{M\bar{\gamma}_0\left(\omega_U+\omega_L\right)}\log\frac{1}{\epsilon}, \tag{5.97}$$

then the functions will be bounded by (5.96) for all times $t \gg 1/(\omega_L - \Omega)$. This result can be treated as an analytical proof of Spectrum Broadcast Structure formation in the studied regime. Similarly to the short-time decay (5.91), the asymptotic behavior of $|\Gamma_{X,X'}(t)|, B_{X,X'}(t)$ is governed by the product $\Delta X^2 N_{mac}$, so that the increase of the macrofraction size is quadratic with decreasing the spatial resolution of the Spectrum Broadcast Structure. This finite spatial resolution of the Spectrum Broadcast Structure for a given error level and a macrofraction size is a manifestation of the "macroscopic objectivity" idea, introduced in the former parts of this Chapter for simplified models of Quantum Brownian Motion. Namely, for a given tolerance ϵ and a macrofraction size, the objective state of the system appear only on the length scales greater than ones given by (5.97).

High temperature

Here we consider the opposite situation of a hot environment: $k_B T \gg \hbar\omega_U$. Intuitively, a formation of the Spectrum Broadcast Structure should be quite compromized now, as high temperature, while increasing the decoherence power of the environment through the increase of its energy appearing in (5.69), decreases its information capacity, by decreasing the purity, on which depends the orthogonalization factor (5.70). Indeed, this is what we show below. In the leading order $\tanh\left(\frac{\tau_T\omega}{2}\right) = \left[\coth\left(\frac{\tau_T\omega}{2}\right)\right]^{-1} \approx \frac{\tau_T\omega}{2}$ and (5.69) and (5.70) read:

$$f_T^{\Gamma}(t;\omega_k) \approx \frac{2}{\tau_T\omega_k}|\alpha_k(t)|^2, \tag{5.98}$$

$$f_T^{B}(t;\omega_k) \approx \frac{\tau_T\omega_k}{2}|\alpha_k(t)|^2. \tag{5.99}$$

The relevant means (5.74) can be calculated analytically again. We start with decoherence factor

$$\begin{aligned}&\left\langle\left\langle f_T^{\Gamma}(t;\omega_k)\right\rangle\right\rangle = \\ &\frac{4M\bar{\gamma}_0}{\hbar\pi\tau_T\omega_L\omega_U}\int_{\omega_L}^{\omega_U}\frac{1}{(\omega_k^2-\Omega^2)^2}\Bigg(\left(1-\cos^2(\Omega t)\right)+\frac{\Omega^2}{\omega_k^2}\left(1+\cos^2(\Omega t)\right) \\ &-2\cos(\Omega t)\cos(\omega_k t)-\frac{2\Omega}{\omega_k}\sin(\Omega t)\sin(\omega_k t)\Bigg) = \frac{2M\bar{\gamma}_0}{\hbar\pi\tau_T\omega_L\omega_U}\left(I_1^{\Gamma}+I_2^{\Gamma}-2I_3^{\Gamma}-2I_4^{\Gamma}\right).\end{aligned} \tag{5.100}$$

Computing integrals we obtain:

$$I_1^{\Gamma} = \int_{\omega_L}^{\omega_U} d\omega \frac{\Omega^2}{\omega^2(\omega^2-\Omega^2)^2}\left(1-\cos^2(\Omega t)\right) = \tag{5.101}$$

$$\frac{\left(1-\cos^2(\Omega t)\right)}{\Omega^2}\left(\frac{\omega_U-\omega_L}{\omega_U\omega_L}-\frac{\omega_U}{2(\omega_U^2-\Omega^2)}+\frac{\omega_L}{2(\omega_L^2-\Omega^2)}+\frac{3}{4\Omega}\log\frac{(\omega_U+\Omega)(\omega_L-\Omega)}{(\omega_U-\Omega)(\omega_L+\Omega)}\right)$$

$$I_2^\Gamma=\int_{\omega_L}^{\omega_U}d\omega\frac{1}{(\omega^2-\Omega^2)^2}\left(1+\cos^2(\Omega t)\right)= \tag{5.102}$$
$$\frac{1}{4\Omega^2}\left(1+\cos^2(\Omega t)\right)\left(\frac{2\omega_L}{\omega_L^2-\Omega^2}-\frac{2\omega_U}{\omega_U^2-\Omega^2}+\frac{1}{\Omega}\log\frac{(\omega_U+\Omega)(\omega_L-\Omega)}{(\omega_U-\Omega)(\omega_L+\Omega)}\right)$$

$$I_3^\Gamma=\int_{\omega_L}^{\omega_U}d\omega\frac{1}{(\omega^2-\Omega^2)^2}\cos(\omega t)\cos(\Omega t)= \tag{5.103}$$
$$\frac{1}{4\Omega^2}\cos\Omega t\left[\frac{2\omega_L\cos(\omega_L t)}{\omega_L^2-\Omega^2}-\frac{2\omega_U\cos(\omega_U t)}{\omega_U^2-\Omega^2}+t\cos(\Omega t)F_{\mathrm{Si}}(+,-,+,-)+\right.$$
$$\left.t\sin(\Omega t)F_{\mathrm{Ci}}(+,-,-,+)+\frac{1}{\Omega}(\cos(\Omega t)\,F_{\mathrm{Ci}}(+,-,-,+)+\sin(\Omega t)\,F_{\mathrm{Si}}(-,+,-,+)\right]$$

$$I_4^\Gamma=\int_{\omega_L}^{\omega_U}d\omega\frac{\Omega}{\omega(\omega^2-\Omega^2)^2}\sin(\omega t)\sin(\Omega t)= \tag{5.104}$$
$$\frac{1}{2\Omega^3}\sin(\Omega t)\left[2\left(\mathrm{Si}\left(\omega_U t\right)-\mathrm{Si}\left(\omega_L t\right)\right)-\cos(\Omega t)F_{\mathrm{Si}}(-,+,-,+)-\sin(\Omega t)F_{\mathrm{Ci}}(-,+,+,-)\right.$$
$$\left.+\frac{\Omega}{2}\left(\frac{2\Omega\sin(\omega_L t)}{\omega_L^2-\Omega^2}-\frac{2\Omega\sin(\omega_U t)}{\omega_U^2-\Omega^2}+t\cos(\Omega t)F_{\mathrm{Ci}}(-,+,+,-)+t\sin(\Omega t)F_{\mathrm{Si}}(+,-,+,-)\right)\right].$$

In the case of generalized overlap the mean is given by

$$\left\langle\left\langle f_T^B(t;\omega_k)\right\rangle\right\rangle= \tag{5.105}$$
$$\frac{M\bar{\gamma}_0\tau_T}{\hbar\pi\Delta\omega}\int_{\omega_L}^{\omega_U}\frac{\omega^2}{(\omega_k^2-\Omega^2)^2}\left(\left(1+\cos^2(\Omega t)+\right)+\frac{\Omega^2}{\omega_k^2}\left(1-\cos^2(\Omega t)\right)\right.$$
$$\left.-2\cos(\Omega t)\cos(\omega_k t)-\frac{2\Omega}{\omega_k}\sin(\Omega t)\sin(\omega_k t)\right)=\frac{2M\bar{\gamma}_0\tau_T}{\hbar\pi\Delta\omega}\left(I_1^B+I_2^B-2I_3^B-2I_4^B\right)$$

The results of integration are:

$$I_1^B=\int_{\omega_L}^{\omega_U}d\omega\frac{\omega^2}{(\omega^2-\Omega^2)^2}\left(1+\cos^2(\Omega t)\right)= \tag{5.106}$$
$$\frac{\omega_L}{2(\omega_L^2-\Omega^2)}-\frac{\omega_U}{2(\omega_U^2-\Omega^2)}+\frac{1}{4\Omega}\log\frac{(\omega_U-\Omega)(\omega_L+\Omega)}{(\omega_L-\Omega)(\omega_U+\Omega)}$$

$$I_2^B=\int_{\omega_L}^{\omega_U}d\omega\frac{\Omega^2}{(\omega^2-\Omega^2)^2}\left(1-\cos^2(\Omega t)\right)= \tag{5.107}$$
$$\frac{\omega_L}{2(\omega_L^2-\Omega^2)}-\frac{\omega_U}{2(\omega_U^2-\Omega^2)}+\frac{1}{4\Omega}\log\frac{(\omega_U+\Omega)(\omega_L-\Omega)}{(\omega_L+\Omega)(\omega_U-\Omega)}$$

$$I_3^B=\int_{\omega_L}^{\omega_U}d\omega\frac{\omega^2}{(\omega^2-\Omega^2)^2}\cos(\omega t)\cos(\Omega t)= \tag{5.108}$$

$$
\begin{aligned}
&\frac{1}{4\Omega}\Bigg(\frac{2\omega_L\cos(\omega_L t)}{\omega_L^2-\Omega^2}-\frac{2\omega_U\cos(\omega_U t)}{\omega_U^2-\Omega^2}+\\
&t(\cos(\Omega t)F_{\mathrm{Si}}(+,-,+,-)+\sin(\Omega t)F_{\mathrm{Ci}}(+,-,-,+))+\\
&\frac{1}{\Omega}\cos(\Omega t)\left(\cos(\Omega t)F_{\mathrm{Ci}}(-,+,+,-)+\sin(\Omega t)F_{\mathrm{Si}}(+,-,+,-)\right)\Bigg)\\
I_4^B=\quad&\int_{\omega_L}^{\omega_U}d\omega\frac{\omega\Omega}{(\omega^2-\Omega^2)^2}\sin(\omega t)\sin(\Omega t)= \qquad (5.109)\\
&\frac{1}{4}\sin(\Omega t)\left[\frac{2\Omega\sin(\omega_L t)}{\omega_L^2-\Omega^2}-\frac{2\Omega\sin(\omega_U t)}{\omega_U^2-\Omega^2}+t(\cos(\Omega t)F_{\mathrm{Ci}}(-,+,+,-)+\sin(\Omega t)F_{\mathrm{Si}}(+,-,+,-))\right].
\end{aligned}
$$

To find short-time behavior of the mean, we expand th expressions for decoherence and generalized overlap up to the second order in time. This is a good approximation for $t \ll \omega_U^{-1}$. As a result we obtain in the case of decoherence

$$
\begin{aligned}
&I_1^\Gamma= \qquad (5.110)\\
&\left(\frac{\omega_U-\omega_L}{\omega_U\omega_L}-\frac{\omega_U}{2(\omega_U^2-\Omega^2)}+\frac{\omega_L}{2(\omega_L^2-\Omega^2)}+\frac{3}{4\Omega}\log\frac{(\omega_U+\Omega)(\omega_L-\Omega)}{(\omega_U-\Omega)(\omega_L+\Omega)}\right)t^2+O(t^4)\\
&I_2^\Gamma= \qquad (5.111)\\
&\frac{1}{4\Omega^2}\left(\frac{2\omega_L}{\omega_L^2-\Omega^2}-\frac{2\omega_U}{\omega_U^2-\Omega^2}+\frac{1}{\Omega}\log\frac{(\omega_U+\Omega)(\omega_L-\Omega)}{(\omega_U-\Omega)(\omega_L+\Omega)}\right)(2-\Omega^2t^2)+O(t^4)\\
&I_3^\Gamma=\frac{\Omega^2}{4}\left(\frac{2\omega_L}{\omega_L^2-\Omega^2}-\frac{2\omega_U}{\omega_U^2-\Omega^2}+\frac{1}{\Omega}\log\frac{(\omega_U+\Omega)(\omega_L-\Omega)}{(\omega_U-\Omega)(\omega_L+\Omega)}\right) \qquad (5.112)\\
&+\frac{1}{2(\omega_L^2-\Omega^2)(\omega_U^2-\Omega^2)}\left(\omega_L\Omega^2+\omega_U\omega_L-\omega_L\omega_U^2-\omega_U\Omega^2\right)t^2+O(t^4)\\
&I_4^\Gamma=\left(\frac{1}{2\omega_L^2-\Omega^2}-\frac{1}{2\omega_U^2-\Omega^2}+\frac{1}{4\Omega}\log\frac{(\omega_U+\Omega)(\omega_L-\Omega)}{(\omega_U-\Omega)(\omega_L+\Omega)}\right)t^2+O(t^4), \qquad (5.113)
\end{aligned}
$$

and for generalized overlap

$$
\begin{aligned}
&I_1^B=\left(\frac{\omega_L}{\omega_L^2-\Omega^2}-\frac{\omega_U}{\omega_U^2-\Omega^2}-\frac{1}{2\Omega}\log\frac{(\omega_L-\Omega)(\omega_U+\Omega)}{(\omega_L+\Omega)(\omega_U-\Omega)}\right)\frac{2-\Omega^2t^2}{2}+O(t^4) \qquad (5.114)\\
&I_2^B=\frac{\Omega^2}{2}\left(\frac{\omega_L}{\omega_L^2-\Omega^2}-\frac{\omega_U}{\omega_U^2-\Omega^2}+\frac{1}{2\Omega}\log\frac{(\omega_L-\Omega)(\omega_U+\Omega)}{(\omega_L+\Omega)(\omega_U-\Omega)}\right)t^2+O(t^4) \qquad (5.115)\\
&I_3^B=\frac{1}{2}\left(\frac{\omega_L}{\omega_L^2-\Omega^2}-\frac{\omega_U}{\omega_U^2-\Omega^2}-\frac{1}{2\Omega}\log\frac{(\omega_L-\Omega)(\omega_U+\Omega)}{(\omega_L+\Omega)(\omega_U-\Omega)}\right)+ \qquad (5.116)\\
&\frac{1}{4}\Bigg(\frac{\omega_U}{\omega_U^2-\Omega^2}(\omega_U^2+\Omega^2)-\frac{\omega_L}{\omega_L^2-\Omega^2}(\omega_L^2+\Omega^2)+\\
&3(\omega_L-\omega_U)+2\Omega\log\frac{(\omega_L-\Omega)(\omega_U+\Omega)}{(\omega_L+\Omega)(\omega_U-\Omega)}\Bigg)t^2+O(t^4)\\
&I_4^B=\frac{\Omega^2}{2}\left(\frac{\omega_L}{\omega_L^2-\Omega^2}-\frac{\omega_U}{\omega_U^2-\Omega^2}-\frac{1}{2\Omega}\log\frac{(\omega_L-\Omega)(\omega_U+\Omega)}{(\omega_L+\Omega)(\omega_U-\Omega)}\right)t^2+O(t^4). \qquad (5.117)
\end{aligned}
$$

Finally for short time-scales $t \ll \omega_U^{-1}$ we obtain the following behavior:

$$\left\langle\left\langle f_T^{\Gamma}(t;\omega)\right\rangle\right\rangle = \frac{4M\bar{\gamma}_0}{\hbar\pi\omega_L\omega_U\tau_T}t^2 + O(t^4), \tag{5.118}$$

$$\left\langle\left\langle f_T^{B}(t;\omega)\right\rangle\right\rangle = \frac{M\bar{\gamma}_0\tau_T}{\hbar\pi}\tau_T t^2 + O(t^4), \tag{5.119}$$

resulting again in the initial Gaussian decay:

$$|\Gamma_{X,X'}(t)| \approx \exp\left[-N_{mac}\left(\frac{t}{\tau_{dec}}\right)^2\right] \tag{5.120}$$

$$B_{X,X'}(t) \approx \exp\left[-N_{mac}\left(\frac{t}{\tau_{ort}}\right)^2\right]. \tag{5.121}$$

However, this time the timescales are different. For the decoherence one obtains

$$\frac{\tau_{dec}}{\sqrt{N_{mac}}}, \quad \tau_{dec} = \tau_T\frac{\hbar\pi\omega_L\omega_U}{2\Delta X M\bar{\gamma}_0}, \tag{5.122}$$

whereas for generalized overlap the characteristic time is:

$$\frac{\tau_{ort}}{\sqrt{N_{mac}}}, \quad \tau_{ort} = \tau_T^{-1}\frac{2\hbar\pi}{\Delta X M\bar{\gamma}_0}. \tag{5.123}$$

As one would expect, the key difference is in the temperature dependence through the the thermal time $\tau_T = \hbar/(k_B T)$. While τ_{dec} decreases as T^{-1} indicating faster decoherence with higher temperature, $\tau_{ort} \sim T$ so that it may even happen that the orthogonalization timescale $\tau_{dec}/\sqrt{N_{mac}}$ is larger than the validity of the short-time approximation $t \ll \omega_U^{-1}$. Keeping $\tau_{dec}/\sqrt{N_{mac}} < \omega_U^{-1}$ so that the short-time approximation, and hence the Gaussian decay is valid, puts a constraint on the temperature, the macrofraction size and the separation to be discriminated:

$$\frac{T}{\Delta X\sqrt{N_{mac}}} < \frac{M\bar{\gamma}_0}{2\pi k_B\omega_U}. \tag{5.124}$$

To get some insight into possible revivals of the decoherence and orthogonalization factors, we perform long-time analysis. For $t \gg 1/(\omega_L - \Omega) \approx 1/\omega_L$ the asymptotic expression for $\left\langle\left\langle f_T^{\Gamma}(t;\omega)\right\rangle\right\rangle$ reads:

$$\left\langle\left\langle f_T^{\Gamma}(t;\omega)\right\rangle\right\rangle = \quad \frac{4M\bar{\gamma}_0}{\hbar\pi\Delta\omega\tau_T}\left(A_\Gamma\cos^2(\Omega t) + B_\Gamma\right) + O(t^{-1}) \tag{5.125}$$

with:

$$A_\Gamma \equiv -\frac{1}{4\Omega^2}\left[\frac{\Delta\omega}{\omega_U\omega_L}+\frac{1}{2\Omega}\log\frac{(\omega_U+\Omega)(\omega_L-\Omega)}{(\omega_U-\Omega)(\omega_L+\Omega)}\right], \tag{5.126}$$

$$B_\Gamma \equiv \frac{1}{4\Omega^2}\left(\frac{\omega_L}{\omega_L^2-\Omega^2}-\frac{\omega_U}{\omega_U^2-\Omega^2}\right)-A_\Gamma, \tag{5.127}$$

while for generalized overlap it is:

$$\left\langle\left\langle f_T^B(t;\omega)\right\rangle\right\rangle = \quad \frac{M\bar{\gamma}_0\tau_T}{\hbar\pi\Delta\omega}\left(A_B\cos^2(\Omega t)+B_B\right)+O(t^{-1}), \tag{5.128}$$

where:

$$A_B \equiv \frac{1}{2\Omega}\log\frac{(\omega_U-\Omega)(\omega_L+\Omega)}{(\omega_L-\Omega)(\omega_U+\Omega)} \tag{5.129}$$

$$B_B \equiv \frac{\omega_L}{\omega_L^2-\Omega^2}-\frac{\omega_U}{\omega_U^2-\Omega^2}. \tag{5.130}$$

We observe that unlike in the low T regime, the decoherence asymptotic keeps oscillating with the system frequency Ω even for fast environments as $A_\Gamma \approx \Delta\omega/(4\Omega^2\omega_U\omega_L)$, while $A_B \approx 0$. We are now ready to solve the problem of the Spectrum Broadcast Structure formation in the high temperature regime. We perform minimization of the above expressions. This allows us to establish the size of macrofractions needed, in a given temperature T, to achieve decoherence and distinguishability, and hence the Spectrum Broadcast Structures, on a length-scale ΔX within given errors:

$$|\Gamma_{X,X'}(t)| < \epsilon_{dec},\ B_{X,X'}(t) < \epsilon_{ort}. \tag{5.131}$$

Equations (5.125) and (5.128) give us the answer:

$$T\Delta X_0^2 N_{mac}^\Gamma > \frac{\hbar^2\pi\Delta\omega}{2Mk_B\bar{\gamma}_0 B_\Gamma}\log\frac{1}{\epsilon_{dec}} \approx \frac{\hbar^2\pi\Omega^2\omega_U\omega_L}{Mk_B\bar{\gamma}_0}\log\frac{1}{\epsilon_{dec}}, \tag{5.132}$$

$$\frac{\Delta X_0^2 N_{mac}^B}{T} > \frac{2\pi k_B\Delta\omega}{M\bar{\gamma}_0 B_B}\log\frac{1}{\epsilon_{ort}} \approx \frac{2\pi k_B\omega_U\omega_L}{M\bar{\gamma}_0}\log\frac{1}{\epsilon_{ort}}, \tag{5.133}$$

where N_{mac}^Γ is the size of the traced-over part of the environment $(1-f)E$ and N_{mac}^B is the size of (each of) the observed macrofraction. As predicted, keeping all other parameters fixed, the observed macrofraction size in high temperature must be much larger than the unobserved one in order to come close to Spectrum Broadcast Structure. Indeed, from the above results those sizes scale like the thermal-to-central-system energies:

$$\frac{N_{mac}^B}{N_{mac}^\Gamma} > 2\left(\frac{k_BT}{\hbar\Omega}\right)^2\frac{\log\epsilon_{ort}}{\log\epsilon_{dec}} \tag{5.134}$$

and the later factor is huge for the considered "fast" environments, since $k_B T \gg \hbar\omega_U \gg \hbar\Omega$.

5.5.9 Dynamical aspects of Spectrum Broadcast Structure

Let us assume that a Spectrum Broadcast Structure is formed, this is both $|\Gamma_{X_0,X_0'}(t)|$ and $B^{mac}_{X_0,X_0'}(t)$ are negligible small for $X_0 \neq X_0'$. Then we see that equation (5.36), taking the usual continuum limit of the sum, is approximately (it can never become strictly) diagonal in the position basis:

$$\varrho_{S:fE}(t) \approx \int dX_0 \, |\langle X_0|\phi_0\rangle|^2 \times \\ \times |X(t)\rangle\langle X(t)| \otimes \varrho_{mac_1}(X_0;t) \otimes \cdots \otimes \varrho_{mac_{\mathcal{M}}}(X_0;t), \tag{5.135}$$

where $|X(t)\rangle \equiv e^{-i\hat{H}_S t}|X_0\rangle$, we have grouped fE into $\mathcal{M}$ macro-fractions and $\varrho_{mac_i}(X_0;t)$ have orthogonal supports (for large enough t, see for example Figure 5.3 d) or the results of Subsection 5.5.8). What appears in (5.135) is a novel structure, compared to the previous studies [13, 65], Dynamical Spectrum Broadcast Structure. Because the system now has its own dynamics, the pointers $|X(t)\rangle$ are now states of motion–they evolve on a time-scale $t_S \sim 2\pi/\Omega$, rather than being static as in other models in which the formation of Spectrum Broadcast Structure has been proven [65], and a time-dependent Spectrum Broadcast Structure is formed with a reference to these evolving pointers. For the regime of parameters considered in this Chapter, the respective time-scales are: $t_S \sim 2 \times 10^{-8} s$ – the motion of the central system and $t_{SBS} \sim 2 \times 10^{-10} s$ – the timescale of Spectrum Broadcast Structure formation in the case of the off-resonant "fast" environment (to find the timescale we used the results presented in Figure 5.3 b),d)). As a result, the Spectrum Broadcast Structure is formed two orders of magnitude faster than the intrinsic system evolution. Thanks to it, all the observers will measure the same initial position (this is the oscillation amplitude) X_0, leaving the (by now decohered) system undisturbed in its state of motion. But the traces of this motion are present in the environment not only through X_0 – each state $\varrho_{mac}(X_0;t)$ depends on the whole trajectory $X(t;X_0)$. More precisely, at time t the argument of displacement operator acting on an individual subsystem of the environment is a product of the central system's trajectory and factor steaming from the free evolution of the subsystem, integrated from the initial time $t_0 = 0$ up to final time t (equations (5.29 5.32)). In principle, it should be possible to reconstruct the trajectory by measuring the environment. We have not developed a complete scheme to achieve this. Let us just make some remarks regarding the topic. One can approach this problem from different sides. Firstly, from Chapter 2 we can try to determine the measurement that discriminates optimally the environmental states evolving accordingly X_0 and X_0'. However, we were not able to diagonalize the corresponding operator. On the other hand, we would like to point out that, under assumptions that we have made, central system acts on the environment as a classical driving force. In fact, monitoring

of such a force has been studied in literature, for example in context of gravity-wave detectors [102]. We believe that a closer inspection of these results may solve the problem of recovering the trajectory of the central system. However, due to time constraints, we were forced to postpone this research direction and we hope to address it in near future.

The intuitive picture is that while the system rotates on its intrinsic timescale, the environment follows this movement and past the transient period a spectrum broadcast structure is being continuously formed, leading to a perception of objective position at each moment of time. Due to the neglected back reaction on the system – recoilless limit, the structure (5.135) is only a first approximation to this situation, as for example the central system does not dissipate its energy to the environment. The next logical step would be to include the back reaction.

5.6 Concluding remarks

In this Chapter we conducted the study concerning the emergence of Spectrum Broadcast Structures in the widely studied Quantum Brownian Motion model.

We started our discussion by arguing why the investigation of Spectrum Broadcast Structure cannot be performed using the techniques that has been developed so far in the literature devoted to the model. We also described in detail why we do not follow the common way of modeling the environment in terms of continuous spectral density function, but instead in most cases keep the description of the environment to be discrete. We discussed the advantages and disadvantages of this approach.

We started the actual investigation of the model with the highly simplified case, in which the self-Hamiltonians of the system and the environment were not included into the consideration (the Full Measurement Limit). We have shown that there is always a formation of the Spectrum Broadcast Structure for thermal environment, irrespectively of how high the temperature is, if one waits long enough and/or takes large enough macrofractions. We derived the Gaussian character of this formation and the timescales of the process. Although the considered situation is a great simplification it allowed to gain some insights into the full model.

Subsequently, we made a step towards the full model by including self-Hamiltonian of the environment. Here, we investigated the time averages of the indicator functions (decoherence factor and generalized overlap) using a form of ergodicity for almost periodic functions. In the limit of low temperatures and for large separations of the system's initial positions X_0, X_0' we showed that these averages decay exponentially. Although the results were still obtained for simplified model there are interesting at least for two reasons. Firstly, to the author's knowledge, the technique concerning averages of almost periodic functions has not been applied previously to study decoherence. We believe that it can prove to be useful also in other models, in which the almost periodic function appear, such as spin models of decoherence. Moreover,

the large separation assumption opens here an interesting possibility of a space coarse-grained Spectrum Broadcast Structure, where such a structure appears for large distances only but for small not. This would lead to a sort of a macroscopic objectivity, emerging only at large scales.

Finally, we addressed the full model in the recoilless limit. We assumed that the back-reaction of the environment on the system can be neglected, what allowed us to use Born-Oppenheimer type of approximation and to arrive at a manageable form of the evolved system-environment state. Subsequently, we restricted our considerations to the particular initial states of the central system - momentum and position squeezed states. There were two reasons to do so. Firstly, the choice was motivated by the fact that the system couples to the environment via position operator and thus, from this fact and the results obtained for simplified models, it could be expected that the decoherence process happens in the basis related to the position eigenstates. Moreover, for the considered states the evolution operator takes a particular simple form that allowed us to use the expression developed in Chapter 4. We provided a case study of continuous spectral density in the Calderia- Leggett approximation, known also as Fokker-Planck limit. Subsequently, we studied the functions indicating the Spectrum Broadcast structure formation for different regimes of discrete environmental spectrum (resonant, "slow" and "fast" off-resonant) and discussed the differences between the obtained results. Firstly, the analysis was performed by plotting the function of interest (in some cases also their averages). The influence of squeezing of the initial state of the environment on the formation of Spectrum Broadcast Structure was also investigated. We developed an analytical treatment of almost periodic functions appearing in the Quantum Brownian Motion model basing on the Law of Large Numbers. It allowed us to answer relevant questions concerning the time-scales of Spectrum Broadcast Structure formation as well as the numbers of environmental subsystems needed to achieve this process in a mathematically rigorous way. Finally, we commented on novel, dynamical character of the Spectrum Broadcast Structure formed in the considered model.

Chapter 6

Conclusions and open problems

In this thesis our aim was to study selected problems concerning role of correlations in Quantum Information Theory and Quantum to Classical transition. We investigated Remote State Preparation protocol and Spectrum Broadcast Structures formation in models with environments consisting of harmonic oscillators.

More precisely, in Chapter 3 we showed that quantum separable correlations cannot provide better efficiency of Remote State Preparation Protocol than that obtained with entangled states. We proved this statement for the most general version of the protocol, working under the natural assumptions for the problem. In this way we resolved the important issue that attracted the interest of some members of Quantum Information Theory community. Subsequently, we provided also two examples of restricted protocols, in which the above statement does not hold. Both of them concern restrictions imposed on decoding operations. As a result, we gained a more complete understanding of power of different kinds of quantum correlations in Remote State Preparation protocol.

In the second part of the thesis, Chapters 4 and 5 we studied the formation of Spectrum Broadcast Structure in the context of physical models with environments consisting of harmonic oscillators. Firstly, in Chapter 4 we derived formulas for functions indicating Spectrum Broadcast Structures formation – decoherence factor and generalized overlap, assuming that the environment is driven by a central system and that the initial state of the environment is thermal. We generalized these results to arbitrary tensor products of single mode Gaussian states of the environment. Subsequently, the dependence of the indicator functions on temperature was discussed. In Chapter 5 we investigated the model of Quantum Brownian Motion, initially studying simplified versions of the model. Working the in recoilless limit we derived the approximated solution for the dynamics in the full model and discussed the formation of Spectrum Broadcast Structures in the case of different descriptions of the environment: continuous and discrete one. In the former case we provided expression for indicator functions (decoherence factor and generalized overlap) in the so called Caldeira-Leggett limit. In the latter we argued that the indicator function become almost periodic functions of time and analyze their time-behavior with respect to the different choices of frequencies of the environment and

its initial state. Finally we developed the analytical technique of analysis basing on the Law of Large Numbers. This allowed us to find regimes of parameters, for which in Quantum Brownian Motion, in recoilless limit, Spectrum Broadcast Structures are approximately formed. We discussed the novel, dynamical character of Spectrum Broadcast Structure, which is formed in the model. This are main results of the second part of the thesis.

Let us now list some open problems. Regarding Chapter 2:

- It would be interesting to investigate if the lack of common reference frame results in advantage also in protocols other than Remote State Preparation.
- As we mentioned, the thermodynamical perspective of the protocol could be examined in future.

For the second part of the thesis:

- To prove in a rigorous way condition indicating the enhancement of decoherence process with temperature for continuous variable systems.
- To understand in quantitative way why some controlled evolutions lead the enhancement of decoherence process with temperature. The results obtained in Chapter 4 concerning this problem are preliminary.
- To try to quantify, what is the cost of writing information about the central system in the environment. Does it scale with number of records present in the environment?
- To try to answer the question: is there a fundamental bound on the amount of information that can be written in the environment? If the answer is affirmative, what are consequences for Spectrum Broadcast Structure formation? The results of the analysis should be compared with [103].
- To explore connections between dynamical Spectrum Broadcast Structures and consistent histories framework. Investigation along these lines has been initiated in [104]. Once more, an especially interesting issue concerns the information-capacity of the environment: what happens when there are not enough environmental subsystems to store records about full consistent history of the system? Does such fact introduce irreversibility to the problem?
- To generalize results of Chapter 5 by restoring dissipation into considerations.
- To analyze if the Quantum Speed Limits [105] can be used to bound timescales of Spectrum Broadcast Structures formation.

- We know that in some cases there is a connection between consistent histories and quantum trajectories [106, 107]. It would be interesting between quantum trajectories and Spectrum Broadcast Structures.

Bibliography

[1] P. A. Schilpp Ed. *Albert Einstein, Philosopher-Scientist: The Library of Living Philosophers, Vol. VII*. La Salle: Open Court, 1949.

[2] A. Einstein, B. Podolsky, and N. Rosen. "Can Quantum-Mechanical Description of Physical Reality Be Considered Complete?" In: *Phys. Rev.* 47 (10 1935), pp. 777–780.

[3] N. Bohr. "Can Quantum-Mechanical Description of Physical Reality be Considered Complete?" In: *Phys. Rev.* 48 (8 1935), pp. 696–702.

[4] J. S. Bell. "On the Einstein Podolsky Rosen paradox". In: *Physics* 1.3 (1964), pp. 195–200.

[5] W. Joos and H. D. Zeh. "The Emergence of Classical Properties Through Interaction with the Environment". In: *Z. Phys. B* 59 (1985).

[6] W. H. Zurek. "Pointer basis of quantum apparatus: Into what mixture does the wave packet collapse?" In: *Phys. Rev. D* 24 (6 1981), pp. 1516–1525.

[7] W. H. Zurek. "Environment-induced superselection rules". In: *Phys. Rev. D* 26 (8 1982), pp. 1862–1880.

[8] E. Joos, H. Zeh, C. Kiefer, D. Giulini, J. Kupsch, and I. Stamatescu. *Decoherence and the Appearance of a Classical World in Quantum Theory*. Springer Berlin Heidelberg, 2013.

[9] W. H. Zurek. "Decoherence, einselection, and the quantum origins of the classical". In: *Rev. Mod. Phys.* 75 (3 2003), pp. 715–775.

[10] H. Ollivier, D. Poulin, and W. H. Zurek. "Objective Properties from Subjective Quantum States: Environment as a Witness". In: *Phys. Rev. Lett.* 93 (22 2004), p. 220401.

[11] W. H. Zurek. "Quantum Darwinism". In: *Nat Phys* 5.3 (2009), pp. 181–188.

[12] M. Schlosshauer. *Decoherence: And the Quantum-To-Classical Transition*. The Frontiers Collection. Springer, 2007.

[13] R. Horodecki, J. K. Korbicz, and P. Horodecki. "Quantum origins of objectivity". In: *Phys. Rev. A* 91 (3 2015), p. 032122.

[14] J. Rosaler. "Local reduction in physics". In: *Studies in History and Philosophy of Science Part B: Studies in History and Philosophy of Modern Physics* 50 (2015), pp. 54 –69.

[15] W. K. Wootters and W. H. Zurek. "A single quantum cannot be cloned". In: *Nature* 299.5886 (1982), pp. 802–803.

[16] J. A. Wheeler and W. H. Zurek Eds. *Quantum Theory and Measurement*. Princeton University Press, 1983.

[17] B. Dakic, Y. O. Lipp, X. Ma, M. Ringbauer, S. Kropatschek, S. Barz, T. Paterek, V. Vedral, A. Zeilinger, C. Brukner, and P. Walther. "Quantum discord as resource for remote state preparation". In: *Nat Phys* 8.9 (2012), pp. 666–670.

[18] A. Galindo and P. Pascual. *Quantum Mechanics I*. Berlin: Springer, 1990.

[19] A. Galindo and P. Pascual. *Quantum Mechanics II*. Berlin: Springer, 1990.

[20] M. A. Nielsen and I. L. Chuang. *Quantum Computation and Quantum Information: 10th Anniversary Edition*. 10th. New York, NY, USA: Cambridge University Press, 2011.

[21] M. M. Wilde. *Quantum Information Theory*. 1st. New York, NY, USA: Cambridge University Press, 2013.

[22] B. Hall. *Quantum Theory for Mathematicians*. Graduate Texts in Mathematics. Springer New York, 2013.

[23] M.-D. Choi. "Completely positive linear maps on complex matrices". In: *Linear Algebra and its Applications* 10.3 (1975), pp. 285 –290.

[24] K. Kraus, A. Böhm, J. Dollard, and W. Wootters. *States, effects, and operations: fundamental notions of quantum theory : lectures in mathematical physics at the University of Texas at Austin*. Lecture notes in physics. Springer-Verlag, 1983.

[25] W. F. Stinespring. "Positive Functions on C*-Algebras". In: *Proceedings of the American Mathematical Society* 6.2 (1955), pp. 211–216.

[26] R. Horodecki, P. Horodecki, M. Horodecki, and K. Horodecki. "Quantum entanglement". In: *Rev. Mod. Phys.* 81 (2 2009), pp. 865–942.

[27] K. Modi, A. Brodutch, H. Cable, T. Paterek, and V. Vedral. "The classical-quantum boundary for correlations: Discord and related measures". In: *Rev. Mod. Phys.* 84 (4 2012), pp. 1655–1707.

[28] M. Piani, P. Horodecki, and R. Horodecki. "No-Local-Broadcasting Theorem for Multipartite Quantum Correlations". In: *Phys. Rev. Lett.* 100 (9 2008), p. 090502.

[29] M. Horodecki, P. Horodecki, R. Horodecki, J. Oppenheim, A. Sen(De), U. Sen, and B. Synak-Radtke. "Local versus nonlocal information in quantum-information theory: Formalism and phenomena". In: *Phys. Rev. A* 71 (6 2005), p. 062307.

[30] K. Modi, T. Paterek, W. Son, V. Vedral, and M. Williamson. "Unified View of Quantum and Classical Correlations". In: *Phys. Rev. Lett.* 104 (8 2010), p. 080501.

[31] M. Ozawa. "Entanglement measures and the Hilbert–Schmidt distance". In: *Physics Letters A* 268.3 (2000), pp. 158 –160.

[32] F. G.S. L. Brandão and G. Gour. "Reversible Framework for Quantum Resource Theories". In: *Phys. Rev. Lett.* 115 (7 2015), p. 070503.

[33] C. H. Bennett, G. Brassard, C. Crépeau, R. Jozsa, A. Peres, and W. K. Wootters. "Teleporting an unknown quantum state via dual classical and Einstein-Podolsky-Rosen channels". In: *Phys. Rev. Lett.* 70 (13 1993), pp. 1895–1899.

[34] A. K. Pati. "Minimum classical bit for remote preparation and measurement of a qubit". In: *Phys. Rev. A* 63 (1 2000), p. 014302.

[35] C. H. Bennett, D. P. DiVincenzo, P. W. Shor, J. A. Smolin, B. M. Terhal, and W. K. Wootters. "Remote State Preparation". In: *Phys. Rev. Lett.* 87 (7 2001), p. 077902.

[36] C. H. Bennett and S. J. Wiesner. "Communication via one- and two-particle operators on Einstein-Podolsky-Rosen states". In: *Phys. Rev. Lett.* 69 (20 1992), pp. 2881–2884.

[37] P. W. Shor. "Algorithms for Quantum Computation: Discrete Logarithms and Factoring". In: *Proceedings of the 35th Annual Symposium on Foundations of Computer Science*. SFCS '94. Washington, DC, USA: IEEE Computer Society, 1994, pp. 124–134.

[38] D. Kenigsberg, T. Mor, and G. Ratsaby. "Quantum Advantage Without Entanglement". In: *Quantum Info. Comput.* 6.7 (2006), pp. 606–615.

[39] E. Biham, G. Brassard, D. Kenigsberg, and T. Mor. "Quantum computing without entanglement". In: *Theoretical Computer Science* 320.1 (2004), pp. 15 –33.

[40] A. Datta, A. Shaji, and C. M. Caves. "Quantum Discord and the Power of One Qubit". In: *Phys. Rev. Lett.* 100 (5 2008), p. 050502.

[41] T. Baumgratz, M. Cramer, and M. B. Plenio. "Quantifying Coherence". In: *Phys. Rev. Lett.* 113 (14 2014), p. 140401.

[42] E. Chitambar and G. Gour. "Critical Examination of Incoherent Operations and a Physically Consistent Resource Theory of Quantum Coherence". In: *Phys. Rev. Lett.* 117 (3 2016), p. 030401.

[43] A. Winter and D. Yang. "Operational Resource Theory of Coherence". In: *Phys. Rev. Lett.* 116 (12 2016), p. 120404.

[44] F. G.S. L. Brandão, M. Horodecki, J. Oppenheim, J. M. Renes, and R. W. Spekkens. "Resource Theory of Quantum States Out of Thermal Equilibrium". In: *Phys. Rev. Lett.* 111 (25 2013), p. 250404.

[45] M. Navascués and L. P. García-Pintos. "Nonthermal Quantum Channels as a Thermodynamical Resource". In: *Phys. Rev. Lett.* 115 (1 2015), p. 010405.

[46] M. Lostaglio, M. P. Müller, and M. Pastena. "Stochastic Independence as a Resource in Small-Scale Thermodynamics". In: *Phys. Rev. Lett.* 115 (15 2015), p. 150402.

[47] I. Marvian and R. W. Spekkens. "Modes of asymmetry: The application of harmonic analysis to symmetric quantum dynamics and quantum reference frames". In: *Phys. Rev. A* 90 (6 2014), p. 062110.

[48] H. Ollivier, D. Poulin, and W. H. Zurek. "Environment as a witness: Selective proliferation of information and emergence of objectivity in a quantum universe". In: *Phys. Rev. A* 72 (4 2005), p. 042113.

[49] H.-P. Breuer and F. Petruccione. *The Theory of Open Quantum Systems*. Oxford: Oxford University Press, 2002.

[50] U. Weiss. *Quantum Dissipative Systems*. Series in modern condensed matter physics. World Scientific, 1999.

[51] V. Hakim and V. Ambegaokar. "Quantum theory of a free particle interacting with a linearly dissipative environment". In: *Phys. Rev. A* 32 (1 1985), pp. 423–434.

[52] R. Blume-Kohout and W. H. Zurek. "Quantum Darwinism: Entanglement, branches, and the emergent classicality of redundantly stored quantum information". In: *Phys. Rev. A* 73 (6 2006), p. 062310.

[53] M. Zwolak and W. H. Zurek. "Complementarity of quantum discord and classically accessible information". In: *Scientific reports* 3 (2013), p. 1729.

[54] M. Zwolak, C. J. Riedel, and W. H. Zurek. "Amplification, redundancy, and quantum Chernoff information". In: *Physical review letters* 112.14 (2014), p. 140406.

[55] R. Blume-Kohout and W. H. Zurek. "A Simple Example of "Quantum Darwinism": Redundant Information Storage in Many-Spin Environments". In: *Foundations of Physics* 35.11 (2005), pp. 1857–1876.

[56] R. Blume-Kohout and W. H. Zurek. "Quantum Darwinism in Quantum Brownian Motion". In: *Phys. Rev. Lett* 10.240405 (2008).

[57] M. Zwolak, H. Quan, and W. H. Zurek. "Quantum Darwinism in a mixed environment". In: *Physical review letters* 103.11 (2009), p. 110402.

[58] M. Zwolak, H. Quan, and W. H. Zurek. "Redundant imprinting of information in nonideal environments: Objective reality via a noisy channel". In: *Physical Review A* 81.6 (2010), p. 062110.

[59] C. J. Riedel and W. H. Zurek. "Quantum Darwinism in an Everyday Environment: Huge Redundancy in Scattered Photons". In: *Phys. Rev. Lett* 105 (2010).

[60] C. J. Riedel and W. H. Zurek. "Redundant information from thermal illumination: Quantum Darwinism in scattered photons". In: *New Journal of Physics* 13.7 (2011), p. 073038.

[61] C. J. Riedel, W. H. Zurek, and M. Zwolak. "The rise and fall of redundancy in decoherence and quantum Darwinism". In: *New Journal of Physics* 14.8 (2012), p. 083010.

[62] M. Zwolak, C. J. Riedel, and W. H. Zurek. "Amplification, Decoherence, and the Acquisition of Information by Spin Environments". In: *Scientific reports* 6 (2016), p. 25277.

[63] W. H. Zurek. "Quantum Darwinism". In: *Nature* 5 (2009).

[64] "Quantum discord is Bohr's notion of non-mechanical disturbance introduced to counter the Einstein–Podolsky–Rosen argument". In: *Annals of Physics* 338 (2013), pp. 361 –374.

[65] J. K. Korbicz, P. Horodecki, and R. Horodecki. "Objectivity in a Noisy Photonic Environment through Quantum State Information Broadcasting". In: *Phys. Rev. Lett.* 112 (12 2014), p. 120402.

[66] J. K. Korbicz, E. A. Aguilar, P. Ćwikliński, and P. Horodecki. "Do objective results typically appear in quantum measurements?" In: *arXiv preprint arXiv:1604.02011* (2016).

[67] F. G.S. L. Brandão, M. Piani, and P. Horodecki. "Generic emergence of classical features in quantum Darwinism". In: *Nature communications* 6 (2015).

[68] C. A. Fuchs and C. M. Caves. "Mathematical techniques for quantum communication theory". In: *Open Systems & Information Dynamics* 3.3 (1995), pp. 345–356.

[69] C. A. Fuchs and J. van de Graaf. "Cryptographic distinguishability measures for quantum-mechanical states". In: *IEEE Transactions on Information Theory* 45.4 (1999), pp. 1216–1227.

[70] T. Tufarelli, D. Girolami, R. Vasile, S. Bose, and G. Adesso. "Quantum resources for hybrid communication via qubit-oscillator states". In: *Phys. Rev. A* 86 (5 2012), p. 052326.

[71] P. Horodecki, J. Tuziemski, P. Mazurek, and R. Horodecki. "Can Communication Power of Separable Correlations Exceed That of Entanglement Resource?" In: *Phys. Rev. Lett.* 112 (14 2014), p. 140507.

[72] R. Horodecki and M. Horodecki. "Information-theoretic aspects of inseparability of mixed states". In: *Phys. Rev. A* 54 (3 1996), pp. 1838–1843.

[73] M. B. Ruskai, S. Szarek, and E. Werner. "An analysis of completely-positive trace-preserving maps on M2". In: *Linear Algebra and its Applications* 347.1 (2002), pp. 159 –187.

[74] F. W. J. Olver, D. W. Lozier, B. R. F., and W. Clark Charles Eds. *NIST Handbook of Mathematical Functions*. Cambridge University Press, 2010.

[75] J. Oppenheim, M. Horodecki, P. Horodecki, and R. Horodecki. "Thermodynamical Approach to Quantifying Quantum Correlations". In: *Phys. Rev. Lett.* 89 (18 2002), p. 180402.

[76] W. H. Zurek. "Quantum discord and Maxwell's demons". In: *Phys. Rev. A* 67 (1 2003), p. 012320.

[77] J. Tuziemski and J. K. Korbicz. "Dynamical objectivity in quantum Brownian motion". In: *EPL (Europhysics Letters)* 112.4 (2015), p. 40008.

[78] C. Fleming, A. Roura, and B. Hu. "Exact analytical solutions to the master equation of quantum Brownian motion for a general environment". In: *Annals of Physics* 326.5 (2011), pp. 1207 –1258.

[79] J. K. Korbicz and M. Lewenstein. "Remark on a Group-Theoretical Formalism for Quantum Mechanics and the Quantum-to-Classical Transition". In: *Found. Phys* 37 (2007), p. 879.

[80] E. C. G. Sudarshan. "Equivalence of Semiclassical and Quantum Mechanical Descriptions of Statistical Light Beams". In: *Phys. Rev. Lett.* 10 (7 1963), pp. 277–279.

[81] R. J. Glauber. "Coherent and Incoherent States of the Radiation Field". In: *Phys. Rev.* 131 (6 1963), pp. 2766–2788.

[82] M. M. Miller and E. A. Mishkin. "Representation of Operators in Quantum Optics". In: *Phys. Rev.* 164 (5 1967), pp. 1610–1617.

[83] A. Perelomov. *Generalized Coherent States and Their Applications*. Springer-Verlag, 1986.

[84] C. Weedbrook, S. Pirandola, R. García-Patrón, N. J. Cerf, T. C. Ralph, J. H. Shapiro, and S. Lloyd. "Gaussian quantum information". In: *Rev. Mod. Phys.* 84 (2 2012), pp. 621–669.

[85] P. Massignan, A. Lampo, J. Wehr, and M. Lewenstein. "Quantum Brownian motion with inhomogeneous damping and diffusion". In: *Phys. Rev. A* 91 (3 2015), p. 033627.

[86] A. Caldeira and A. Leggett. "Path integral approach to quantum Brownian motion". In: *Physica A: Statistical Mechanics and its Applications* 121.3 (1983), pp. 587 –616.

[87] J. Tuziemski and J. K. Korbicz. "Objectivisation In Simplified Quantum Brownian Motion Models". In: *Photonics* 2.1 (2015), p. 228.

[88] J. Tuziemski and J. K. Korbicz. "Analytical studies of Spectrum Broadcast Structures in Quantum Brownian Motion". In: *J. Phys. A* to appear ().

[89] P. Ullersma. "An exactly solvable model for Brownian motion: I Derivation of the Langevin equation". In: *Physica* 32 (1966), p. 27.

[90] A. J. Roncaglia and J. P. Paz. "Redundancy of classical and quantum correlations during decoherence". In: *Phys. Rev. A* 80 (2009), p. 042111.

[91] A. Besicovitch. *Almost Periodic Functions*. Dover science books. Dover Publications, 1954.

[92] P. W. Aanderson. "Local moments and localized states". In: *Nobel Lecture* (1977).

[93] J. von Neumann. *Mathematical Foundations of Quantum Mechanics transl Beyer R T*. Princeton: Princeton University Press, 1955.

[94] A. Gut. *Probability: A Graduate Course*. Springer, 2013.

[95] A. Wintner. "Upon a Statistical Method in the Theory of Diophantine Approximations". In: *American Journal of Mathematics* 55.1 (1933), pp. 309–331.

[96] F. Haake and R. Reibold. "Strong damping and low-temperature anomalies for the harmonic oscillator". In: *Phys. Rev. A* 32 (1985), p. 2462.

[97] A. W. Jasper and D. G. Truhlar. "Non-Born-Oppenheimer Molecular Dynamics for Conical Intersections, Avoided Crossings, and Weak Interactions". In: *Conical Intersections: Theory, Computation and Experiment ed Domcke W, Yarkony D R and Köppel H (World Scientific) World Scientific, Singapore* 2011 (2011).

[98] R. P. Feynmann and A. R. Hibbs. *Quantum Mechanics and Path Integrals*. Mineola: Dover Publications, 2005.

[99] R. Feynman and F. Vernon. "The Theory of a General Quantum System Interacting with a Linear Dissipative System". In: *Annals of Physics* 281.1 (2000), pp. 547 –607.

[100] G. Mahan. *Many-Particle Physics*. Physics of Solids and Liquids. Springer, 2000.

[101] H. A. Gersch. "Time evolution of minimum uncertainty states of a harmonic oscillator". In: *American Journal of Physics* 60.11 (1992), pp. 1024–1030.

[102] C. M. Caves, K. S. Thorne, R. W. P. Drever, V. D. Sandberg, and M. Zimmermann. "On the measurement of a weak classical force coupled to a quantum-mechanical oscillator. I. Issues of principle". In: *Rev. Mod. Phys.* 52 (2 1980), pp. 341–392.

[103] J. J. Halliwell. "Somewhere in the universe: Where is the information stored when histories decohere?" In: *Phys. Rev. D* 60 (10 1999), p. 105031.

[104] C. J. Riedel, W. H. Zurek, and M. Zwolak. "Objective past of a quantum universe: Redundant records of consistent histories". In: *Phys. Rev. A* 93 (3 2016), p. 032126.

[105] D. P. Pires, M. Cianciaruso, L. C. Céleri, G. Adesso, and D. O. Soares-Pinto. "Generalized Geometric Quantum Speed Limits". In: *Phys. Rev. X* 6 (2 2016), p. 021031.

[106] L. Diósi, N. Gisin, J. Halliwell, and I. C. Percival. "Decoherent Histories and Quantum State Diffusion". In: *Phys. Rev. Lett.* 74 (2 1995), pp. 203–207.

[107] T. A. Brun. "Continuous measurements, quantum trajectories, and decoherent histories". In: *Phys. Rev. A* 61 (4 2000), p. 042107.